Some Considerations of Strong, Electromagnetic and Gravitational Interactions of Hadrons

by

Andrew Rothery

A thesis presented for the degree of Doctor of Philosophy of the University of London and the Diploma of Imperial College.

April 1971

GENERAL INTRODUCTION AND ABSTRACT

Part One of this thesis is concerned solely with the "strong" interaction of hadrons. The concept of "resonance" dominates the descriptions of all such processes. Though it is debateable whether or not one can give the status of "elementary particle" to a resonance, the resonances certainly have sufficient identity to be detected as final or intermediary states of different reactions. A dynamical resonance model (originated by Veneziano) is used to describe antiproton-neutron annihilation at rest into three pions.

Part Two looks into recent ideas on gravitational effects in elementary particle physics. It has often been thought that the gravitational interaction is too weak to be of any consequence in the subnuclear world. However, it is now believed that gravity is capable of causing a natural renormalization of infinite quantities in field theory. It is shown how gravity-modified hadron electrodynamics gives a finite and experimentally testable value for the $\pi^+ - \pi^0$ mass difference.

P R E F A C E

The work presented here was carried out in the Department of Theoretical Physics, Imperial College, commencing October 1968: except where stated in the text, it is original and has not been submitted in this or any other university for any other degree.

I would like to thank all the members of the I.C. Theoretical Physics Department for many illuminating discussions over the last three years, especially Professor T. W. Kibble, Professor P. T. Matthews and Professor A. Salam, who have given invaluable support and encouragement.

I am particularly indebted to those with whom I have collaborated at one time or another during my stay at I.C., namely Dr. R. Migneron, Dr. G. P. Gopal, Mr. M. J. Duff and Mr. J. Huskins.

I am also grateful to Dr. R. J. Rivers for helpful advice on writing this thesis.

Finally, I wish to thank the Science Research Council for a maintenance grant.

CONTENTS

Part One

Part Two

PART ONE

1 INTRODUCTION TO PART ONE

1-1 A dynamical model for strong interactions, based on one originally suggested by Veneziano[1], is applied in the $N\bar{N}_{T=1} \rightarrow 3\pi$ decay channel. This enables the basic structure of this type of model to be directly confronted with experimental data, leading to insight into the phenomenological nature of both the theoretical model and the observed production of pions and their resonances. Indeed, one of the first successes of Veneziano's model was its application by Lovelace[2] to antiproton-neutron annihilation at rest into three pions[3]. Doubts over the accuracy of this prediction have led to alternative prescriptions for describing this process, either within the Veneziano formalism or even by turning back to non-Veneziano sums of resonances. A detailed investigation of the relationship between this experiment and the various Veneziano prescriptions for it is carried out - including a new and more accurate determination of the form of the relevant four-point amplitude. Essential parameters are found by fitting the two-dimensional surface of the Dalitz plot distribution directly. A phenomenological interpretation is given - i.e. a description is made in terms of pion resonances, which are directly or indirectly observed in other processes.

1-2 The Veneziano model has had success in being able to correlate different particle reactions with few arbitrary parameters. Such "global" predictions have not been very accurate, however.[4] It has been hard to obtain really close agreement in any one particular process because of the difficulties in implementing unitarity and unambiguously fixing the coefficients of so-called "secondary" Veneziano terms. The accurate investigation of the low-energy $\bar{p}n \to 3\pi$ is thus especially relevant to these problems.

1-3 Section 2 outlines the features of the experimental data on $\bar{p}n \to 3\pi$, stressing the inconclusive results of Breit-Wigner parameterizations. Section 3 is a brief statement of the kinematical notation required for the description of the various $N\bar{N}_{T=1}$ channels, and a brief derivation of some of the relations between the different isospin amplitudes. These relations are important in choosing the manner in which the Veneziano ansatz is introduced, and also in evaluating its predictive power. Section 4 introduces the concepts encountered in the Veneziano formalism and its extensions. Section 5[5] firstly reviews the earlier Veneziano model descriptions of $\bar{p}n \to 3\pi$, showing their detailed structure in a two-dimensional Dalitz plot representation. Use of a technique for fitting directly to the Dalitz plot surface, thus using all available information, shows a secondary term structure contrary to earlier analyses. Agreement with data is obtained using far fewer parameters than the phase-shift approaches.

Section 6 gives an account of the partial-wave structure of the amplitude so constructed.[6] The major items of significance are recalled in Section 7.

2 EXPERIMENTAL AND PHENOMENOLOGICAL FEATURES OF $\bar{p}n \rightarrow 3\pi$.

2-1 In the experimental Dalitz plot[3] (Figures 1, 2) the outstanding structural features are the central absence of events and the strong enhancements near the s-axis. Such features have their origins in the dynamics of the process since the kinematic phase space is a constant distribution over the area of the Dalitz plot. The details of the phase space are summarized in Figure 3. Since the $\bar{p}n$ system decays at rest in a $^1S_0$, isospin $T=1$ state it has the quantum numbers of a heavy pion; Mandelstam variables s,t,u can be used, with $s=(p_{\pi^+}+p_{\pi_1^-})^2$, $t=(p_{\pi^+}+p_{\pi_2^-})^2$ and $u=(p_{\pi_1^-}+p_{\pi_2^-})^2$.

One would expect to see bands across the Dalitz plot corresponding to $\pi^+\pi^-$ resonances, for example at $s,t=m_\varsigma^2, m_f^2, m_g^2$, and no bands at $u=$ constant, which would mean exotic $\pi^-\pi^-$ resonances. The expected band structure is drawn in Figure 4; though the data is not inconsistent with this - for example, the major enhancements correspond to some of the intersections of the bands - band features are not clearly defined and an unambiguous resonance interpretation is by no means immediate.

2-2 No satisfactory phenomenological explanation of the $\bar{p}n$ pion final state in terms of resonances has previously been given. Attempts to fit the distribution using Breit-Wigner parameterizations usually consider as candidate final-state resonances those particles classifiable as Regge recurrences and their "daughters" (Figure 5).

Recurrences are particles whose spins and masses are approximately linearly related - in $\bar{p}n \to 3\pi$, for example, the ρ, f and g mesons (with spins 1, 2 and 3, respectively) lie on the ρ-f degenerate trajectory:

$$\alpha(s) = 0.483 + 0.885\, s \qquad (2.1)$$

so that $\alpha(m_\rho^2) = 1$

$\alpha(m_f^2) = 2$

$\alpha(m_g^2) = 3$

The daughters are those particles which have approximately the same mass as a particle on the trajectory but lower spin values; they will lie on lower trajectories parallel to the "leading" one. It should be stressed that this is, for the purposes of this section, only a classification - graced by hindsight. Thus one might expect the ρ, f and g mesons to be participants in this region of phase space and also any of their daughters, though other possibilities are not excluded. The g-meson mass occurs close to the phase space boundary so consideration of the ρ-f region is usually stressed.

2-3 The Syracuse-Rome group[3] who carried out the experiment tried fits with coherent sums of Breit-Wigner terms for the ρ, f, ϵ and an exotic $T = 2$ resonance. Added background contributions were found to be little help. Their results were inconclusive. The best fit indicates that the ρ contribution is, surprisingly, consistent with zero; also, the f contribution is large, but presence of other resonances in the f region could not be ruled out.

A more recent phase-shift analysis[7] uses fourteen parameters to effect a fit using more daughters and no exotics. They agree with the absence of ϱ, but support an S-wave ϵ' particle in the f region - indeed they indicate (but not conclusively) that the S-wave final state resonances dominate. The hole in such formalisms is accounted for by the cancellation of overlapping Breit-Wigner tails, though no statistics are quoted for this.

To summarise the general attitude of the phenomenological analyses: there appears to be a "decoupling" of the higher spin resonances, especially the ϱ, and a daughter contribution not easy to handle using standard Breit-Wigner type parameterizations.

3 KINEMATICS: SU(2) - SYMMETRIC AMPLITUDES FOR $N\bar{N}_{T=1} \to 3\pi$ PROCESSES

3-1 Following Shapiro's version[8] of the standard notation for $\pi\pi \to \pi\pi$ scattering (see Figure 6) the S matrix is written:

$$S = 1 - i\,(2\pi)^4\,\delta^4\left(\sum_{i=1}^{4} p_i\right) F. \tag{3.1}$$

$$M^{dcba}(s,t,u) = -\frac{F^{dcba}(s,t,u)}{16\pi} \tag{3.2}$$

where a,b,c and d are isospin components in a system of Cartesian basis vectors and

$$s = (p_a + p_b)^2$$

$$t = (p_a + p_c)^2$$

$$u = (p_a + p_d)^2$$

$$s + t + u = m_a^2 + m_b^2 + m_c^2 + m_d^2 \tag{3.3}$$

The physical particle states are

$$\begin{aligned} |\pi^+\rangle &= \frac{1}{\sqrt{2}}\left(|\pi_1\rangle + i\,|\pi_2\rangle\right) \\ |\pi^-\rangle &= \frac{1}{\sqrt{2}}\left(|\pi_1\rangle - i\,|\pi_2\rangle\right) \\ |\pi^0\rangle &= |\pi_3\rangle \end{aligned} \tag{3.4}$$

The most general amplitude satisfying Bose statistics, isospin conservation and crossing symmetry is

$$\begin{aligned} M^{dcba}(s,t,u) = {} & A(s,t,u)\,\delta_{ab}\,\delta_{cd} + B(s,t,u)\,\delta_{ac}\,\delta_{bd} \\ & + C(s,t,u)\,\delta_{ad}\,\delta_{bc} \end{aligned} \tag{3.5}$$

where $A(s,t,u) = A(s,u,t) = B(t,s,u) = C(u,t,s)$.

If one works with the function defined as

$$A(t,u) \equiv B(s,t,u) + C(s,t,u) \tag{3.6}$$

which is symmetric in its two arguments, then it completely determines the amplitude via

$$A(s,t,u) = \tfrac{1}{2}\left[A(s,t) + A(u,s) - A(t,u)\right] \tag{3.7}$$

The s-channel isospin - T amplitudes A_s^T are given in general by

$$\begin{aligned} A_s^0 &= 3A(s,t,u) + B(s,t,u) + C(s,t,u) \\ A_s^1 &= B(s,t,u) - C(s,t,u) \\ A_s^2 &= B(s,t,u) + C(s,t,u) \end{aligned} \tag{3.8}$$

and so in terms of the s-channel T = 2 amplitude, which is $A(t,u)$ as defined in equation (3.6),

$$\begin{aligned} A_s^0 &= \tfrac{3}{2}\left[A(s,t) + A(s,u)\right] - \tfrac{1}{2}A(t,u) \\ A_s^1 &= A(s,t) - A(s,u) \\ A_s^2 &= A(t,u) \end{aligned} \tag{3.9}$$

3-2 The Veneziano ansatz is usually written down for $A(t,u)$[8,9] Though the most general form of $A(t,u)$ in terms of a possible symmetric ansatz $V(x,y)$, having poles in x and y, is

$$A_s^2 \equiv A(t,u) = gV(t,u) + f\left[V(s,u) + V(s,t)\right] \tag{3.10}$$

one can use the condition that there be no $T=2$ resonances to set $f=0$. Thus given a structure of V from a dynamical Veneziano model, the assumption of absence of exotics leads to the postulate that $A(t,u) = gV(t,u)$.

3-3 In the decay channel $X \to 3\pi$ for a particle X having the quantum numbers of a π meson, the matrix elements for the various decays are picked out of the function M of equation (3.5) as follows:

$$M(X^- \to \pi^+ \pi_1^- \pi_2^-) = C(u,t,s) + B(u,t,s) \equiv A(s,t)$$

where $s = (p_{\pi^+} + p_{\pi_1^-})^2$

$t = (p_{\pi^+} + p_{\pi_2^-})^2$

$$M(X^- \to \pi_1^0 \pi_2^0 \pi^-) = A(s,t,u) \equiv \tfrac{1}{2}[A(s,t)+A(u,s)-A(t,u)]$$

where $s = (p_{\pi_1^0} + p_{\pi_2^0})^2$

$t = (p_{\pi^0} + p_{\pi^-})^2$

$$M(X^0 \to \pi^+ \pi^- \pi^0) = A(s,t,u) \equiv \tfrac{1}{2}[A(s,t)+A(u,s)-A(t,u)]$$

where $s = (p_{\pi^+} + p_{\pi^-})^2$

$t = (p_{\pi^+} + p_{\pi^0})^2$

$$M(X^0 \to \pi^0 \pi^0 \pi^0) = A(s,t,u) + B(s,t,u) + C(s,t,u) \equiv \tfrac{1}{2}[A(s,t) + A(s,u) + A(t,u)]$$

where $s = (p_{\pi_1^0} + p_{\pi_2^0})^2$

$t = (p_{\pi_1^0} + p_{\pi_3^0})^2$ (3.11)

Hence the decay rates (proportional to the Dalitz plot densities) for the different $N\bar{N}_{T=1}$ channels are:

$$R(\bar{p}n \to \pi^+\pi^-\pi^-) = N|A(s,t)|^2$$

$$R(\bar{p}n \to \pi^-\pi^0\pi^0) = \tfrac{1}{4}N|A(s,t)+A(s,u)-A(t,u)|^2$$

$$R(\bar{p}p \to \pi^0\pi^0\pi^0) = \tfrac{1}{4}N|A(s,t)+A(s,u)+A(t,u)|^2$$

$$R(\bar{p}p \to \pi^+\pi^-\pi^0) = \tfrac{1}{4}N|A(s,t)+A(s,u)-A(t,u)|^2 \quad (3.12)$$

where N is the normalization constant.

3-4 This last paragraph will derive relationships between the total decay rates of the processes in equation (3.12) resulting from the various symmetries of the three-pion final state. Especially useful in later considerations will be the bounds on the ratio

$$R \equiv \frac{R_{TOT}(\bar{p}p \to \pi^+\pi^-\pi^0)}{R_{TOT}(\bar{p}n \to \pi^+\pi^-\pi^-)} \quad (3.13)$$

given in equation (3.21). R_{TOT} is obtained by integrating over the available phase space, accounting for the symmetry of any identical particles in the final state. The basic phase space is that for a $\pi^+\pi^-\pi^0$ final state where s,t,u (subject to $s + t + u = 4m_N^2 + 3\mu^2$) take all values allowed by energy-momentum conservation (see Figure 3); if there are two identical particles one must divide the integral by two; if there are three one must divide by six, corresponding to the six equivalent permutations of (s,t,u). Thus one has immediately:

$$2\,R_{TOT}(\bar{p}n \to \pi^-\pi^0\pi^0) = R_{TOT}(\bar{p}p \to \pi^+\pi^-\pi^0) \qquad (3.14)$$

with $R_{TOT} = \int_D R(s,t,u)\,ds\,dt$ where D is the region of Figure 3.

One may obtain a second relation between these decay rates and bounds on their ratios by exploiting the symmetry properties of the amplitudes in the phase space integration, using a trick similar to one used by Zemach in Reference 10.

Defining

$$F(s,t) = A(s,t) + A(t,u) + A(s,u), \qquad (3.15)$$

which is totally symmetric in s,t, and u, then

$$\int_D F^*(s,t)\,A(s,t)\,ds\,dt = \int_D F^*(s,t)\,A(s,u)\,ds\,dt = \int_D F^*(s,t)\,A(t,u)\,ds\,dt \qquad (3.16)$$

The complex conjugates of the three integrals in equation (3.16)

are also equal. The decay rates of equations (3.11) may be re-written in the form below in order that the total decay rates simplify, i.e.

$$\begin{aligned} M(\pi^+\pi^-\pi^-) &= \tfrac{1}{3}F(s,t) - \tfrac{1}{3}\left[A(t,u)+A(s,u)-2A(s,t)\right] \\ M(\pi^-\pi^0\pi^0) &= \tfrac{1}{6}F(s,t) - \tfrac{1}{3}\left[2A(t,u)-A(s,t)-A(s,u)\right] \\ M(\pi^0\pi^0\pi^0) &= \tfrac{1}{2}F(s,t) \\ M(\pi^+\pi^-\pi^0) &= M(\pi^-\pi^0\pi^0) \end{aligned} \tag{3.17}$$

In evaluating the phase space integrals, the interference between the symmetric and non-symmetric parts vanishes in view of equalities (3.16) and

$$\begin{aligned} &R_{TOT}(\bar{p}n \to \pi^+\pi^-\pi^-) = \\ &\qquad \frac{N}{2}\frac{1}{9}\left[\int_D |F(s,t)|^2 ds\,dt + \int_D |A(t,u)+A(s,u)-2A(s,t)|^2 ds\,dt\right] \\ &R_{TOT}(\bar{p}n \to \pi^-\pi^0\pi^0) = \\ &\qquad \frac{N}{2}\frac{1}{36}\left[\int_D |F(s,t)|^2 ds\,dt + 4\int_D |2A(t,u)-A(s,t)-A(s,u)|^2 ds\,dt\right] \\ &R_{TOT}(\bar{p}p \to 3\pi^0) = \frac{N}{6}\frac{1}{4}\int_D |F(s,t)|^2 ds\,dt \end{aligned} \tag{3.18}$$

the integrals of the non-symmetric parts in the first and second equation of equations (3.18) above are the same, so

$$\begin{aligned} R_{TOT}(\bar{p}p \to \pi^+\pi^-\pi^0) &= 2\,R_{TOT}(\bar{p}n \to \pi^-\pi^0\pi^0) \\ &= 2\left[R_{TOT}(\bar{p}n \to \pi^+\pi^-\pi^-) - R_{TOT}(\bar{p}p \to 3\pi^0)\right] \end{aligned} \tag{3.19}$$

The ratio

$$\begin{aligned} R &= R_{TOT}(\bar{p}p \to \pi^+\pi^-\pi^0) \,/\, R_{TOT}(\bar{p}n \to \pi^+\pi^-\pi^-) \\ &= 2\left\{1 - \frac{3}{4}\cdot\frac{\int_D |F(s,t)|^2 ds\,dt}{\int_D |F(s,t)|^2 ds\,dt + \int_D |A(t,u)+A(s,u)-2A(s,t)|^2 ds\,dt}\right\} \end{aligned} \tag{3.20}$$

In this form it can be seen that whatever model predicts $A(s,t)$,

$$\frac{1}{2} \leq R \leq 2 \tag{3.21}$$

4 VENEZIANO THEORY

4-1 Veneziano[1] presented a model amplitude which is a crossing-symmetric sum of narrow resonances having the correct Regge behaviour in all channels. These resonances all lie on parallel linear Regge trajectories $\alpha(s)$ - a condition strongly supported by the mass spectrum of the observed resonances. The form of this model relies on the asymptotic behaviour of the Γ-function (Stirling's formula) for its Regge limit and the pole structure of the Γ-function to represent resonances. The basic Veneziano-style amplitude for $\pi\pi$ scattering (presented in 1968 by Shapiro and Yellin[9, 8] and also Lovelace[2]) is, with the kinematical notation of section 3,

$$A(s,t) = g \cdot \frac{\Gamma(1-\alpha_s)\Gamma(1-\alpha_t)}{\Gamma(1-\alpha_s-\alpha_t)} \qquad (4.1)$$

where $\alpha_s = \alpha_0 + \alpha' s$ (4.2)

In making this ansatz, absence of exotic resonances has been assumed, as explained in section 3-2. Strictly speaking the properties of the model are valid in the narrow resonance approximation ($\mathrm{Im}\alpha = 0$), which violates unitarity. For any comparison of this theory with experiment the poles in s and t at integer values of α_s and α_t must be shifted off the real axis. This point will be dealt with in paragraph 4-5.

That the amplitude is "dual"[11] - either in the sense of being a sum of poles simultaneously in the s and t channels or in the sense of Regge-resonance duality - may be seen from the expansion of the beta function:

$$B(-\alpha_s,-\alpha_t) = \frac{\Gamma(-\alpha_s)\Gamma(-\alpha_t)}{\Gamma(-\alpha_s-\alpha_t)}$$

$$= \sum_{j=0}^{\infty} \binom{\alpha_t+j}{j} \frac{1}{j-\alpha_s} \qquad (4.3)$$

The symmetry in s and t of the beta function demonstrates that sum of poles may be in the s or t channel. Duality may be schematically indicated using quark "duality diagrams", the one appropriate to $\pi\pi$ scattering being shown in Figure 7.

Using the limit

$$\lim_{z\to\infty} z^{b-a} \frac{\Gamma(z+a)}{\Gamma(z+b)} = 1 \qquad (4.4)$$

then in the complex t plane, for any fixed value of $\arg t$ other than zero, it can be shown[8] that for large t and fixed s

$$A_s^0 \longrightarrow \frac{3}{2}\pi g \frac{1+e^{-i\pi\alpha(s)}}{\sin\pi\alpha(s)} \frac{[\alpha(t)]^{\alpha(s)}}{\Gamma(\alpha(s))}$$

$$A_s^1 \longrightarrow \pi g \frac{-1+e^{-i\pi\alpha(s)}}{\sin\pi\alpha(s)} \frac{[\alpha(t)]^{\alpha(s)}}{\Gamma(\alpha(s))}$$

$$A_s^2 \longrightarrow 0 \qquad (4.5)$$

Equation (4.5) shows that the isospin amplitudes, related to $A(s,t)$ by equations (3.9) have the proper Regge behaviour.

4-2 The expansion of A as a sum of poles (equation (4.3) shows that in any finite region of phase space, A can always be approximated by a finite set of poles in that region. Attempts to fit data by parameterizing a set of poles whose positions are indicated by Regge trajectories may violate duality, crossing symmetry or even Regge behaviour. For this reason, the discussions here on $\bar{p}n\to 3\pi$ do not consider such models (for example Boguta[12] and Pokorski/Thomas[13]) especially in view of the accuracy of the

full Veneziano formula described later in Section 5.

4-3 The existence of daughter particles occurs naturally in this formalism. The residue at a pole when $\alpha(s)=j$ is a polynomial in t of order $\leq j$. The residue is thus expressible as a sum of Legendre polynomials $P_\ell(\cos\theta_s)$ with $\ell=0,1\ldots j$ and represents a series of resonances with the same mass but with spins $\lambda = 0, 1, \ldots j$.

As an example, consider the $s=m_\rho^2$ (i.e. $\alpha(m_\rho^2)=1$) pole for a real trajectory in (4.1). Using $z\,\Gamma(z)=\Gamma(1+z)$,

$$
\begin{aligned}
A(s,t) &= g\,\frac{\Gamma(2-\alpha_s)}{1-\alpha_s}\,\frac{\Gamma(1-\alpha_t)}{\Gamma(1-\alpha_s-\alpha_t)} \\
&= \frac{g}{\alpha'}\,\frac{1}{m_\rho^2-s}\,\frac{\Gamma(1-\alpha_t)}{\Gamma(-\alpha_t)} \qquad \text{near } \alpha_s=1 \\
&= \frac{g}{\alpha'}\,\frac{1}{s-m_\rho^2}\,\left[\alpha_0+\alpha' t\right] \\
&= \frac{g}{\alpha'}\,\frac{1}{s-m_\rho^2}\,\left[a_0 P_0 + a_1 P_1\right] \qquad (4.6)
\end{aligned}
$$

where a_0 and a_1 depend on the expression for $\cos\theta_{s=m_\rho^2}$, which is linear in t. A detailed discussion of daughter structure will be made with specific reference to $\bar{p}n\to 3\pi$ in section 6, using complex trajectories to give physical, finite poles. Equation (4.6) shows how the amplitude's pole at $s=m_\rho^2$ contains both the ρ meson and ϵ meson with well-determined contributions. It will be seen that this ability of Veneziano to specify daughter contributions can be used to eliminate some of the guesswork involved in fitting data, where with Breit-Wigners one has to choose all the possible candidate resonances.

4-4 Without altering any of the basic properties (crossing, Regge &c.) the most general Veneziano-style amplitude is actually

$$A(s,t) = \sum_{n=1}^{\infty} \sum_{m=0}^{n} c_{nm} \Gamma_{nm}(s,t) \qquad (4.7)$$

where $$\Gamma_{nm}(s,t) = \Gamma(n-\alpha_s)\Gamma(n-\alpha_t) \Big/ \Gamma(n+m-\alpha_s-\alpha_t) \qquad (4.8)$$

The addition of such secondary terms (or "satellites") only alters the residue structure at a pole i.e. it changes the relative amounts of the various daughters at a pole. For example, for real trajectories the residue at $s=m_\rho^2$ is not α_t but $c_{10}\alpha_t + c_{11}$ which simply has a different mixture of ρ and ϵ.

Though the possibility of adding secondary terms is known as "the satellite ambiguity" - interpreting the c_{nm}'s as ambiguity-constants - a more optimistic attitude (voiced for example in Lovelace's review, Reference 4) treats the satellites as occuring necessarily. Here, in some N-point function formalism a basic amplitude would be unambiguous and the satellite coefficients for all other processes could be specified by factorization of the N-point amplitude.

A simple example to demonstrate the occurence of secondary terms is to consider the Veneziano five-point function[14] for scalar particles, with identical trajectories in all channels. It has poles in all five variables $s_{i,i+1}$ (see Figure 8) where

$$\begin{aligned} s_{i,i+1} &= (p_i + p_{i+1})^2 \qquad i = 1, 2 \ldots 5 \\ p_i^2 &= 1 \\ p_6 &= p_1 \end{aligned} \qquad (4.9)$$

Generalising the Beta function of equation (4.3), which has the integral representation

$$B(-\alpha_s, -\alpha_t) = \int_0^1 du\, u^{-\alpha_s - 1} (1-u)^{-\alpha_t - 1} \tag{4.10}$$

the five-point function $F(s_{12}, s_{23}, s_{34}, s_{45}, s_{51})$ is

$$F = \int_0^1 \int_0^1 \frac{du_i\, du_j}{1-u_i u_j} u_1^{-\alpha_{12}-1} u_2^{-\alpha_{23}-1} u_3^{-\alpha_{34}-1} u_4^{-\alpha_{45}-1} u_5^{-\alpha_{51}-1} \tag{4.11}$$

where $\alpha_{12} \equiv \alpha(s_{12}) = \alpha' s_{12} + \alpha_0$, et cetera. The variables u_i are not independent and all the u's can be expressed in terms of two of them. The symmetric form (4.11) can thus be written, after eliminating some of the variables,

$$F = \int_0^1 du_1 \int_0^1 du_4\, u_1^{-\alpha_{12}-1} u_4^{-\alpha_{45}-1} \left(\frac{1-u_1}{1-u_1u_4}\right)^{-\alpha_{23}-1} \left(\frac{1-u_4}{1-u_1u_4}\right)^{-\alpha_{34}-1} \times (1-u_1u_4)^{-\alpha_{15}-2} \tag{4.12}$$

Variables u_1 and u_4 can approach the lower limits of integration at the same time, and so the non-adjacent variables s_{12} and s_{45} may develop simultaneous poles, corresponding to Figure 9. The residue at a pole in one of the variables, say s_{45}, may be evaluated: first write

$$F = \int_0^1 du_1\, u_1^{-\alpha_{12}-1} (1-u_1)^{-\alpha_{23}-1} \int_0^1 du_4\, u_4^{-\alpha_{45}-1} (1-u_4)^{-\alpha_{34}-1} \times (1-u_1u_4)^{\alpha_{23}+\alpha_{34}-\alpha_{15}} \tag{4.13}$$

So at a pole $\alpha_{45} = j$,

$$\operatorname*{Res}_{\alpha_{45}=j} F = \int_0^1 du_1\, u_1^{-\alpha_{12}-1} (1-u_1)^{-\alpha_{23}-1} \times \frac{(-1)^j}{j!} \frac{\partial^j}{\partial u_4^j} \left[(1-u_4)^{-\alpha_{34}-1} (1-u_1u_4)^{\alpha_{23}+\alpha_{34}-\alpha_{15}} \right] \Bigg|_{u_4=0} \tag{4.14}$$

It is now clear that the residue at $j=0$ is simply the four-point function of equation (4.10) for four scalar particles, with $s=s_{12}$ and $t=s_{23}$. For higher values of j, corresponding to recurrences along the α_{45} trajectory (Figure 10) this basic Beta function will be multiplied by additional powers of u_1 and polynomials in α_{12} and α_{23}. Thus for a particle of high mass m_j ($\alpha_{45}(m_j^2)=j$) on the fourth leg of the four-point function, secondary terms will accompany the basic Beta function. Note that the satellite structure obtained from evaluating (4.14) corresponds to the particle mass m_j, spin j plus all the daughters (mass m_j, spins $\ell=0,1..j$). If one requires the satellites for a particular daughter, the spin ℓ component must be extracted. Thus the $j=0$ ($\ell=0$) four-point function has no satellites, and as the mass of this "excited leg" increases, more and more satellites come in.

If the $\pi\pi$ amplitude has few satellites then one would expect to see many satellites for $\bar{p}n\to 3\pi$ in this approach, as one of the external particles is a daughter. Since Regge trajectories cannot depemd on the external masses, (only c's do), extrapolation of the formula (4.7) to $X\to 3\pi$ decays is permissible. (For $\bar{p}n\to 3\pi$, $|A(s,t)|^2$ is proportional to the Dalitz plot density). The $N\bar{N}_{T=1}$ "particle" with pion quantum numbers is seen as a spin 0 daughter of a pion recurrence at $s=4m_N^2$; since $4m_N^2 > \frac{1}{\alpha'}$ ($\sim 1.1\,GeV^2$), $N\bar{N}$ is in the region where secondary terms are expected. An example of this is the analysis of Squires, Rubinstein and Chaichan [15] which obtains

five secondary β_4 terms from two β_5 terms for $\bar{p}, n, \pi^+, \pi^-, \pi^-$ by mass extrapolation and extraction of the pion pole at $\alpha_\pi(4m_N^2) \sim 3$ Further comments on this occur in section 5. However, since physics is currently lacking a global theory as indicated above, the c_{nm}'s will be regarded as unknown structure constants in the model.

4-5 To implement unitarity, or at least to obtain a complex amplitude to compare with experiment, the resonance poles in (4.7) must be off the real axis. One approach, supported recently by Lovelace[16], treats the real Veneziano as a K-matrix. Here, the Veneziano amplitude is projected into partial waves $v_\ell(s)$ which are interpreted as being the K-matrix - i.e. the T-matrix is given by the formula

$$T_\ell(s) = \frac{R_\ell(s)}{1 + \rho(s)\, R_\ell(s)} \tag{4.15}$$

$\rho(s)$ is used to carry the resonance properties. Unitarity determines the imaginary part of $T_\ell(s)$ on the right-hand cut. However, such unitarization in one channel loses low-energy crossing symmetry. Another, older, approach, which will be followed here, is to add an imaginary part to the trajectory α_s,

$$\mathrm{Im}\,\alpha(s) = A\,(s-4\mu^2)^\beta\,\theta(s-4\mu^2) \quad ; \quad \beta > 0 \tag{4.16}$$

Imα is real below threshold.

Lovelace[2] originally used the form (4.16) in his amplitude for $\bar{p}n \to 3\pi$, with $\beta = \frac{1}{2}$. The motivation for taking $\beta = \frac{1}{2}$ is that the pole, for example at $\alpha(s) = 1$ will then take the form

$$\frac{1}{1-\alpha(s)} = \frac{1}{\alpha'} \cdot \frac{1}{m_\epsilon^2 - s - i(A/\alpha')(s-4\mu^2)^{1/2}} \qquad (4.17)$$

(4.16) roughly correlates with the Breit-Wigner form $(m_\epsilon^2 - s - i m_\epsilon \Gamma)^{-1}$ Similar considerations probably led to the original Lovelace estimate of $A = 0.28\ (\mathrm{GeV}/c^2)^{-1}$ in looking at $\bar{p}n \to 3\pi$, since this roughly tallied with the ϵ-width in the proposed amplitude $\Gamma_{11}(s,t)$.

The Regge behaviour of A_s^T, Equation (4.5), is guaranteed along the real axis now, since $\mathrm{Im}\,\alpha(s) \to \infty$ as $s \to \infty$.

The major objection to the kind of parameterization given in equation (4.16) is that besides particles on leading trajectories and their daughters, infinite numbers of "ancestor" particles arise. An "ancestor" to a leading particle is one with the same mass but higher spin. These appear since the residue at a pole, being a polynomial in α_t will contain terms no longer finite polynomials in t. The power series expansion of $(t-4\mu^2)^\beta$ in the residue shows that the residue now is expressible as an infinite sum of $P_l(\cos\theta_s)$'s, with $l = 0, 1 \ldots \infty$. For example, the residue in (4.6) is α_t, corresponding to a ρ and an ϵ if α is real.

With an imaginary part as in equation (4.16), the expansion

$$(t-4\mu^2)^\beta = \sum_{l=0}^{\infty} b_l \, P_l(\cos\theta(s=m_\varsigma^2, t)) \qquad (4.18)$$

will not only modify the contribution of ς and ϵ but also introduce an infinite sequence of ancestors. With complex trajectories it is not easy to see what the partial-wave structure of the amplitude is, and thus judge whether ancestors will be important in a realistic situation. However, the partial-wave analysis of section 6 (in which the functions $\int_{-1}^{+1} A(s,t) P_l(\cos\theta)\, d(\cos\theta)$ are explicitly evaluated) will show that the ancestor contributions are negligibly small. So in fact (4.16) may be used as a good phenomenological smoothing-mechanism.

4-6 To summarize briefly, the Veneziano model provides a sum of narrow resonances satisfying duality. The daughter structure is controlled by the secondary term composition. Ancestors arise in the attempt to have finite widths to the particles, though this is not necessarily phenomenologically worrying.

5 VENEZIANO SECONDARY TERMS FOR $\bar{p}n \rightarrow 3\pi$.

5-1 It has already been shown in section 3 that with a Veneziano ansatz for $A(s,t)$ with full satellite structure (equations (4.7) and (4.8)), the predicted decay rate for $\bar{p}n \rightarrow 3\pi$ - and hence the Dalitz plot density - is proportional to $|A(s,t)|^2$ (with $s = M^2(\pi^+, \pi_1^-)$, $t = M^2(\pi^+, \pi_2^-)$). To have a more physical understanding of the relative importance of the secondary terms it is often better to think in terms of the coefficients $\tilde{c}_{nm}$ which multiply individually - normalized Γ_{nm} terms; i.e. $A(s,t)$ may be written:

$$A(s,t) = \sum_{n=1}^{\infty} \sum_{m=0}^{n} \tilde{c}_{nm} \frac{\Gamma_{nm}(s,t)}{\left[\int_D |\Gamma_{nm}(s,t)|^2 ds\, dt\right]^{1/2}} \qquad (5.1)$$

5-2 The original attempt to explain this process using a Veneziano amplitude was Lovelace's[2]. In the first part of his paper, he constructs the $\pi\pi$ scattering amplitude Γ_{10} (Equation 4.1). Then, to judge the effect of mass extrapolation of one of the external pions, he recalls the ρ-meson "decoupling effect" indicated in the earlier phenomenological analyses (see section 2). The only term which contains poles at $\alpha = 1$, 2 and 3 with no ρ-meson is Γ_{11} . So by making this indirect appeal to the data he chooses to use a single term $\Gamma_{11}(s,t)$ i.e. $c_{11} = 1.0$ and all other c_{nm}'s zero.

The form $$\Gamma_{11}(s,t) = \frac{\Gamma(1-\alpha_s)\Gamma(1-\alpha_t)}{\Gamma(2-\alpha_s-\alpha_t)} \qquad (5.2)$$

contains only the ϵ-meson, its recurrences, and their daughters. ρ-Regge behaviour is lost since the leading trajectory is missing. The Regge trajectory used is

$$\alpha_s = 0.483 + 0.885s + i\,0.28(s-4\mu^2)^{1/2}\theta(s-4\mu^2) \qquad (5.3)$$

The value 0.28 is claimed to give the ϵ a width of 280 MeV.

It is interesting to note that of all the individual Γ_{nm}'s, Γ_{11} shows closest agreement with the data, even though it is not particularly good. The Dalitz plot distribution given by Γ_{11} is shown in Figure 11 (a). The Lovelace model predicts a depletion in the centre of the Dalitz plot but it is not steep enough to satisfy experiment (Figures 12 (d), (e) and (f). In addition, the experimental distribution shows concentrations of events along bands of s and t, enhanced at some intersections. This model does not show quite the same enhancements away from the two major ones ($s=t=m_\rho^2$; $s=t=m_f^2$)

5-2 Altarelli and Rubinstein[17] (hereafter referred to as AR) concluded that a single term in (5.1) is insufficient to explain the Dalitz plot distribution satisfactorily. Its most striking feature is the hole in the middle which occurs at values of s and t such that

$$Re(\alpha_s + \alpha_t) = 3 \qquad (5.4)$$

Due to the pole structure in $\Gamma(n+m-\alpha_s-\alpha_t)$, a large denominator occurs in those terms of (5.1) for which

$$n+m \leq 3 \qquad (5.5)$$

So, motivated by direct considerations of the data, they proposed

$$A(s,t) = c_{10}\frac{\Gamma(1-\alpha_s)\Gamma(1-\alpha_t)}{\Gamma(1-\alpha_s-\alpha_t)} + c_{11}\frac{\Gamma(1-\alpha_s)\Gamma(1-\alpha_t)}{\Gamma(2-\alpha_s-\alpha_t)} + c_{20}\frac{\Gamma(2-\alpha_s)\Gamma(2-\alpha_t)}{\Gamma(2-\alpha_s-\alpha_t)}$$

$$+ c_{21}\frac{\Gamma(2-\alpha_s)\Gamma(2-\alpha_t)}{\Gamma(3-\alpha_s-\alpha_t)} + c_{30}\frac{\Gamma(3-\alpha_s)\Gamma(3-\alpha_t)}{\Gamma(3-\alpha_s-\alpha_t)} \qquad (5.6)$$

They fit the two invariant (π^+,π^-) and (π^-,π^-) mass-squared histogram projections with the five coefficients c_{nm} in (5.6). The Regge trajectory used in each of the five terms is (5.3) - and, in particular, the same imaginary part occurs in each. Their best values obtained imply that the first two terms completely dominate (Table 1).

Figure 11 (b) shows the corresponding Dalitz plot distribution. The "hole" in the centre is now more accurately fitted. But the distribution shows a general depletion, in contradiction to experiment all along the line $u \sim 1.5\ (GeV/c^2)^2$ - which corresponds to $Re(\alpha_s+\alpha_t)=3$ (see Figures 12 (e) and (f). Moreover, the concentration close to the boundary at $s=t=m_f^2$ (around $1.7\ (GeV/c^2)^2$) is present with a density twice that in the experimental distribution (Figures 1 & 2). In fact, the overall fit is worse than Lovelace's.

5-3 This failure of the AR analysis probably arises from the fact that the parameters c_{nm} are determined by fitting the two experimental $M^2(\pi^+,\pi^-)$ and $M^2(\pi^-,\pi^-)$ histograms. Their method thus ignores the strong correlation between these two variables.

Furthermore, the use of the form $0.28(s-4\mu^2)^{1/2}$ for the imaginary part of the trajectory for each of the five terms is unduly restrictive. The residue at a pole in s in the representation (5.6) is a polynomial in t whose coefficients are functions of the five c_{nm}'s . The partial wave decomposition of this residue implies the presence of certain particles at this pole. The imaginary part gives it a finite width which relates to the widths and masses of the individual particles present. The width of the poles in the overall amplitude (5.6) depend on the c_{nm}'s and the form of $\mathrm{Im}\alpha$. As such, the c_{nm}'s are related to the imaginary part of the trajectory. The more general expression $A(s-4\mu^2)^B$, with A and B as variable parameters, would treat this correlation in a better way.

To find the best parameters, we use the Dalitz plot $M^2_{\pi^-\pi^-}(=u)$ vs. $M^2_{\pi^-\pi^+}(=s)$. The lower and upper limits of u and s, fixed by the pion mass and the total centre of mass energy, are used to define a 30 x 30 grid across the Dalitz plot. The experimental number of events, N_i, in each square i, with at least one corner within the boundary, are determined. For a given set of values of the free parameters, the predicted probability distribution p_i over the significance squares $\{i\}$ is found by integrating the expression

$$\frac{d^2p}{ds\,du} = c\,.\,|A(s,t)|^2 \qquad (5.7)$$

over the area of the square i within the boundary (c is the overall normalization constant such that $\Sigma_i p_i = 1$) . The predicted distribution of events is simply $\mu_i = N p_i$ $(N = \sum_i N_i)$. As we are compelled to use

a fine grid to retain the unique features of the experimental Dalitz plot the conventional χ^2 method is not applicable in view of the small values of N_i encountered. Instead we directly maximise the likelihood of the observation to find the best parameters. The probability of the observation $\{N_i\}$ is

$$P = \prod_{i=1}^{n} p_i^{N_i} \tag{5.8}$$

where n is the total number of significant squares ($n = 561$ in this case). The likelihood is defined as

$$L \equiv \log P = \sum_{i=1}^{n} N_i \log p_i \tag{5.9}$$

Maximization of L is equivalent to maximizing the Poisson probability $\mathcal{P}$, with means μ_i,

$$\mathcal{P} = \prod_{i=1}^{n} e^{-\mu_i} \frac{\mu_i^{N_i}}{(N_i)!} \tag{5.10}$$

The maximum likelihood with unrestricted probabilities p_i is given by

$$L_{un}(max) = \sum_i N_i \log (N_i / N) \tag{5.11}$$

and the ratio $$\frac{P(max)}{P_{un}(max)} = \exp\left\{-\left[L_{un}(max) - L(max)\right]\right\}$$

enables us to define an indication of goodness of fit G as

$$G = 2\,\frac{L_{un}(max) - L(max)}{\text{Number of degrees of freedom}} \qquad (5.12)$$

Equation (5.12) is consistent with the usual definition of goodness of fit since, writing $\epsilon_i = (\mu_i - N_i)/N_i$,

$$2\left[L_{un}(max) - L(max)\right] = -2\sum_i N_i \log(1+\epsilon_i) \qquad (5.13)$$

If ϵ_i is small, the right hand side of equation (5.13) becomes

$$\sum_i \frac{(\mu_i - N_i)^2}{N_i} \qquad (5.14)$$

which is simple the usual χ^2.

With the above procedure the four free coefficients of equation (5.6) are re-determined with the original Lovelace form for the trajectory as in equation (5.3). The best values of c_{nm} (or equivalently $\tilde{c}_{nm}$) obtained are given in Table I. No term or pair of terms is dominant, as is indicated by the relative equality of the first four $\tilde{c}_{nm}$'s and the important role of the destructive interference. The interference term has an intensity roughly equal to that of the direct contribution and its structure is complex since the relative sign of the five terms varies over the Dalitz plot. Figure 11 (c) shows the corresponding Dalitz plot distribution. The main defects of the AR fit are remedied. The concentration of events along the line $Re(\alpha_s + \alpha_t) = 3$ is now reproduced correctly - see also Figures 12 (c), (d), (e), and (f). Furthermore, the central hole and the concentration close to the boundary at $s = t = m_f^2$ now have the correct densities. Figure 13 compares two distributions in full 30x30 bin detail.

These improvements are reflected in the values of G compared with those obtained using the Lovelace and AR amplitudes as shown in Table I.

Using the more general representation, $A(s-4m_\pi^2)^B$ for $\mathrm{Im}\alpha$ we find that no value of B other than 0.5 gives any significant improvement. However, a better value for A is found to be 0.33 with some slight re-adjustment of the c_{nm}'s as expected from their correlation to A. The corresponding distribution is shown in Fig. 11(d) and the values of c_{nm} and G are shown in Table I.

5-4 The Lovelace and AR analyses were unable to explain all the features of $\bar{p}n$ annihilation at rest into three pions because the strong correlation between the two physical variables describing this process were ignored. This has led to a belief that the Veneziano model is inadequate for this process, but the excellent agreement with experiment over the whole region of the Dalitz plot shown by the fit described in section 5-3 provides ample evidence to the contrary. It can be seen that all the secondary terms expected are in fact necessary to describe the data accurately.

That the five terms of equation (5.6) are the only five needed is indicated by physical considerations. Owing to the imaginary part of the trajectory, none of the five Γ_{nm}'s are exactly zero at $\mathrm{Re}(\alpha_s+\alpha_t)=3$, and the argument that one chooses only those satellites with "holes" is not so straightforward.

Indeed, the "hole" obtained in our final amplitude is obtained from the interference of the five terms. However, since Γ_{nm}'s with $n>3$ would only contribute small background tails the most terms allowed in principle are $\Gamma_{10}, \Gamma_{11}, \Gamma_{20}, \Gamma_{21}, \Gamma_{30}$ and also Γ_{22}, Γ_{31}, Γ_{32}, and Γ_{33}. The extra terms with $n=3$ only contribute in the small η-meson region of the phase space and so the fit would be rather insensitive to them, yielding inconclusive results. The only significant term is Γ_{22}, but since its value in the centre of the Dalitz plot is so large, cancellation to produce a zero there could only be effected by taking large values for $c_{10}, c_{11}, c_{20}, c_{21}$ and c_{30} i.e. a very small relative magnitude for c_{22}. In other words, especially in view of the accuracy of fit obtained, the data does not require the existence of further secondary terms.

The skill of the Veneziano amplitude in specifying the contribution of large numbers of parent and daughter resonances with only a few parameters has been demonstrated. Full details of the phenomenological content (i.e. particle structure) are given in Section 6.

5-5 There has been an attempt to predict the satellite structure for $\bar{p}n$, from mass extrapolation in a higher-point formalism, as described in Section 4. Chaichan, Rubinstein and Squires[15] construct an amplitude for $\bar{p}, n, \pi^+, \pi^-, \pi^-$ which is a sum of only two basic five-point functions (F). As they point out, it is not possible to

consider purely mesonic processes (e.g. $\pi\sigma \to \pi\pi\pi$) and project out the $\ell=0$ state at $s=4m_N^2$. since one would have to assume that factorization was valid to obtain the $\bar{p}n$ amplitude. Daughter degeneracies[18] (where each mass and spin value corresponds to a number of particle states of the formalism) prevent factorization being true. So by going to $N\bar{N}\pi\pi\pi$ directly, factorization is not required. An added advantage is that no angular momentum projection is needed, since the process is at physical threshold. There is however no satisfactory theoretical framework available for treating spin $\frac{1}{2}$ but they are led to adopt the following procedure:- taking $s_{45}=(p_{\bar{p}}+p_n)^2$, and noting the important fact that $\alpha^{\pi}(4m_N^2)\sim 3$, $A(s=s_{12}, t=s_{23})$ is given by the non-exotic terms in the residue of the pole at $\alpha^{\pi}_{45}=3$. The full details of the arguments that lead to the expression adopted are not relevant here. Assuming real trajectories,

$$A(s,t) = \underset{\alpha^{\pi}_{45}=3}{Res}\Big[\alpha^{f}_{12}\, F\left(\alpha^{f}_{12},\ \alpha^{f}_{23}-1,\ \alpha^{B}_{34}-\tfrac{1}{2},\ \alpha^{\pi}_{45},\ \alpha^{B}_{15}-\tfrac{3}{2}\right) + c.(\alpha^{B}_{34}-\tfrac{1}{2})\, F\left(\alpha^{f}_{12}-1, \alpha^{f}_{23}-1, \alpha^{B}_{34}-\tfrac{1}{2}, \alpha^{\pi}_{45}-1, \alpha^{B}_{15}-\tfrac{1}{2}\right)\Big] \qquad (5.15)$$

where α^{B} refers to either the N or Δ trajectory (Ref. 15 says the results turn out to be essentially the same whichever is used) and c is an arbitrary constant.

$A(s,t)$ derived in this way can indeed be put into the form of equation (5.1) with c_{10}, c_{11}, c_{20}, c_{21}, c_{22} all functions of c and the Regge trajectory parameters, and all other $c_{nm}=0$

Unfortunately these are not compatible with the data, since demanding $c_{22} = 0$ (to eliminate c) gives $c_{10} = 1$ (normalization) $c_{11} = 1.80$, $c_{20} = 0.26$, $c_{21} = 0$ There is no $n=3$ term. It is not easy to lay the blame in any particular area (spin-$\frac{1}{2}$ treatment, unitarity etc.). Certainly this shows how the satellite "arbitrariness" of one level can be reduced by going to a higher-point formalism. As reference 15 reminds us, the qualitative results are not trivial since if $\alpha_\pi(4m_N^2)$ had been other than 3, quite different Γ_{nm}'s would have appeared. The general problems of this approach are not yet fully understood.

5-6 At first sight, it would appear that an immediate prediction of the $A(s,t)$ determined previously is that of the $T=1$, $\bar{p}p$ decay into three pions, for which data exists. These are however large errors involved in the separation of singlet and triplet states. The only experimentally accessible quantity is the ratio of the total rates

$$R = \frac{R(\bar{p}p_{T=1} \to \pi^+\pi^-\pi^0)}{R(\bar{p}n \to \pi^+\pi^-\pi^-)} \simeq 1.6^{+1.1}_{-0.8} \qquad (5.16)$$

(The numerical value and errors are those quoted in AR[17])

Since $SU(2)$ alone demands

$$\tfrac{1}{2} \leqslant R \leqslant 2 \qquad (5.17)$$

as derived in section 3-4 (equation 3.21) then any model is bound to get an answer within the range of R quoted in (5.16).

On evaluating this ratio (from equations (3.12) or equivalently (3.20) one obtains $R=1.13$ for the fit with $A=0.28$ and $R=1.04$ for $A=.33$. This is not significantly different to the AR amplitude ($R=1.19$) though the Lovelace Γ_{11} term alone gives $R=0.69$ This would indicate that R is insensitive to the detailed satellite structure though sensitive enough to "reject" Γ_{11} alone. Table II gives corresponding values for the ratios $R(\bar{p}p \to 3\pi^0)$: $R(\bar{p}n \to \pi^+\pi^-\pi^-)$: $R(\bar{p}p_{T=1} \to \pi^+\pi^-\pi^0)$ evaluated using equations (3.12).

6 PARTIAL WAVE STRUCTURE OF $\bar{p}n \to 3\pi$

6-1 The Veneziano amplitude with real trajectories is a sum of infinitely narrow resonances (i.e. poles of the form $\frac{1}{s-m^2}$) To avoid these infinities in the comparisons with experiments discussed earlier, complex trajectories enabled the poles to be moved off the real axis. The structure is now no longer a sum of simple poles, nor explicitly a sum of Breit-Wigner amplitudes. However, the resonances will still be shown by the energy-dependence of partial wave amplitudes $a_\ell(s)$ given by

$$a_\ell(s) = \int_{-1}^{+1} A(s,t) P_\ell(\cos\theta_s)\, d\cos\theta_s \qquad (6.1)$$

The integration is effectively over the range of t available at that s-value, with for the case of $X \to 3\pi$

$$\cos\theta_s(t) = \frac{s^{1/2}\left[2t + (s - M^2 - 3\mu^2)\right]}{\left\{(s-4\mu^2)\left[s-(M+\mu)^2\right]\left[s-(M-\mu)^2\right]\right\}^{1/2}} \qquad (6.2)$$

where for $\bar{p}n \to 3\pi$, $M^2 = 4m_N^2$.

This a_ℓ corresponds to the partial wave expansion:

$$A(s,t) = \sum_{\ell=0}^{\infty} \left(\frac{2\ell+1}{2}\right) a_\ell(s)\, P_\ell(\cos\theta_s(t)) \qquad (6.3)$$

for s fixed.

Partial wave cross sections σ_ℓ are defined as follows:

$$\frac{d\sigma}{d\Omega} \propto |A(s,t)|^2 \qquad \text{(s fixed)} \qquad (6.4)$$

then

$$\sigma = \pi \sum_{l} \sigma_l \tag{6.5}$$

with $\sigma_l = (2l+1)|a_l|^2$ (6.6)

6-2 Consideration of resonance structures by putting $Im\alpha = 0$ and examining the polynomial in t at a pole in s is only a rough guide to the possible resonances present (as described in section 4). Even assuming the validity of its approximation to the complex amplitude used for fitting, there is no way of making comparison with Breit-Wigner or any other resonance parameterization without specifying the phase. (An example of use of this method for $\bar{p}n \to 3\pi$ is Pokorski and Thomas's analysis[13] of Lovelace, AR and their own amplitudes). All that one can determine are the relative magnitudes of the numbers $c_R(m_R^2)$ in the expansion

$$A(s,t) = \sum_R \frac{(2l+1)\, c_R(s)\, P_l(\cos\theta_s)}{s - m_R^2} + (s \leftrightarrow t) \tag{6.7}$$

giving restricted information about relative widths and phases of parents to daughters. Table II gives these ratios for the secondary term structure determined, with $Im\,\alpha = 0$.

6-3 In an Argand plot of $Re\, a_\ell(s)$ vs $Im\, a_\ell(s)$ an anticlockwise loop (with respect to increasing s) is usually taken as evidence for the existence of a resonance[19] (a Breit-Wigner gives anticlockwise loops). Argand plots of the partial waves for the amplitude $A(s,t)$ for $\bar{p}n \to 3\pi$ (equation (5.6) with $Im\,\alpha = A(s-4\mu^2)^{1/2}$; $A = 0.33$) are shown in Figures 14 onwards (there is little difference between $A=0.33$ and $A=0.28$). The strongest resonances may be expected to show peaks in the $|a_\ell(s)|^2$, but to interpret less well-defined bumps and shoulders, the Argand diagram must be consulted; even the peaks should be checked in the complex-a_ℓ plane since it is not impossible for interference of resonances to produce freak peaks. Around the loop, the positions where $s = m_R^2$ should come near, the maximum or minimum in $Im\, a_\ell$. More exact criteria for resonances consider maxima in $\left|\frac{da_\ell}{ds}\right|$ and also maxima in the angular velocity around the loop, but these are not considered here.

From a preliminary inspection of $a_\ell(s)$ $(\ell = 0, 1, \ldots 4)$ the existence of four major resonances may be inferred. Figure 14(a) shows three well-defined peaks in $\sigma_0 = |a_0(s)|^2$ at s=0.49, 1.67, 2.73 GeV^2 (note that experimentally $m_f^2 = 0.59$, $m_\epsilon^2 \sim 0.5$, $m_f^2 = 1.60$, $m_g^2 = 2.77$).

The Argand plot of $a_0(s)$, Figure 14(b), has an anticlockwise sense for s close to each of these s values, confirming that these peaks are indeed resonances. Figure 15(a) shows only one well-defined

peak in $|a_1(s)|^2$ near $s=1.67$ which corresponds to a tight anti-clockwise loop in the Argand plot (Figure 15 (b). For the two shoulders in $|a_1(s)|^2$, the Argand loop shows gentle resonance curvature at $s = m_S^2$ and $s = m_g^2$. Thus the possibility of ρ, ρ'' is not ruled out, though they have very diminished intensities. Details of the positions of these resonances are in Table IV. Figure 16(a) has a "freak peak" in $|a_2(s)|^2$ at $s= 1.96$ - the Argand plot (Figure 16 (b) showing a large clockwise loop. The intensity of this peak is much less than any of the others. Higher partial waves show bumps of ever-decreasing magnitude, with no anticlockwise loops in $a_\ell(s)$ .Specifically, $\ell=3$ and $\ell=4$ show gently clockwise spirals, with no maximum in either $|a_\ell(s)|^2$ exceeding 13.0 (arbitrary) units - compare this with the 50.0 units of the freak peak in $|a_2|^2$ and the typical 700.0 units of the resonance peaks of $|a_1|^2$ and $|a_0|^2$.

Relative intensities are given in Table V, but it should be pointed out that "background" or "overlapping tails" effects have not been taken into account. Further, no attempt is made to infer the exact couplings (partial widths) of the particles indicated. The general trend of these results is in qualitative agreement with the residues of the poles in the zero width amplitude (Table II).

6-4 It is interesting to note that a similar analysis of the Lovelace and AR amplitudes shows them to be quite different in Phenomenological structure. This is what might be expected from

the differing goodnesses of fit to experiment, despite the fact that they have poles in almost the same places. For example, the Lovelace amplitude contains essentially only the ϵ and ϵ' mesons. (Table 5) Since none of these other amplitudes correspond closely to the data, no details of their partial waves are considered here.

6-5 "Ancestors" do not arise with any significant intensity, though the higher partial waves are not without structure. It would be very difficult to isolate any effect and attribute it unambiguously to an ancestor particle. (They are not in evidence in any of the other Veneziano versions either). Certainly as far as deciding on the physical content of either the amplitude or the data is concerned, ancestors are as good as absent.

6-6 The results described in (6-3) on the basis of the fit of 5-3 seem to confirm the "decoupling effect". The ρ, f and g mesons all appear to be absent, or, at least, seriously diminished. Most of their daughters appear to be present in varying intensities: the S-wave ϵ, ϵ', and ϵ'' and equal contribution of ρ' with little ρ''. Inspection of the experimental Dalitz plot supports this; whereas along a line $s = m_\rho^2$ the density of events remain constant (corresponding to P_0), along $s = m_f^2$ the density increases (corresponding to significant amount of P_1). Thus the effect would appear, rather than "S-wave dominance" for example, to be a decoupling of the leading trajectory.

7 SUMMARY

The satellite structure of the general Veneziano amplitude, though not completely specified by the current state of the formalism as a whole, nevertheless agrees well with the $\bar{p}n \to 3\pi$ experiment, needing to use only a few free parameters. (Compare the four used here with the fourteen of the most recent phase shift analysis[7]). The use of a dual amplitude, describing low-energy resonances in terms of Regge trajectories proves successful. Incorporation of unitarity remains an unsolved problem - the Veneziano amplitudes in the narrow resonance limit can only be regarded as a first-order contribution of some more comprehensive peturbative scheme.[20] Despite this, the method of smoothing the infinitely narrow poles employed here - though probably a crude approximation to whatever should be done - has proved to be quite satisfactory physically. The main theoretical problem with the $A(s-4\mu^2)^\beta$ form for $\mathrm{Im}\alpha(s)$, namely the existence of ancestors, turns out to be less serious than might at first sight be thought. The results of section 6 show that the amplitude used to fit the data does not correspond to a significant contribution from any ancestors. Also the relative parent/daughter contributions are not drastically altered at a qualitative level.

Apparently, all the secondary Veneziano terms allowed are necessary to be able to handle the inclusion of all the π-π resonances and their daughters. No term, or few terms, dominate. These conclusions contradict those of Lovelace and AR, whose analyses were unable to explain the features of $\bar{p}n$ annihilation probably because strong correlations between the two physical variables describing the process were ignored. Attempts to predict this satellite structure using a naive reduction of the five-point function using mass extrapolation[15] though giving a qualitative explanation, are not yet in quantitative agreement with the fit presented here.

The only immediate prediction of the $\bar{p}n$ amplitude is the ratio $\dfrac{R_{TOT}(\bar{p}p_{T=1} \longrightarrow 3\pi)}{R_{TOT}(\bar{p}n \longrightarrow 3\pi)}$. Though the value given is reasonable, the ratio is insensitive as a test since the experimental errors involved in extracting information about the $T=1$, $\bar{p}p$ state are so large. Until one has a formalism which specifies the secondary terms for a wide range of processes, it is of course impossible to exploit the crossing symmetries of Veneziano with anything better than qualitative accuracy, since satellite structure will be different in each case.

The preliminary analysis of the partial wave structure of

the Veneziano amplitude for $\bar{p}n \to 3\pi$ (described in section 6) indicates that, with the form for $\mathrm{Im}\alpha$ as used, the amplitude does contain resonance structures. The a_ℓ's give strong evidence for the supposition that in the final 3π final state, the resonances on the leading Regge trajectory (ρ, f and g mesons)are in fact absent, or at least very much diminished. There would seem to be a large contribution from the ρ' resonance, and the S-wave. daughters.

The Veneziano approach, in addition to its theoretical skills (especially in incorporating duality), is also then, useful phenomenologically. The resonances of its dual sum of poles are by no means unphysical. Though Veneziano is not the only possible dual formalism, nor completely debugged, it points a way to a correct understanding of the hadrons.

REFERENCES (PART I)

1. G. Veneziano: Nuova Cimento 57A, 190 (1968)

2. C. Lovelace: Phys. Letters 28B, 265 (1968)

3. P. Aninos, L. Gray, P. Hagerty, T. Kalogeropoulos, L. Zenone, R. Bizzari, S. Ciapetti, M. Gaspero, I. Laakso, L. Lichtman and G. C. Moneti: Phys. Rev. Letters 20, 402 (1968); also private communications with R. Bizzari.

4. See the review talk "Veneziano Theory", C. Lovelace; Cern preprint TH 1123 (1969).

5. Section 5 contains material also appearing in G. P. Gopal, R. Migneron, A. Rothery; I.C. preprint ICTP/69/24; (1970). To be published in "The Physical Review".

6. Section 6 contains material arising from private communications with G. P. Gopal.

7. A. M. Gleeson, W. J. Meggs, M. Parkinson: Phys. Rev. Letters, 25, 74 (1970).

8. J. A. Shapiro: Phys. Rev. 179, 1345 (1969).

9. J. A. Shapiro, J. Yellin: UCRL Report no. 18500 (1968), unpublished.

10. C. Zemach: Phys. Rev. 133, B1201 (1964).

11. Many review talks give a good discussion of "duality" and the concepts leading up to Veneziano, for example - M. Jacob: Brandeis 1970 (M.I.T. Press); M. Kugler: Schladming 1970.

12. J. Boguta: Nuclear Phys. B13, 537 (1969); and also J. Boguta: Bonn preprint December 1969.

13. S. Pokorski, G. H. Thomas: Helsinki preprint 17-70 (1970).

14. K. Bardakçi, H. Ruegg: Phys. Letters 28B, 342 (1968).

15. H. R. Rubinstein, E. J. Squires, M. Chaichan: Phys. Letters 30B (1969).

16. See for example C. Lovelace: Proceedings of the Argonne conference on $\pi\pi$ and $K\pi$ interactions, 562 (1969).

17. G. Altarelli, H. R. Rubinstein: Phys. Rev. 183 (1969).

18. See Reference 15 for brief discussion and further references.

19. For example, R. H. Dalitz, R. G. Moorhouse: Proc. Roy. Soc. Lond. A. 318, 279 (1970).

20. See for example, the review talk "An Introduction to Dual Theory" D. Amati: Cern preprint TH.1231 (1970).

TABLES FOR PART ONE

TABLE I

A comparison of the Veneziano versions for $\bar{p}n \to 3\pi$. The c's are the un-normalized coefficients of Eq. (4.7), the $\tilde{c}$'s multiply the physically normalized contributions in Eq. (5.1). One parameter is always fixed by overall normalization and the errors on the others do not exceed 8%. G is the goodness of fit defined by Eq. (5.12).

	Lovelace	Altarelli-Rubinstein	A = 0.28	A = 0.33
c_{10}	-	1.00	1.00	1.00
c_{11}	1.00	1.89	2.55	2.90
c_{20}	-	0.00	2.96	2.14
c_{21}	-	0.00	7.80	7.31
c_{30}	-	0.57	-4.52	-3.74
$\tilde{c}_{10}$	-	1.00	1.00	1.00
$\tilde{c}_{11}$	1.00	0.78	1.05	1.18
$\tilde{c}_{20}$	-	0.00	0.70	0.53
$\tilde{c}_{21}$	-	0.00	1.04	1.02
$\tilde{c}_{30}$	-	0.00	-0.23	-0.19
$2(L_{un}(max)-L(max))$	1244	1458	606	592
G	2.24	2.62	1.09	1.07

TABLE II

Relative magnitudes of parents and daughters at each pole in $A(s,t)$ with $\mathrm{Im}\alpha = 0$ for $A(s,t) = c_{10}\Gamma_{10} + c_{11}\Gamma_{11} + c_{20}\Gamma_{20} + c_{21}\Gamma_{21} + c_{30}\Gamma_{30}$.

The magnitudes are defined by

$$A(s,t) = \sum_R \frac{(2l+1)\, c_R(s)\, P_l(\cos\theta_s)}{s - m_R^2} + (s \leftrightarrow t)$$

$c_{10} : c_{11} : c_{20} : c_{21} : c_{30}$	m_R^2	Relative c_R's
1 : 2.55 : 2.96 : 7.80 : -4.52	m_ϵ^2	$c_\epsilon : c_\delta = 1.0 : 0.5$
	m_f^2	$c_{\epsilon'} : c_{\delta'} : c_f = 1.0 : 2.0 : -0.3$
1: 2.90 : 2.14 : 7.31 : -3.74	m_ρ^2	$c_\epsilon : c_\delta = 1.0 : 0.4$
	m_f^2	$c_{\epsilon'} : c_{\delta'} : c_f = 1.0 : 3.0 : -0.2$

TABLE III

Ratios of the $N\bar{N}_{T=1}$ decay rates predicted from the four Veneziano amplitudes. The ratio $R = \dfrac{R_{TOT}(\bar{p}p_{T=1} \to \pi^+\pi^-\pi^0)}{R_{TOT}(\bar{p}n \to \pi^+\pi^-\pi^-)}$ is also given.

	$R_{TOT}(\bar{p}p \to 3\pi^0)$	$R_{TOT}(\bar{p}n \to \pi^+\pi^-\pi^-)$	$R_{TOT}(\bar{p}p_{T=1} \to 3\pi)$	R
Lovelace	1	1.53	1.05	0.69
AR	1	2.47	2.95	1.19
A=0.28	1	2.30	2.61	1.13
A=0.33	1	1.95	2.03	1.04

TABLE 4

Location of resonant effectsin the partial waves $a_\ell(s)$ (ℓ=0,1,2,3,4) of $A(s,t)$ determined for $\bar{p}n \to \pi^+\pi^-\pi^-$.

Partial Wave	Resonance Position	$\sigma_\ell(s)$	Curvature of $k_s\, a_\ell(s)$
ℓ =0	ϵ	MAX	ANTI-CLOCKWISE AT $s = m_R^2$
	ϵ'	MAX	
	ϵ''	MAX	
ℓ =1	ρ	SHOULDER	ANTI-CLOCKWISE AT $s = m_R^2$
	ρ'	MAX	
	ρ''	SHOULDER	
ℓ =2	$s = m_\rho^2$	SLIGHT SHOULDER	CLOCKWISE MOTION THROUGHOUT LOOP
	f	NOTHING	
	$s = 1.96$	MAX	
	f'	NOTHING	
ℓ =3,4	SMALL EFFECTS UNRELATED TO RESONANCE MASSES		CLOCKWISE MOTION THROUGHOUT LOOP

TABLE 5

Relative Intensities of Resonances in $\bar{p}n \to \pi^+\pi^-\pi^-$

A) is for the A(s,t) determined as described in text.

B) is for the Lovelace term Γ_{11} for comparison.

The intensities of σ_ℓ are evaluated at the mass of the resonance given by the Regge trajectory. Spin 2 and 3 resonances are absent.

Veneziano Model	Spin-0			Spin-1		
	ϵ	ϵ'	ϵ''	ρ	ρ'	ρ''
A	1.0	0.97	0.96	0.12	0.66	0.14
B	1.0	1.14	0	0	0.16	0

FIGURES FOR PART ONE

FIGURE CAPTIONS

Figure 1. Experimental $(M_{\pi^-\pi^-})^2$ vs. $(M_{\pi^+\pi^-})^2$ Dalitz plot for $\bar{p}n \to 3\pi$. There are two entries per event.

Figure 2. Experimental Dalitz plot general features. The contour numbers represent the number of events per (0.098 x 0.098) (GeV / c^2)^4 area of the Dalitz plot. The number in the centre of the contour graph gives the density at the position of the central "hole".

Figure 3. Phase space for $\bar{p}n$ (at rest) $\to 3\pi$ The axes may represent any pair of s, t or u.

Figure 4. Resonance band structure for $\bar{p}n \to 3\pi$

Figure 5. The ρ-f degenerate trajectory and the daughter trajectories.

Figure 6. Kinematics for the $\pi\pi$ scattering amplitude. a,b,c,d represent the isospin components in a Cartesian basis.

Figure 7. Duality diagram for pseudoscalar meson-meson scattering.

Figure 8. Five-point function kinematic notation.

Figure 9. Possible excitations in five-point function.

Figure 10. The Regge trajectory $\alpha(s_{45})$

Figure 11. $(M_{\pi^-\pi^-})^2$ vs $(M_{\pi^+\pi^-})^2$ Dalitz plots;
(a) Lovelace's distribution
(b) Rubinstein - Altarelli distribution
(c) Dalitz plot distribution given by Veneziano secondary terms determined as described in text with $A = 0.28$.
(d) Secondary terms as in text with $A = 0.33$. The contours are labelled as for Fig. 2.

Figure 12. The histograms show the density of events as a function of $M^2_{\pi^+\pi^-}$. Each histogram averages over a 0.294 $(\text{GeV}/c^2)^2$ - wide slice of $M_{\pi^-\pi^-}{}^2$ the dotted, broken, and full lines describe contour figures 11 (a), 11 (b) and 11 (c) respectively.

Figure 13. Histograms again showing the density of events as a function of $M_{\pi^+\pi^-}{}^2$. However, there is no averaging, and each of the 30 histograms correspond to a one-bin slice $(0.098\ (\text{GeV}/c^2)^2$ of $M_{\pi^-\pi^-}{}^2$. Thus each histogram in Fig. 12 is the average of 3 histograms here. The broken and full lines correspond to contour figures 11 (b) and 11 (c) respectively.

Figure 14. $\ell = 0$ partial waves;
(a) $\sigma_0(s)$ vs. s.
Peaks occur at
$s = 0.49, 1.67, 2.73\ (\text{GeV}/c^2)^2$
(b) Argand diagram $k_s\, \text{Im}\, a_0(s)$ vs. $k_s\, \text{Re}\, a_0(s)$
k_s is proportional to $(s - 4\mu^2)^{1/2}$
The dots are equispaced in s.

Figure 15. ℓ = 1 partial waves;
(a) $3|a_1(s)|^2 = \sigma_1$ vs. s. Peak occurs at s = 1.67 $(GeV/c^2)^2$
(b) Argand plot $k\,Ima_1(s)$ vs. $k\,Rea_1(s)$.

Figure 16. ℓ = 2 partial waves;
(a) $\sigma_2(s)$ vs. s. Peak occurs at s = 1.96 (not a resonance mass). Note the small intensity.
(b) Argand plot $k\,Ima_2$ vs. $k\,Rea_2$.

ERRATUM: The vertical axes in Fig. 14(a), 15(a) Fig. 16(a) should be labelled $\sigma_\ell = (2\ell+1)|a_\ell|^2$ and not $|a_\ell|^2$.

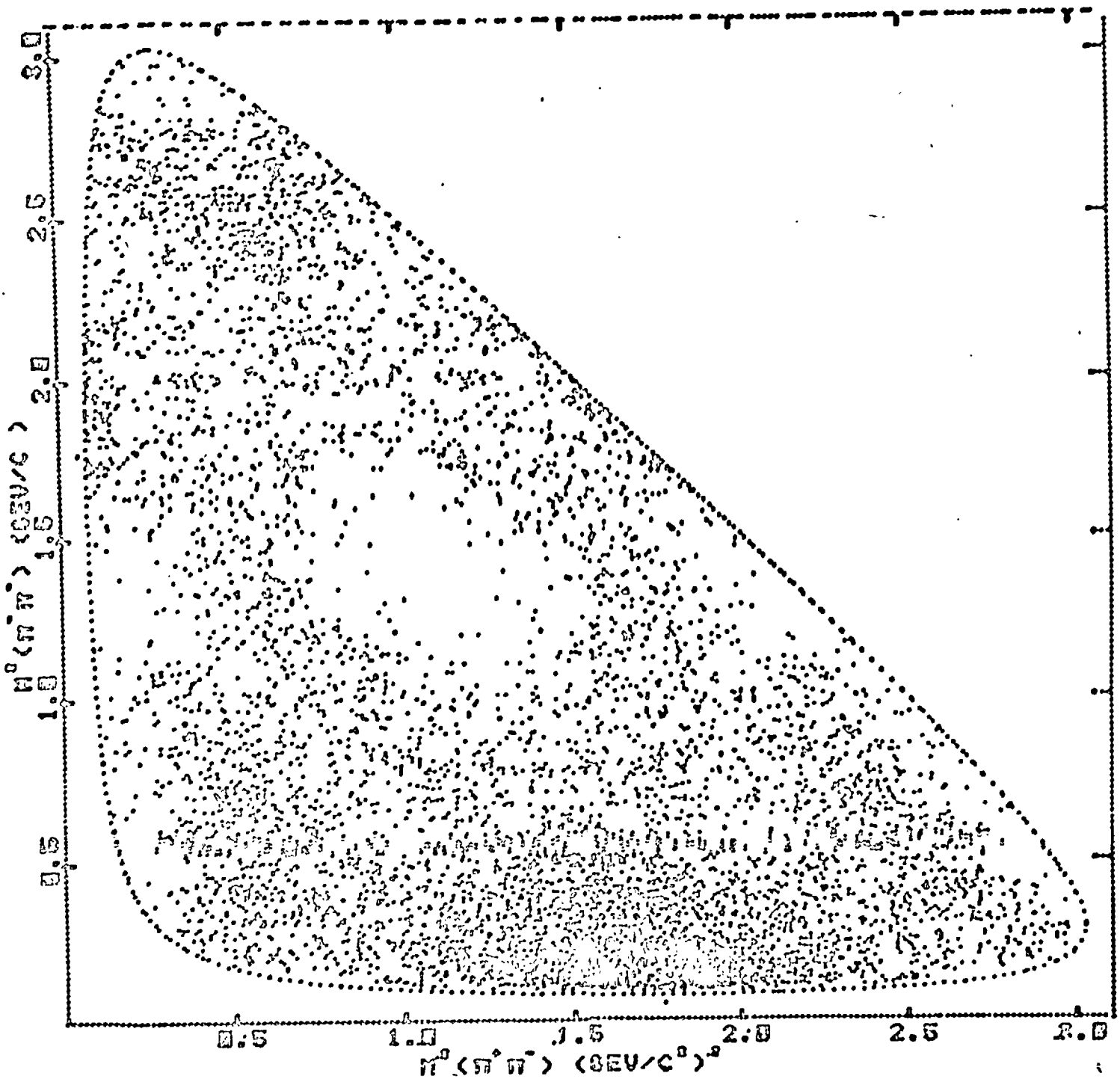

FIG.1

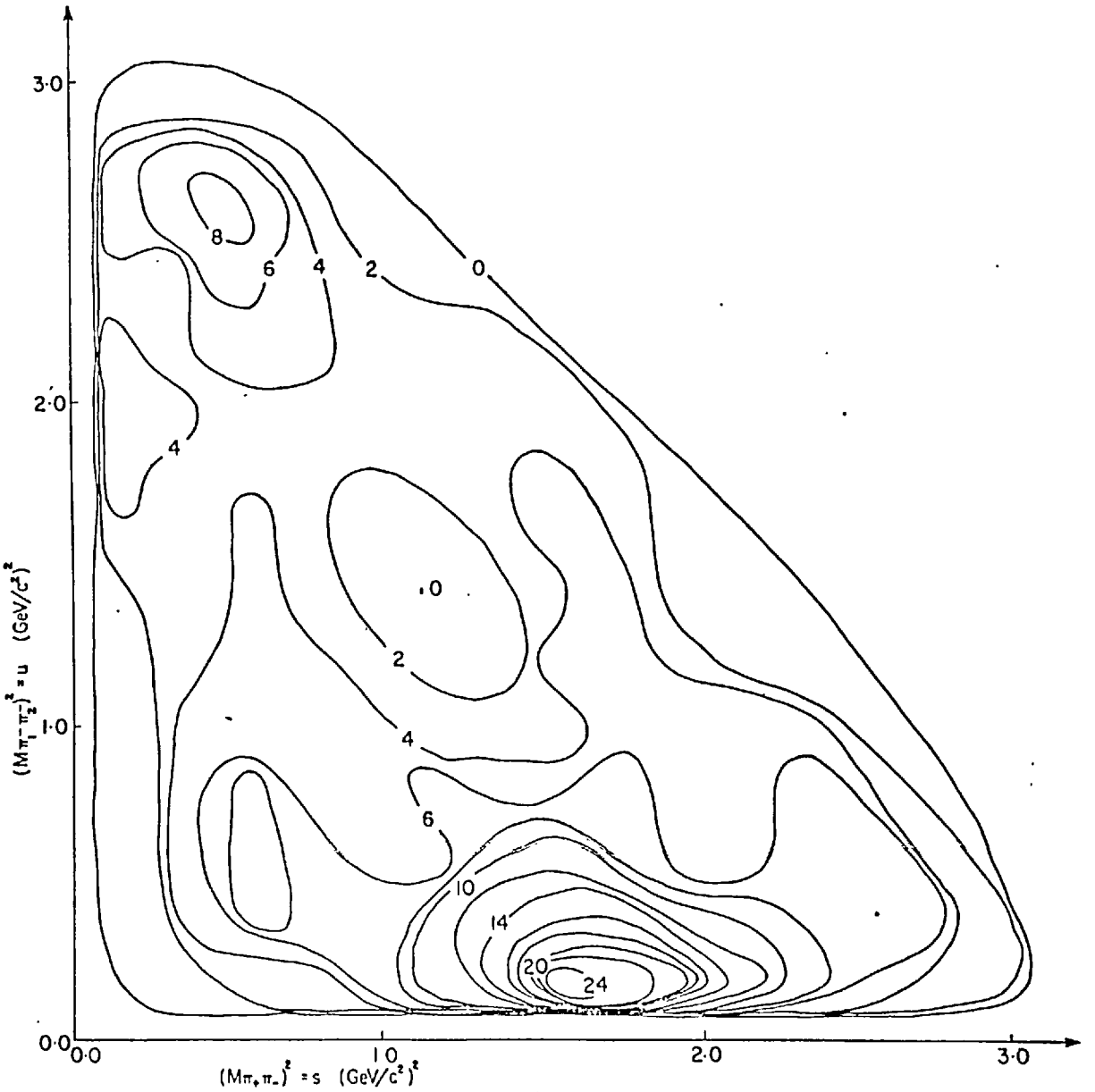

Experimental Features

FIG. 2

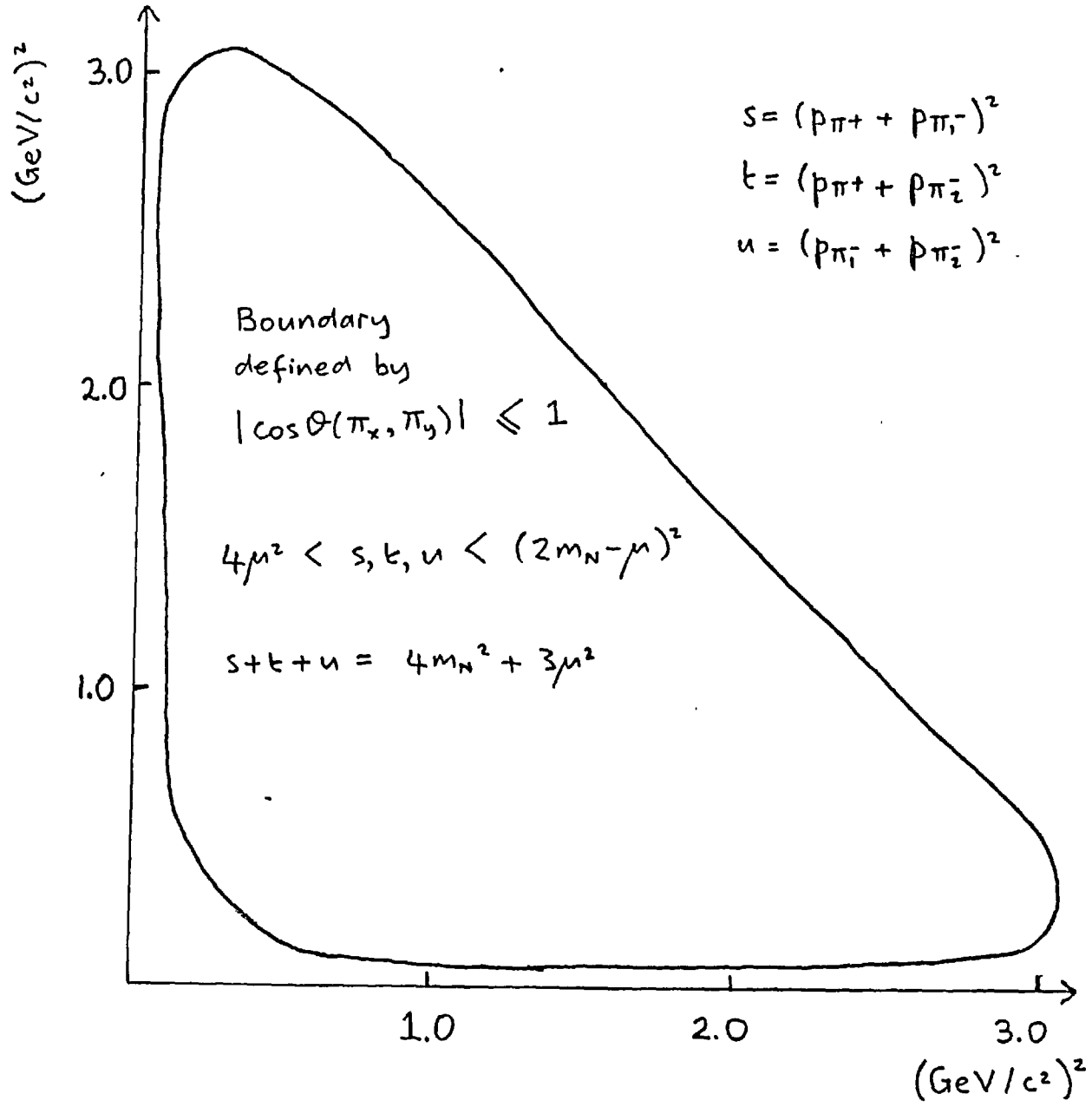
$(GeV/c^2)^2$
3.0
2.0
1.0
$s = (p_{\pi^+} + p_{\pi_1^-})^2$
$t = (p_{\pi^+} + p_{\pi_2^-})^2$
$u = (p_{\pi_1^-} + p_{\pi_2^-})^2$
Boundary defined by
$|\cos\theta(\pi_x, \pi_y)| \leq 1$
$4\mu^2 < s, t, u < (2m_N - \mu)^2$
$s + t + u = 4m_N^2 + 3\mu^2$
1.0
2.0
3.0
$(GeV/c^2)^2$

FIG. 3

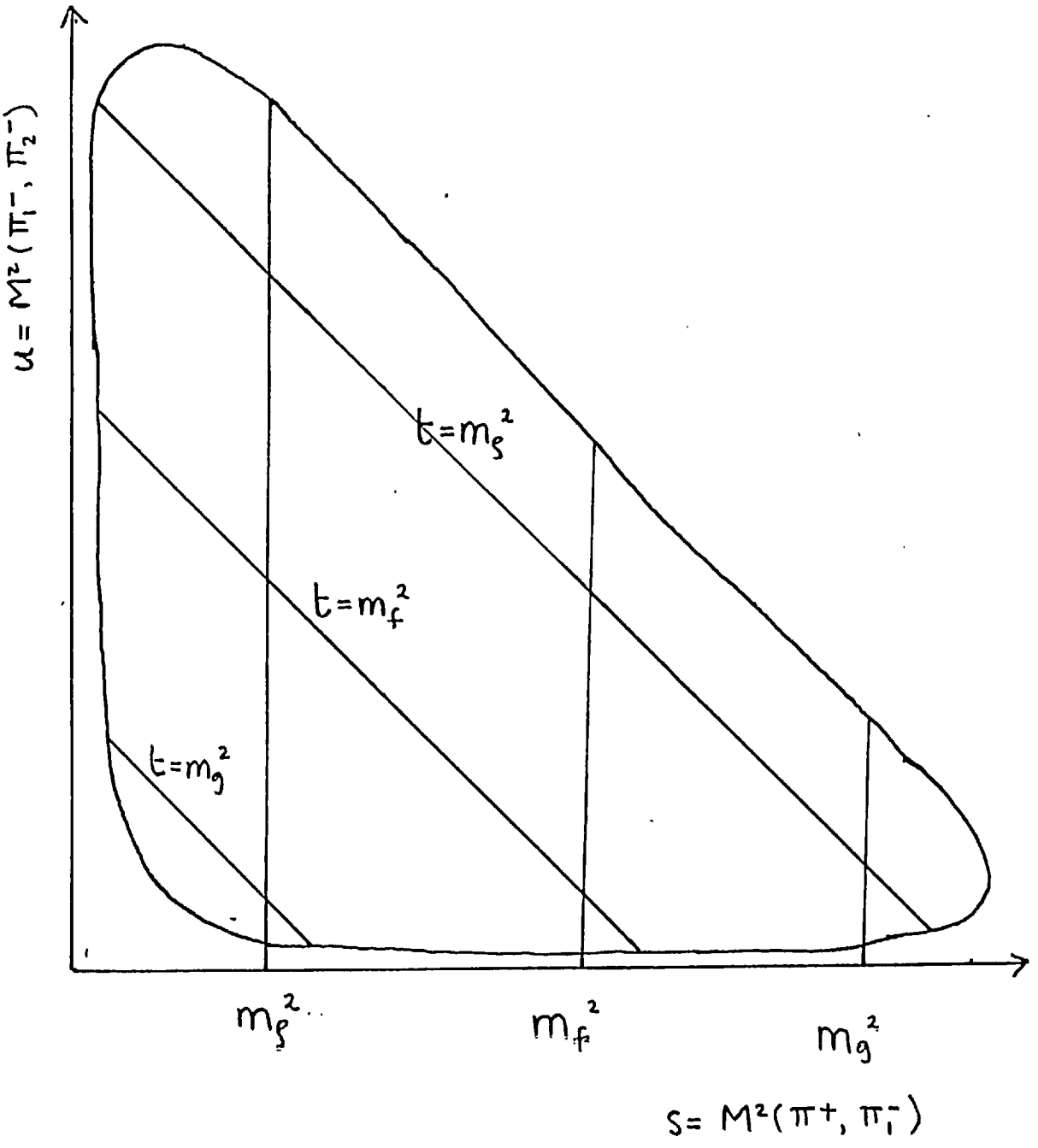

FIG. 4

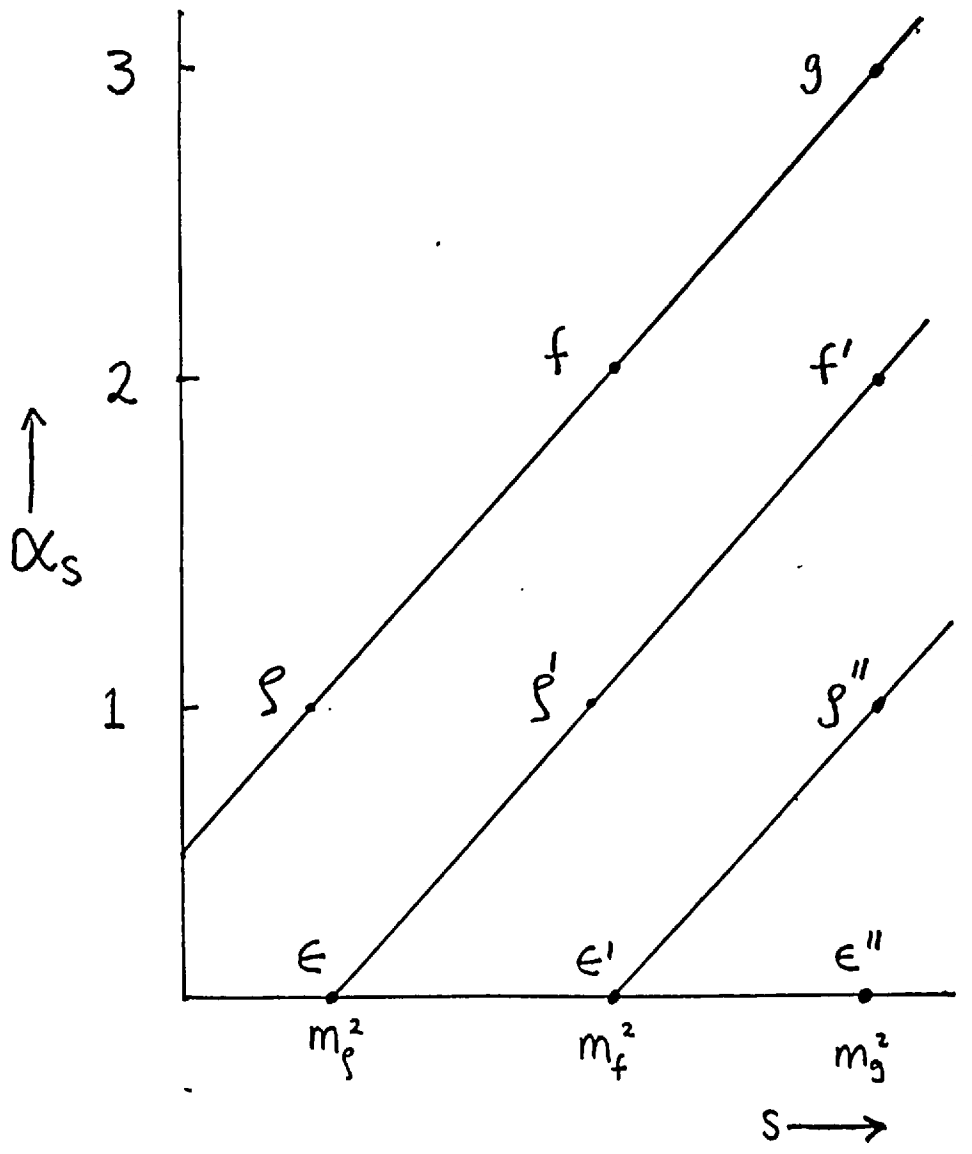

FIG. 5

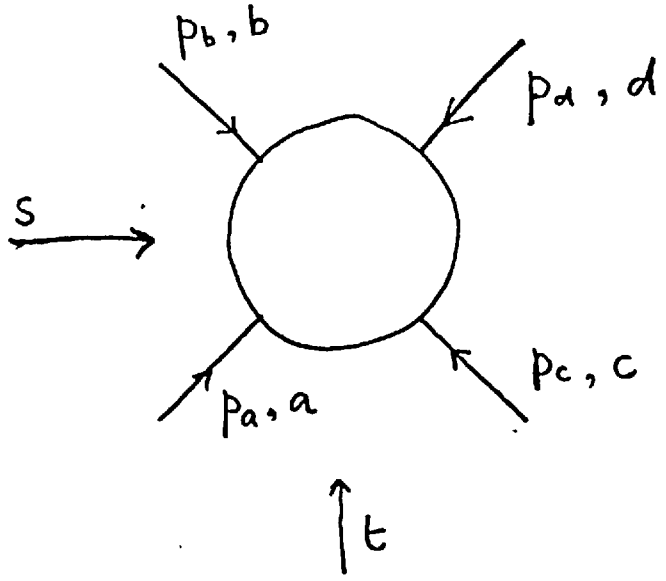

FIG. 6

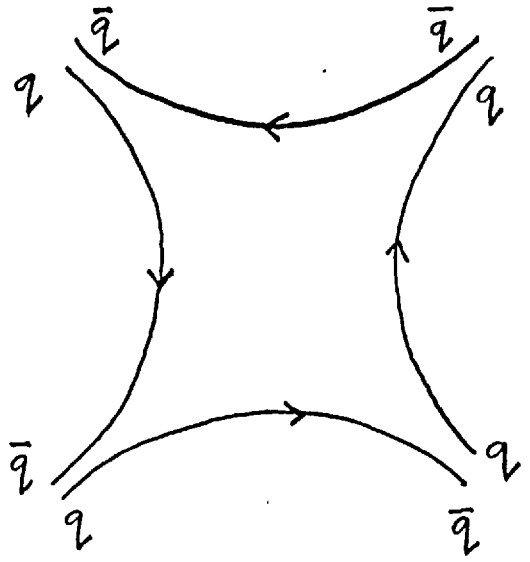

FIG. 7

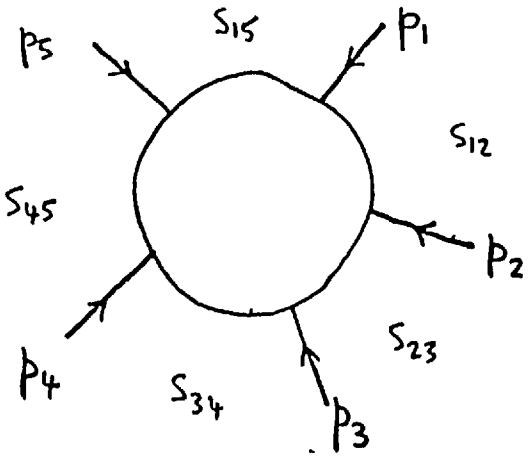

FIG. 8

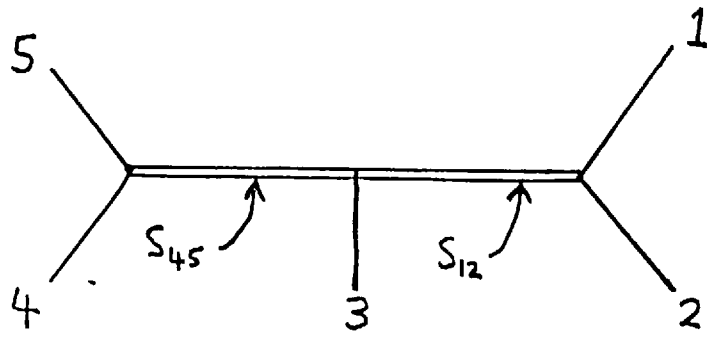

FIG. 9

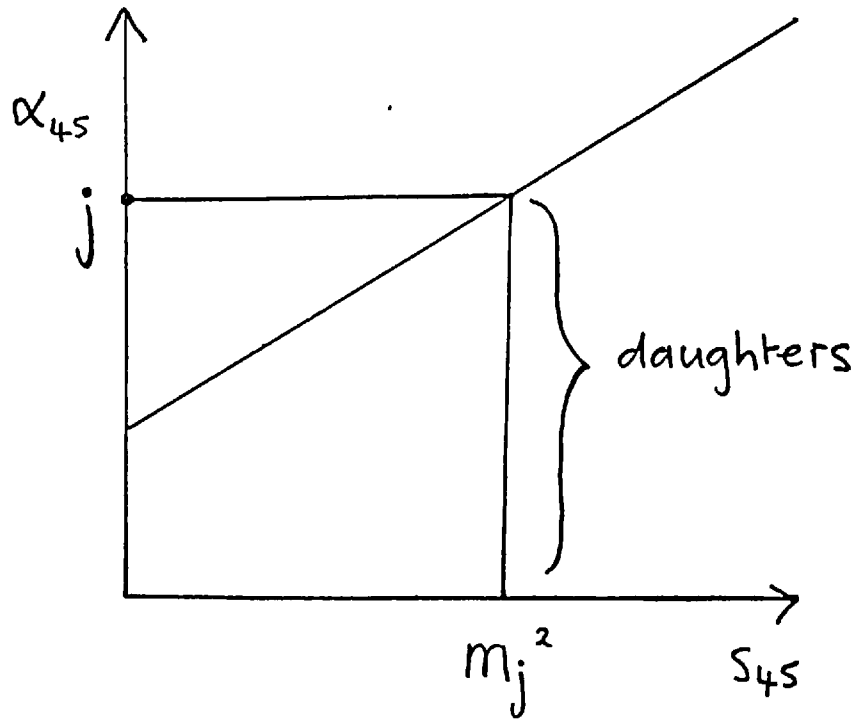

FIG. 10

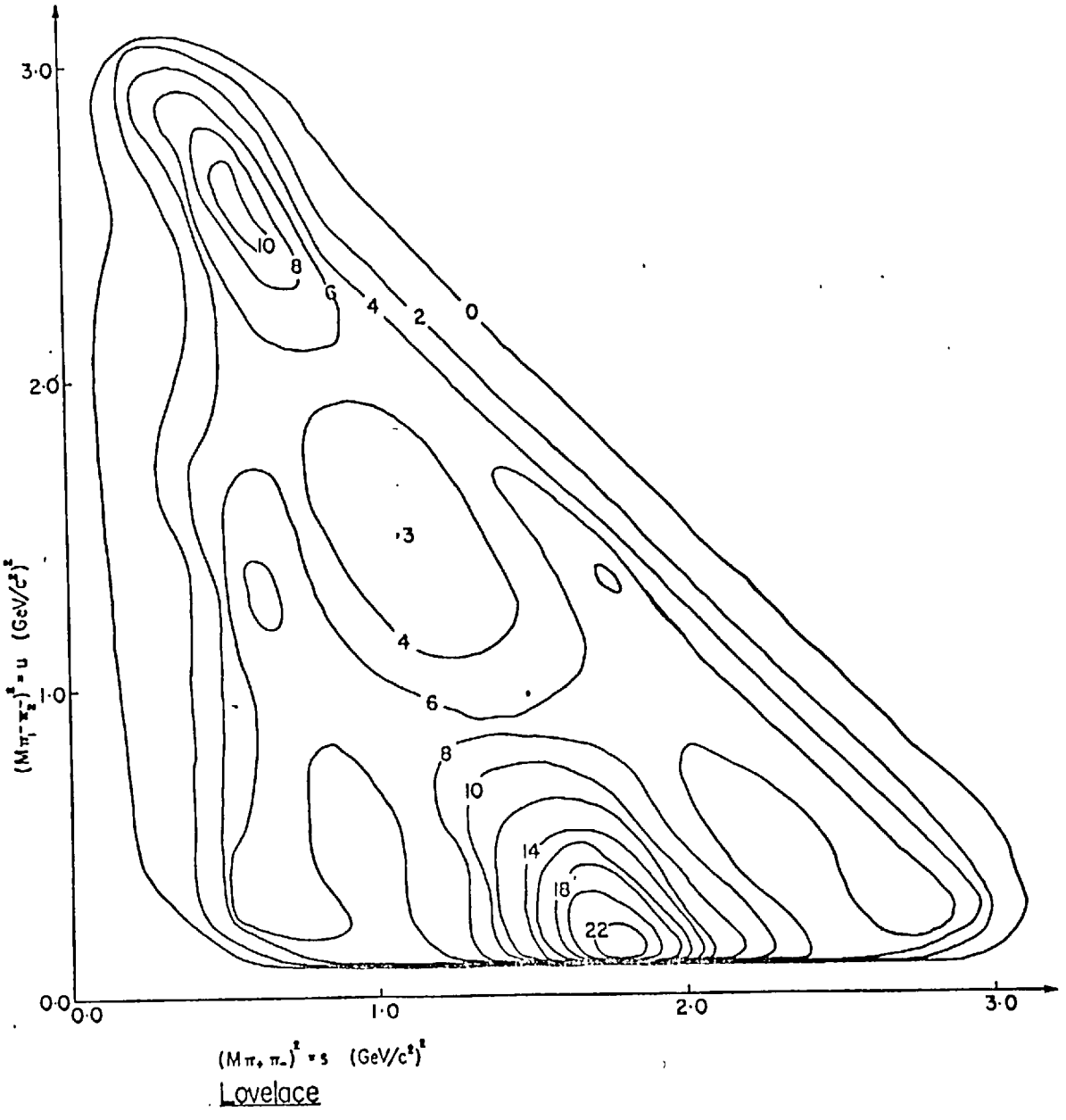
3·0
2·0
1·0
0·0
0·0
1·0
2·0
3·0
10
8
6
4
2
0
3
4
6
8
10
14
18
22
$(M\pi^+\pi^-)^2 = u$ (GeV/c²)²
$(M\pi_+\pi_-)^2 = s$ (GeV/c²)²
Lovelace

FIG.11 (a)

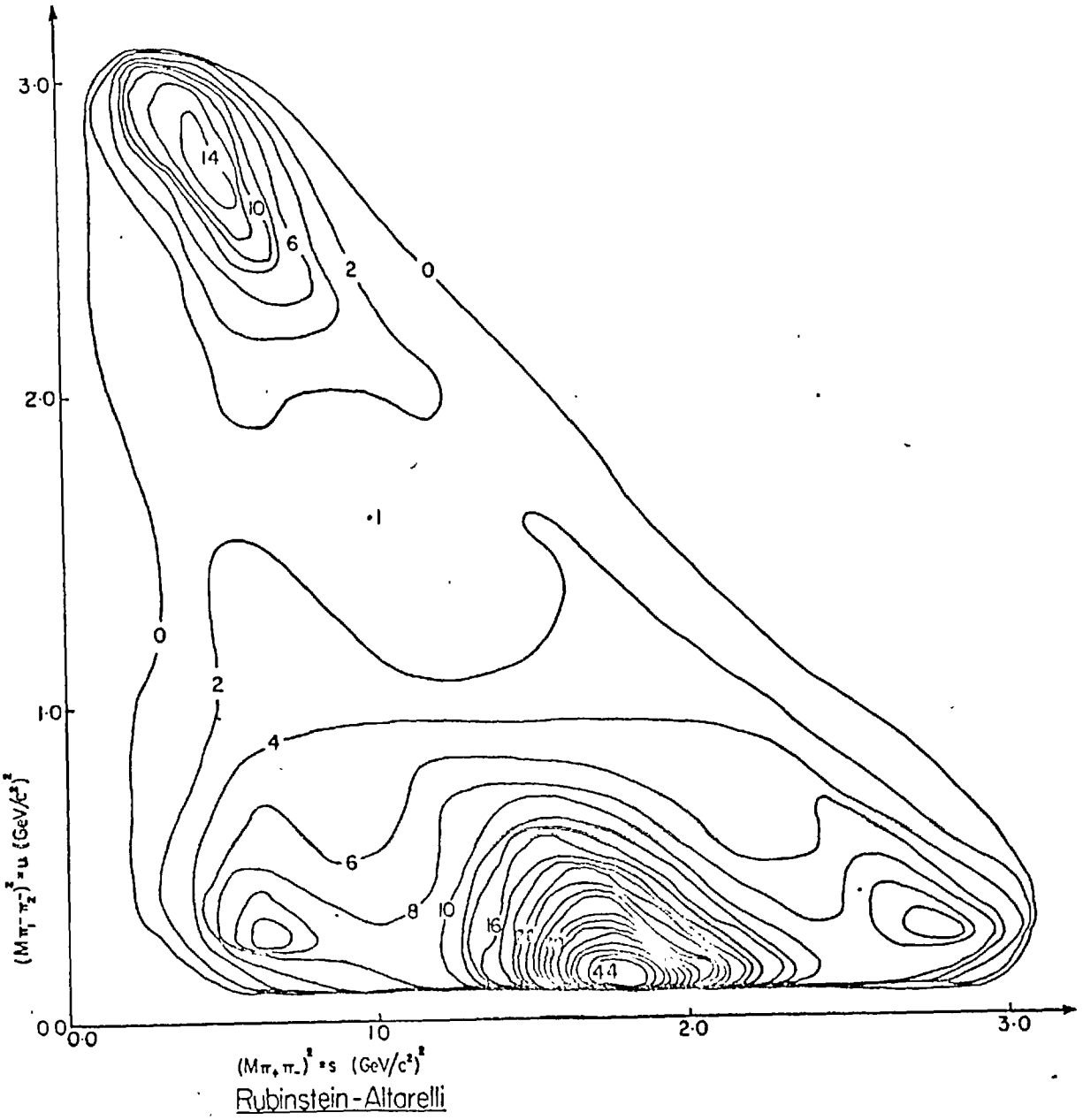
3·0
2·0
1·0
0·0
0
1·0
2·0
3·0
14
10
6
2
0
·1
0
2
4
6
8
10
16
44
$(M\pi_1^- \pi_2^-)^2 = u$ (GeV/c²)²
$(M\pi_+\pi_-)^2 = s$ (GeV/c²)²
Rubinstein-Altarelli

FIG. 11 (b)

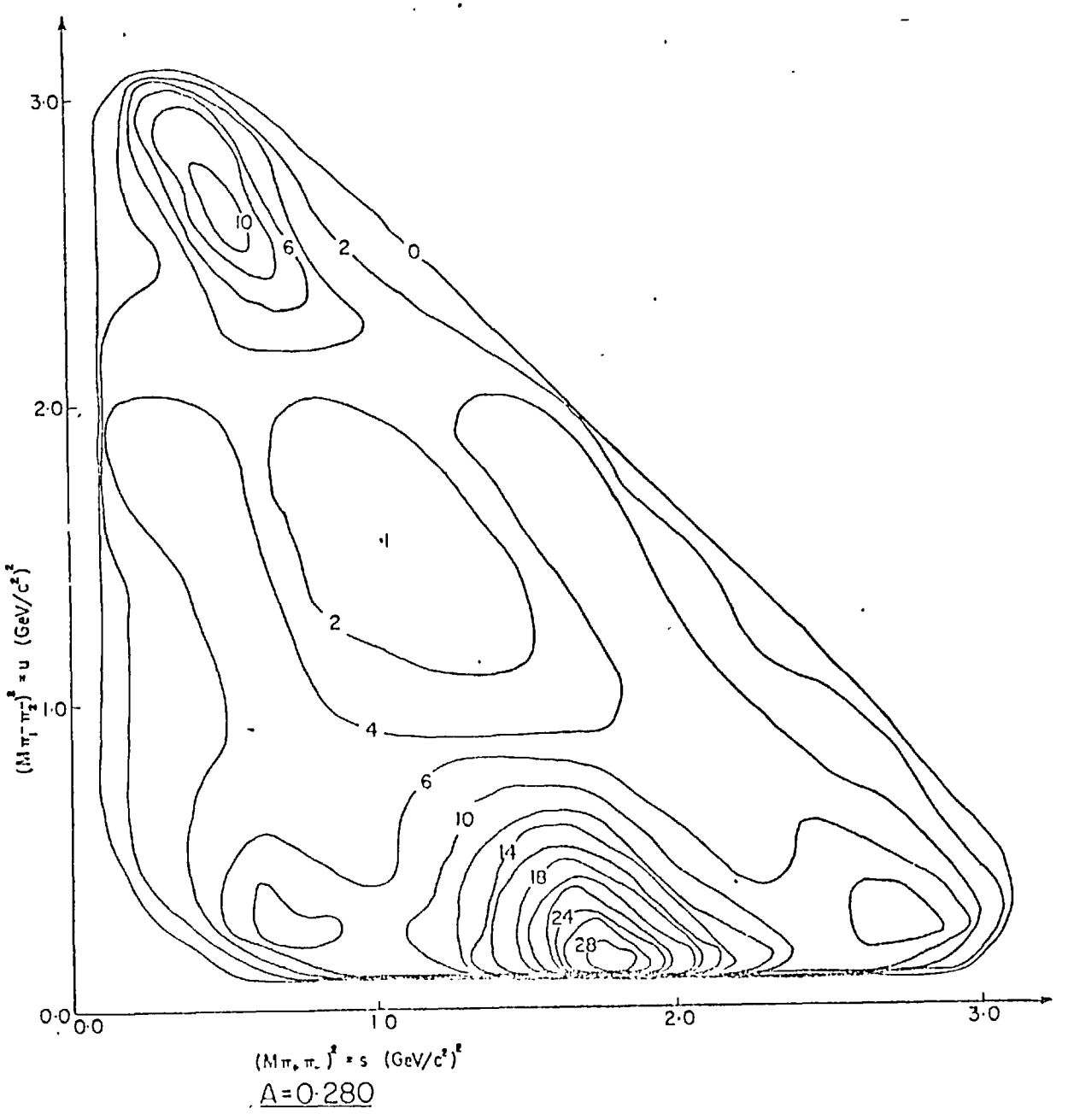
3·0
2·0
1·0
0·0
0·0
1·0
2·0
3·0
10
6
2
0
1
2
4
6
10
14
18
24
28
$(M\pi_1^-\pi_2^-)^2 = u$ (GeV/c²)²
$(M\pi_+\pi_-)^2 = s$ (GeV/c²)²
A=0·280

FIG.11 (c)

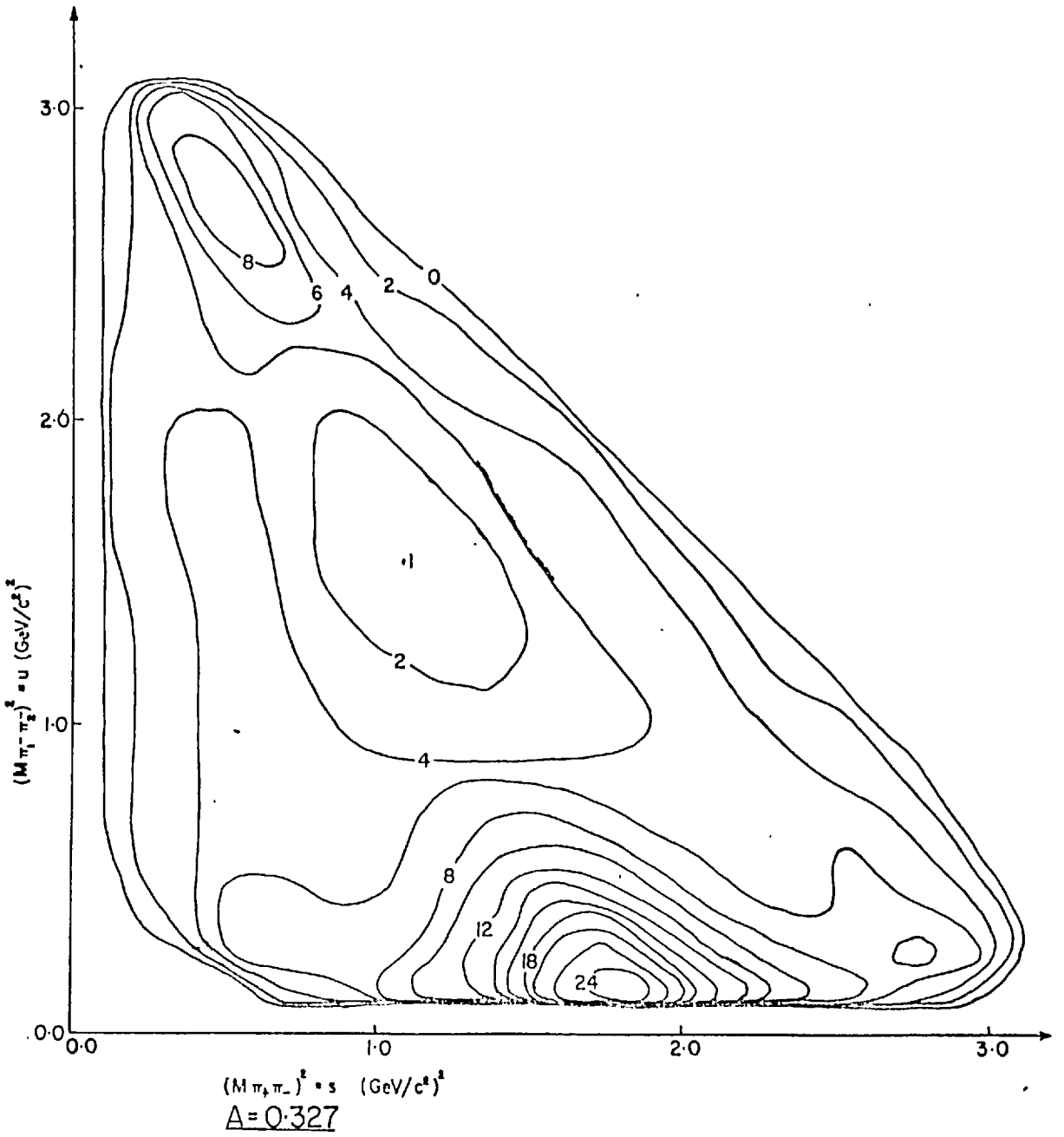
3·0
2·0
1·0
0·0
0·0
1·0
2·0
3·0
8
6
4
2
0
·1
2
4
8
12
18
24
$(M\pi_1^-\pi_2^-)^2$ • u (GeV/c²)²
$(M\pi_+\pi_-)^2$ • s (GeV/c²)²
A=0·327

FIG.11(d)

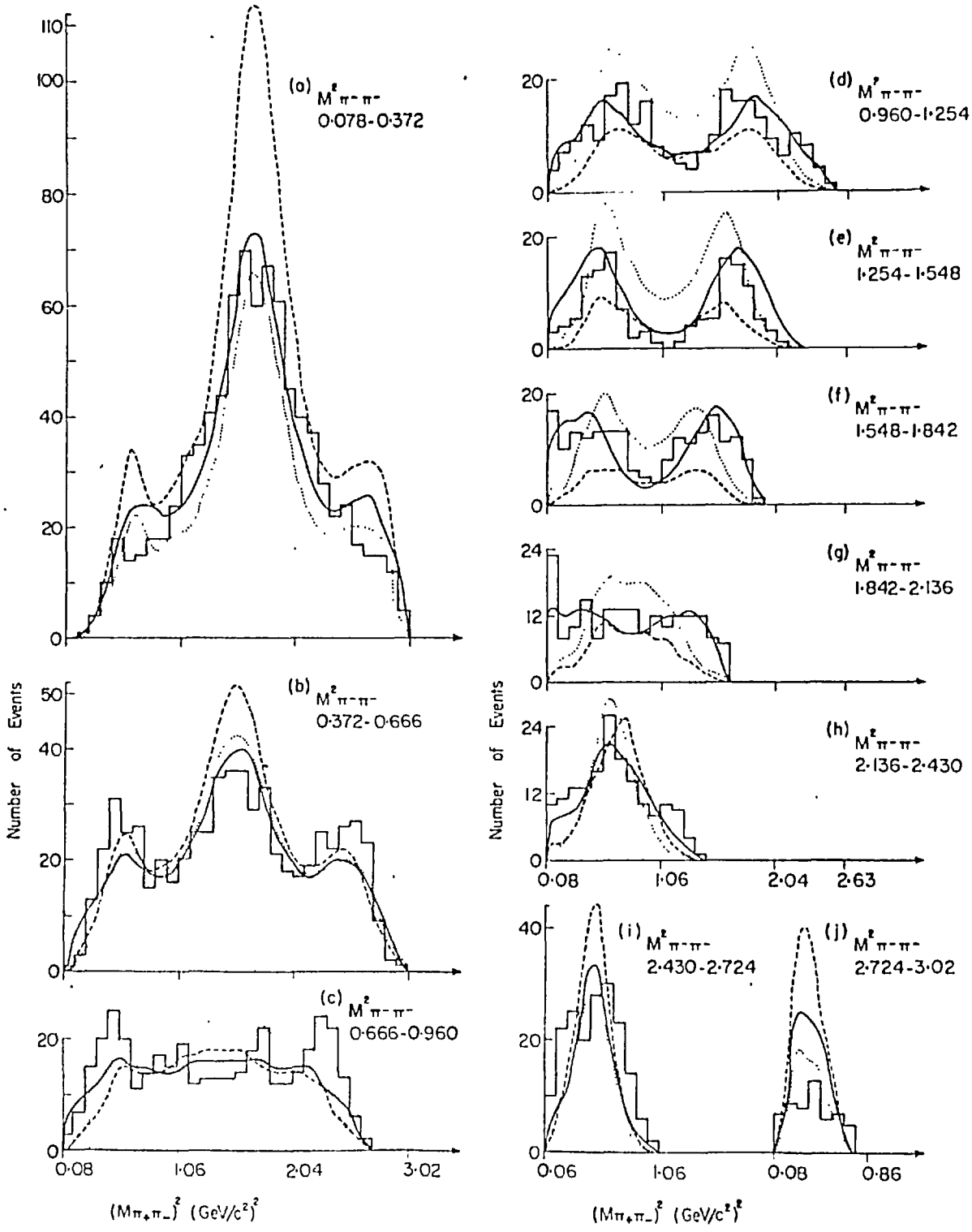
(a) M²π⁻π⁻ 0·078-0·372
(b) M²π⁻π⁻ 0·372-0·666
(c) M²π⁻π⁻ 0·666-0·960
(d) M²π⁻π⁻ 0·960-1·254
(e) M²π⁻π⁻ 1·254-1·548
(f) M²π⁻π⁻ 1·548-1·842
(g) M²π⁻π⁻ 1·842-2·136
(h) M²π⁻π⁻ 2·136-2·430
(i) M²π⁻π⁻ 2·430-2·724
(j) M²π⁻π⁻ 2·724-3·02
Number of Events
0·08
1·06
2·04
3·02
2·63
0·06
0·86
(Mπ₊π₋)² (GeV/c²)²

FIG. 12

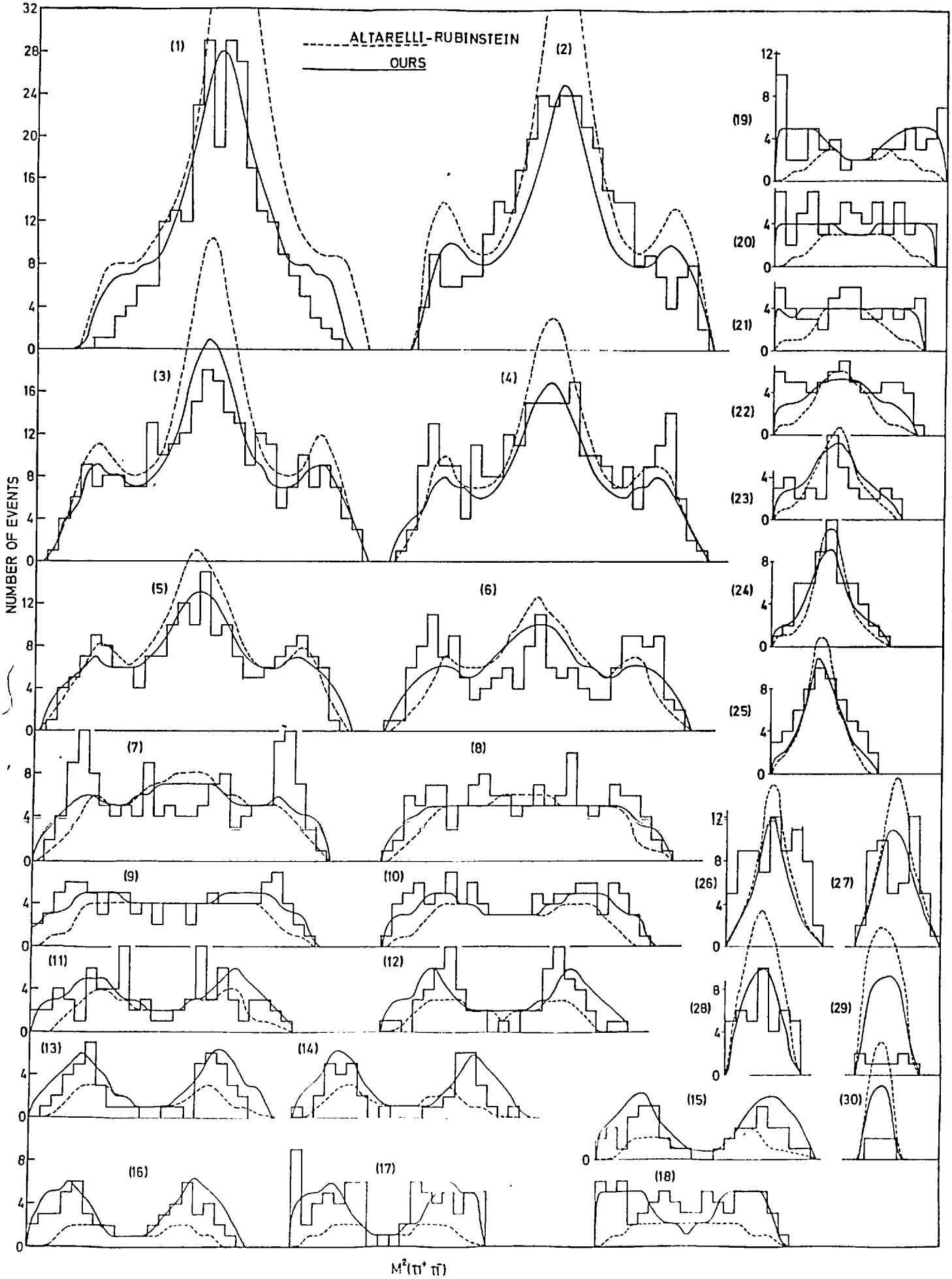
ALTARELLI-RUBINSTEIN
OURS
NUMBER OF EVENTS
$M^2(\pi^+\pi^-)$
(1)
(2)
(3)
(4)
(5)
(6)
(7)
(8)
(9)
(10)
(11)
(12)
(13)
(14)
(15)
(16)
(17)
(18)
(19)
(20)
(21)
(22)
(23)
(24)
(25)
(26)
(27)
(28)
(29)
(30)

FIG.13

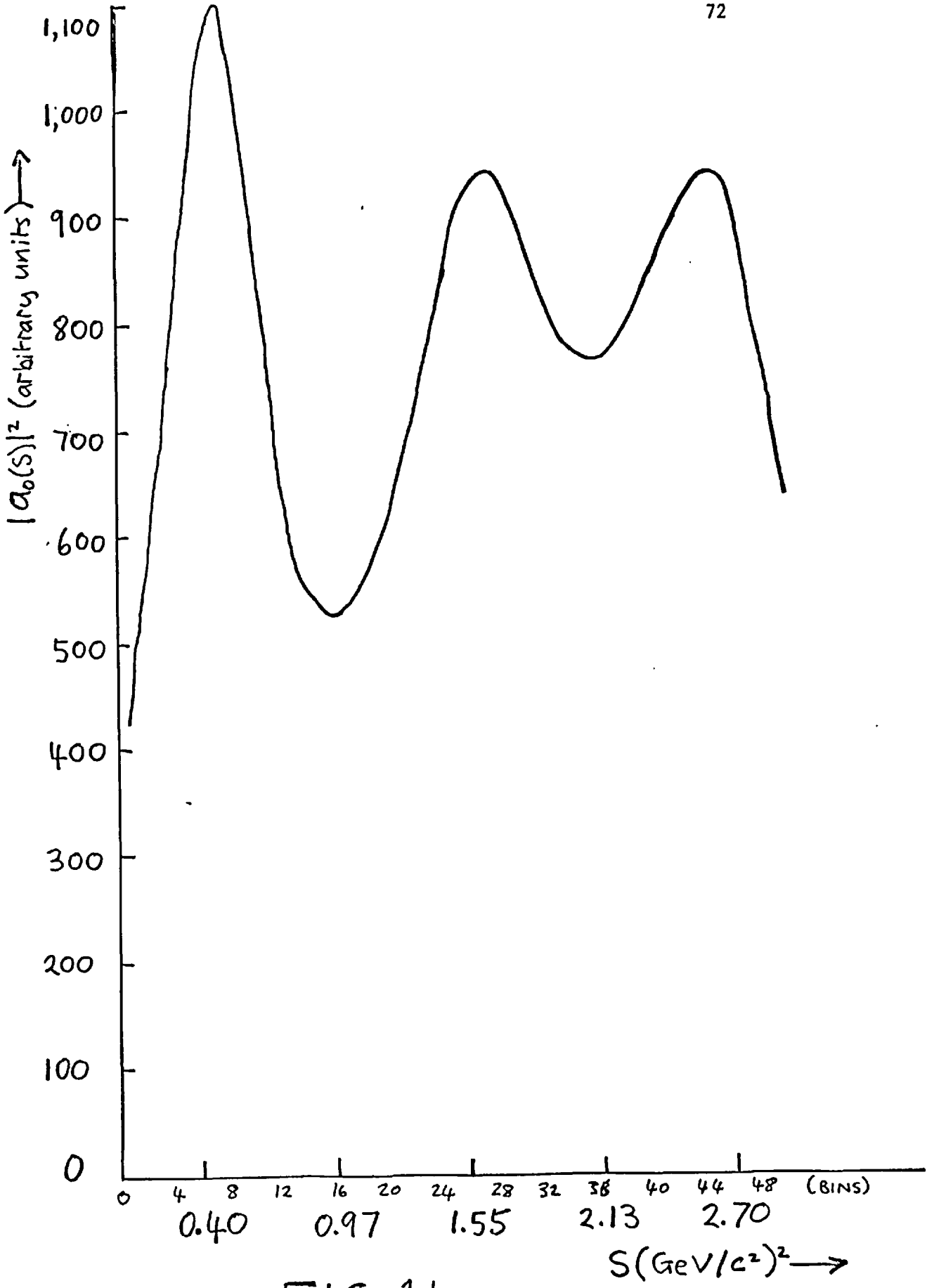
1,100
1,000
900
800
700
600
500
400
300
200
100
0
$|a_0(s)|^2$ (arbitrary units) ⟶
0 4 8 12 16 20 24 28 32 36 40 44 48 (BINS)
0.40 0.97 1.55 2.13 2.70
$s(GeV/c^2)^2$ ⟶

FIG. 14(a)

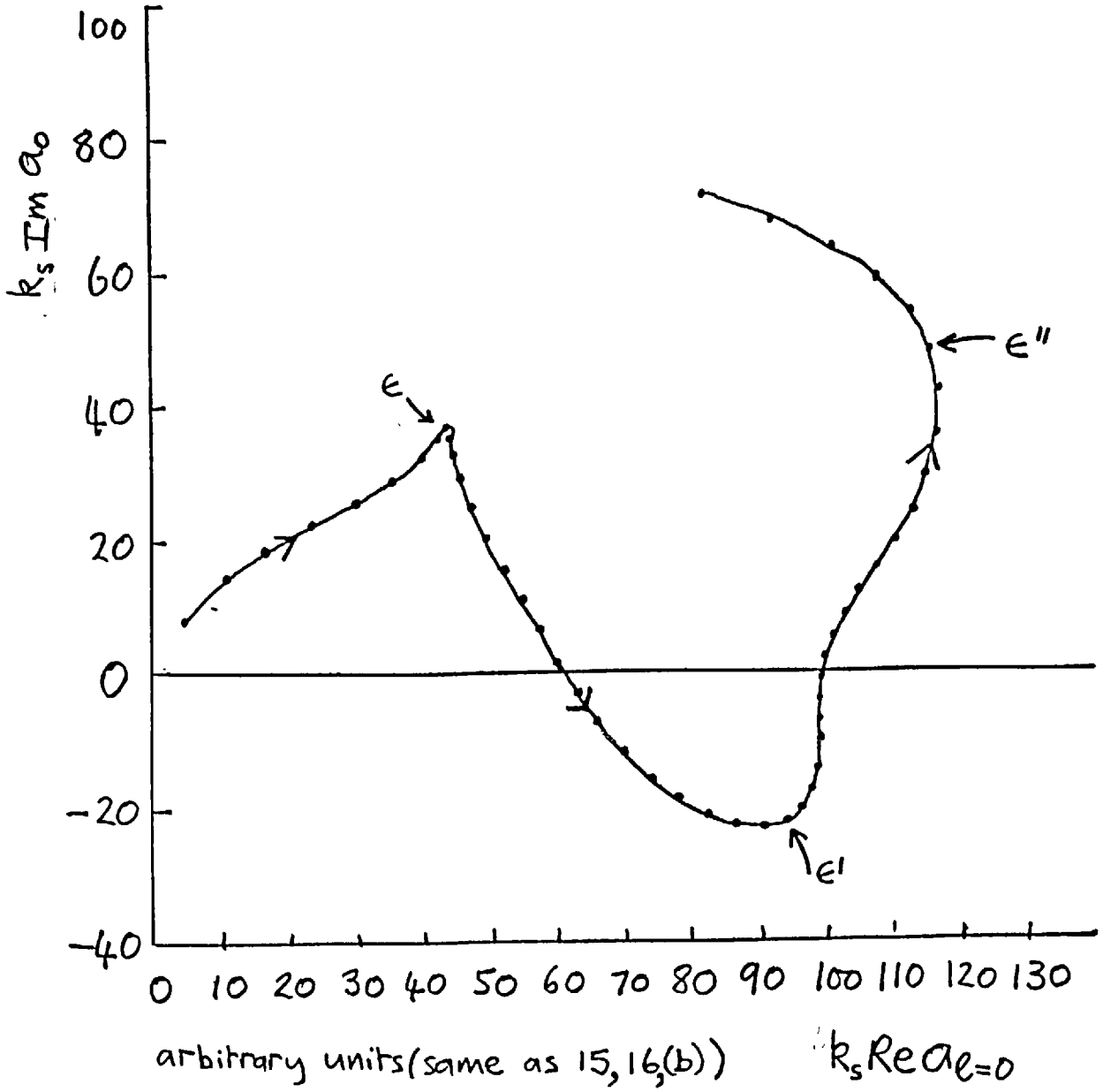
100
80
60
40
20
0
-20
-40
k_s Im a_0
0 10 20 30 40 50 60 70 80 90 100 110 120 130
arbitrary units (same as 15, 16(b))
k_s Re $a_{\ell=0}$
ϵ
ϵ''
ϵ'

FIG 14(b)

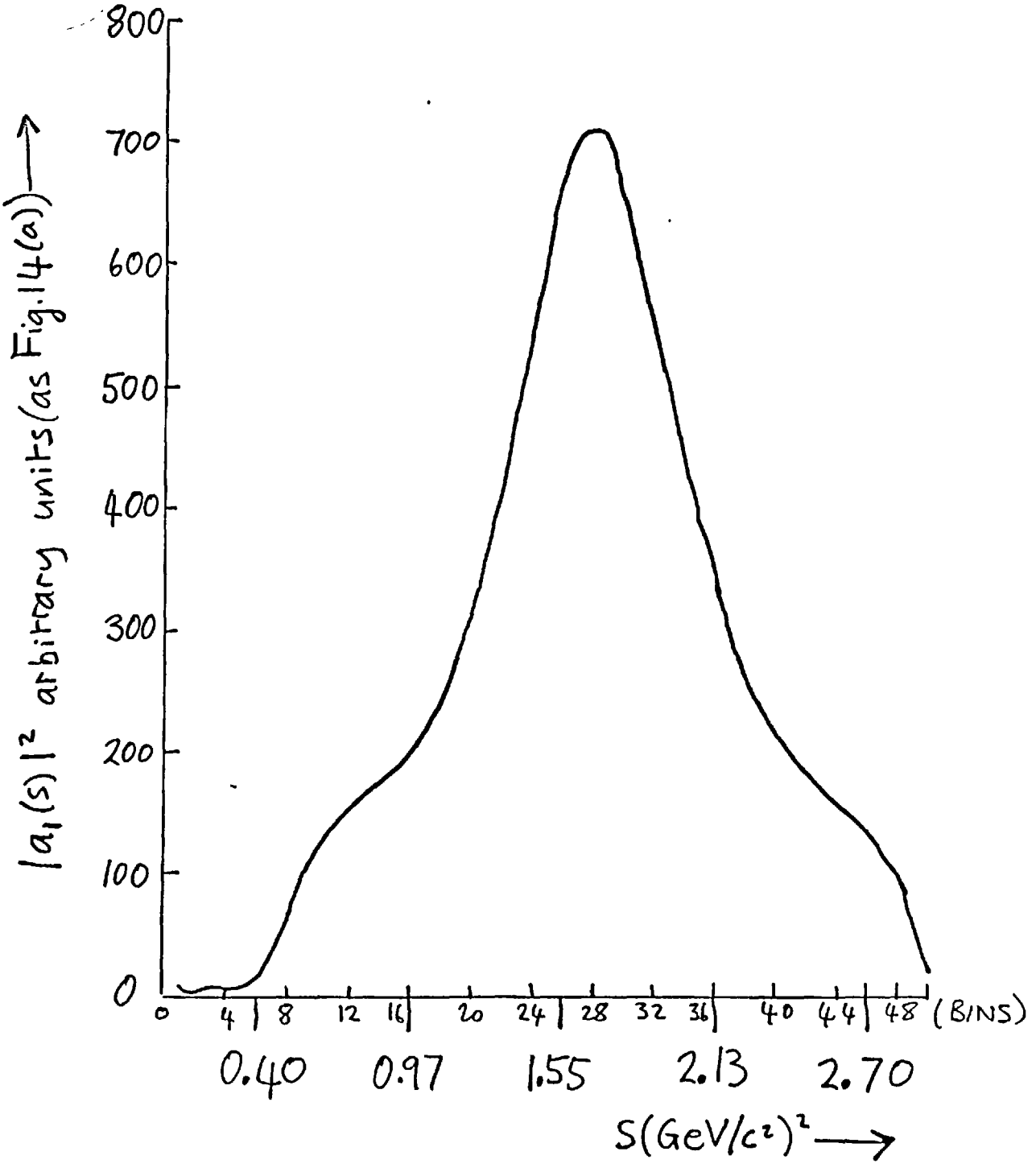
800
700
600
500
400
300
200
100
0
$|a_1(s)|^2$ arbitrary units (as Fig. 14(a)) ⟶
0 4 8 12 16 20 24 28 32 36 40 44 48 (BINS)
0.40 0.97 1.55 2.13 2.70
$s(GeV/c^2)^2$ ⟶

FIG. 15(a)

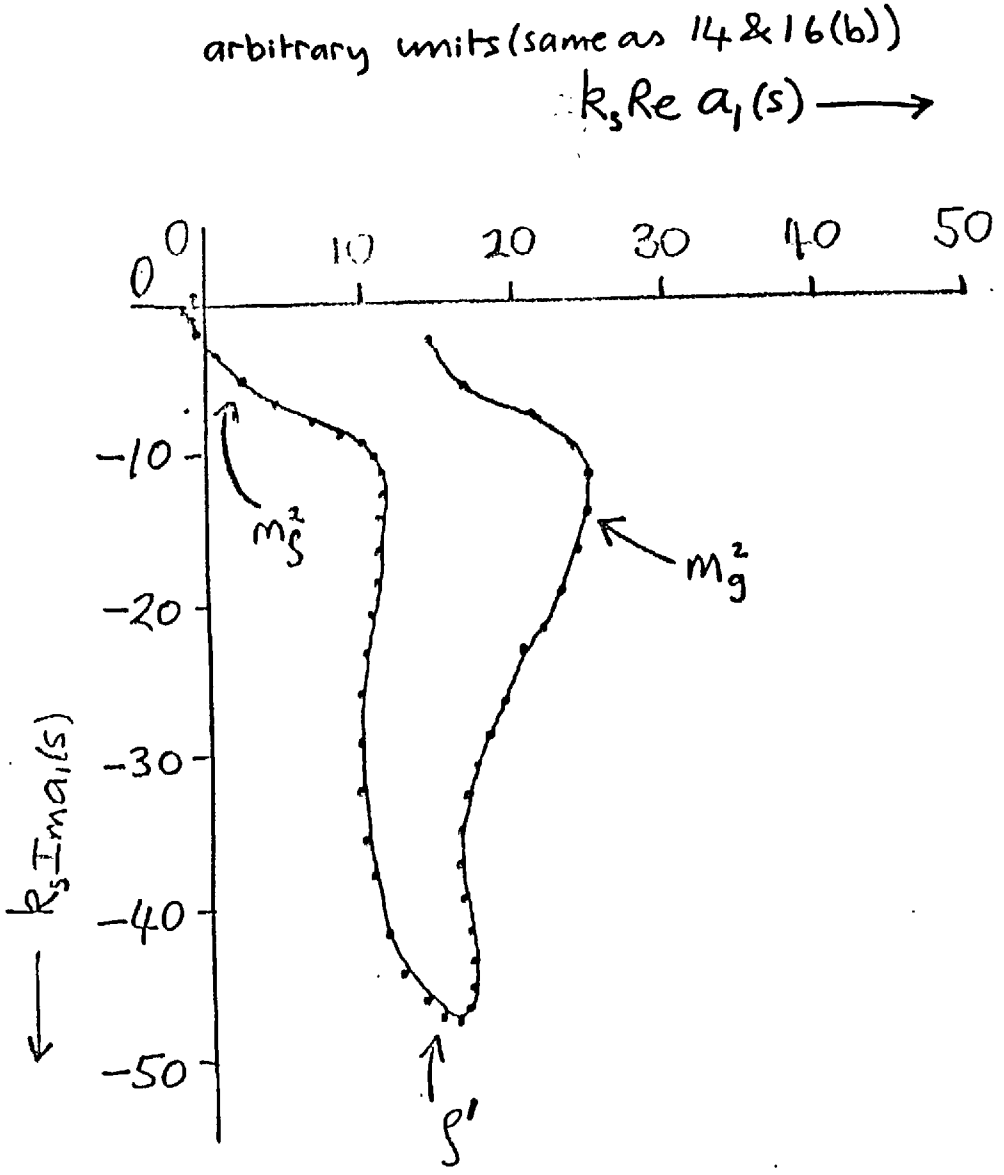
arbitrary units (same as 14 & 16(b))
$k_s Re\, a_1(s) \longrightarrow$
0
10
20
30
40
50
-10
-20
-30
-40
-50
$k_s Im\, a_1(s)$
m_s^2
m_g^2
s'

FIG. 15(b)

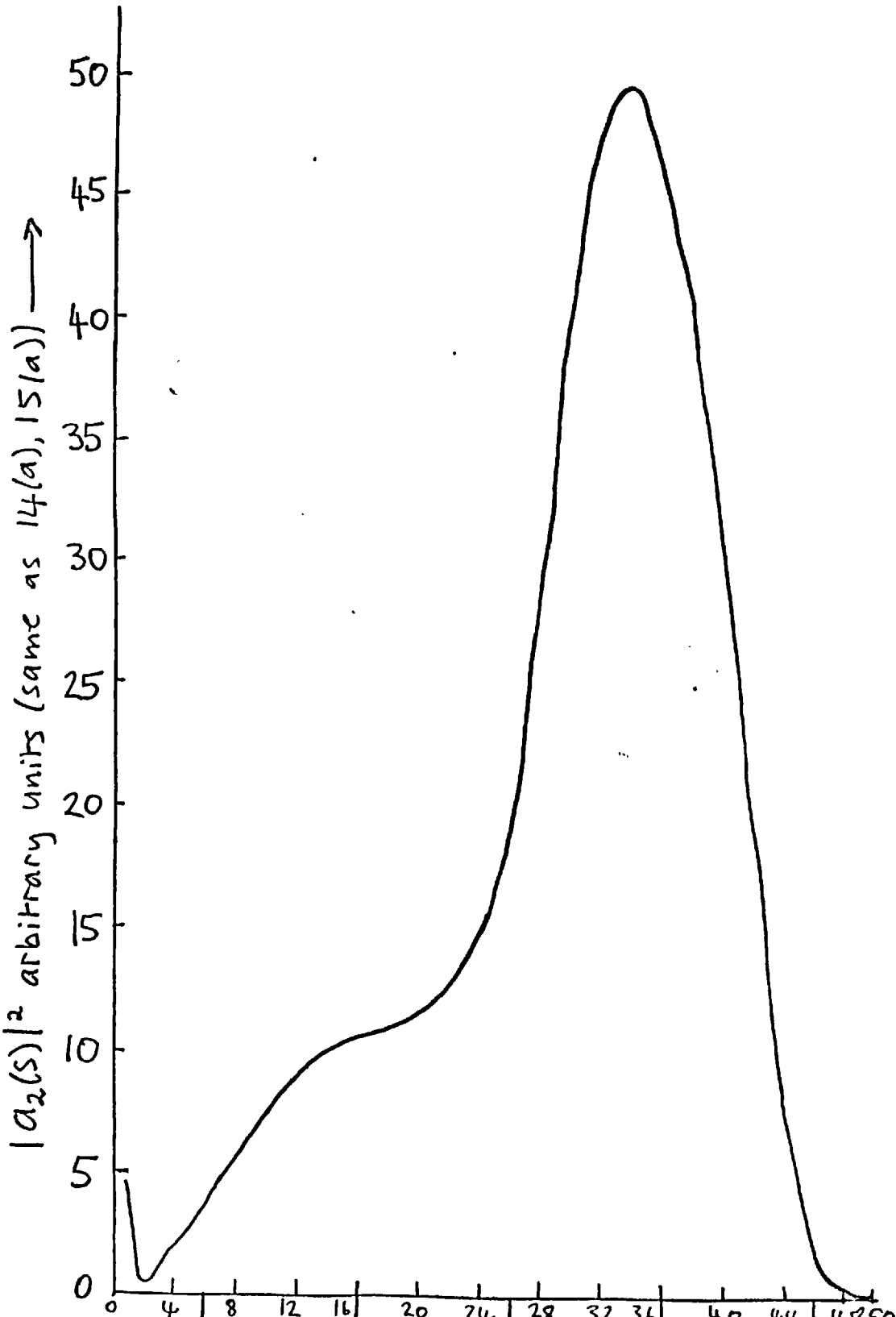
$|a_2(s)|^2$ arbitrary units (same as $|4(a), 15(a)|$) ⟶
0
5
10
15
20
25
30
35
40
45
50
0
4
8
12
16
20
24
28
32
36
40
44
48
50
0.40
0.97
1.55
2.13
2.70
s (GeV/c^2)^2 ⟶

FIG. 16(a)

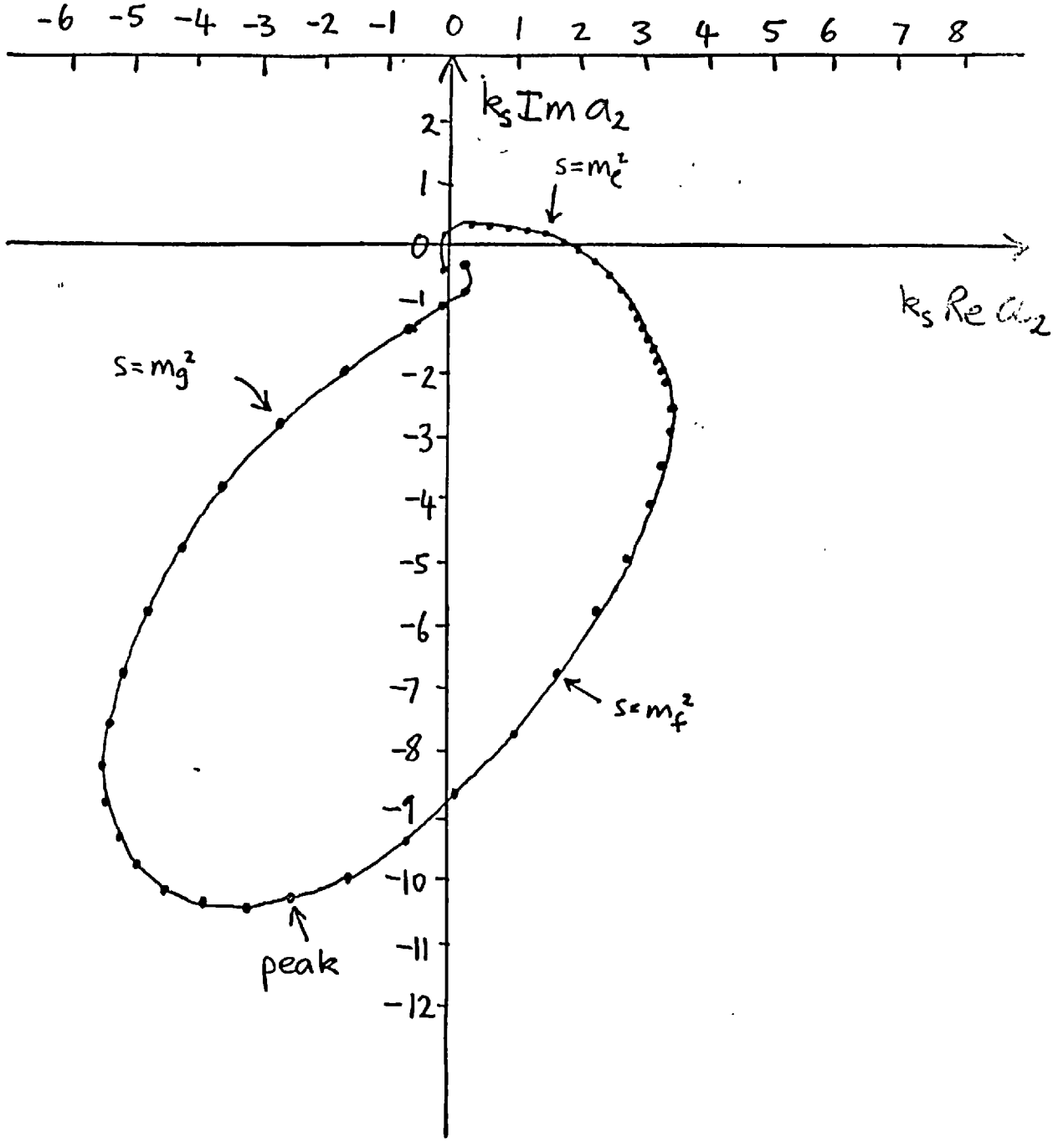
-6 -5 -4 -3 -2 -1 0 1 2 3 4 5 6 7 8
k_s Im a_2
2
1
0
-1
-2
-3
-4
-5
-6
-7
-8
-9
-10
-11
-12
$s=m_c^2$
k_s Re a_2
$s=m_g^2$
$s=m_f^2$
peak

FIG 16(b)

PART TWO

1 INTRODUCTION TO PART TWO

1-1 Over the last few years there have been important developments in the techniques for dealing with non-polynomial Lagrangians - in particular, Lagrangians which are rational or exponential functions of the fields[1,2]. These advances have enabled the gravitational interaction to be treated as a universal non-polynomial coupling[3]. Physically this corresponds to exchange of not one, two or any finite number of gravitons but to an indefinite number, whose propagation is described by a "superpropagator".

In quantum electrodynamics, inclusion of gravity has the effect of removing the ultra-violet divergences of the theory. The conventionally infinite quantities: self-mass (δm) and self-charge (δe) turn out to have finite, computable values[4,5]. The gravitational interaction has altered the small scale behaviour of the system such that the divergence encountered $\lim_{R\to 0} \log' \frac{1}{R}$ in x-space ; $\lim_{\Lambda\to\infty} \log\Lambda$ in p-space) is damped out.

A typical example of a matter-field in curved space-time is (for ϕ a spin-zero field)

$$\mathcal{L}_{matter} = g^{\mu\nu} \frac{\partial_\mu \phi \, \partial_\nu \phi}{\sqrt{-\det g^{\mu\nu}}} \qquad (1.1)$$

The metric tensor is conventionally parameterized as

$$g^{\mu\nu} = \eta^{\mu\nu} + \kappa_g \phi^{\mu\nu} \tag{1.2}$$

with

$$\eta^{\mu\nu} = \begin{pmatrix} 1 & & & \\ & -1 & & \\ & & -1 & \\ & & & -1 \end{pmatrix} \tag{1.3}$$

Alternative non-polynomial co-ordinates for the gravitons are exponential, e.g.

$$g^{\mu\nu} = \left[\exp \left(\kappa_g \gamma_{ab} \phi^{ab} \right) \right]^{\mu\nu} \tag{1.4}$$

where γ_{ab} are 4 x 4 pseudosymmetric matrices. With $g^{\mu\nu}$ as in (1.4) above,

$$\det g^{\mu\nu} = \exp \left(\kappa_g \phi^{a}{}_{a} \right) \tag{1.5}$$

The coupling constant κ_g (κ_g^2 is 8π times G, the Newtonian gravitational constant) which enters the theory, determines the numerical values of δe and δm. The regularizion induced by gravity provides an effective cut-off mass equal to κ_g^{-1}.

1-2 Conventional electrodynamics, of course, treats the infinities in δe and δm as unmeasurable. Just as the physically observable masses and charges are thus blind to the infinities, the numerical values predicted by gravity modifications are equally unobservable. In hadron physics, however, the existence of internal

symmetry breaking enables these quantities to be tested. The electromagnetic breaking of SU(2) (isospin) symmetry in pions will be considered here. It will be shown how inclusion of gravity removes the infinity occuring in a calculation of the $\pi^+ - \pi^0$ mass shift from a physically reasonable Lagrangian. This model will also be used to investigate the hypothesis of "strong" gravity[6]. Here, hadrons do not couple directly to gravitons, but only through their mixing with a massive spin-two meson in analogy with vector dominance (ρ -photon mixing).

1-3 Section 2 reviews the techniques involved in using non-polynomial Lagrangians. The applications to gravitation are sketched in Section 3. This includes the regularization of quantum electrodynamics naturally induced by gravity, "strong" gravity and an outline of the general procedure for including gravity into any given Lagrangian. Section 4 describes the calculation of the pion mass difference using a gravity-modified Lagrangian of pions, photons, vector and axial-vector mesons[7]. In the absence of gravity this Lagrangian gives a reasonable value for the pion mass difference only for massless pions; for physical pions, a logarithmic ultra-violet divergence occurs.

The numerical results of this calculation are presented and discussed in section 5. A mass difference of 6.9 MeV is obtained for massive pions - compared to the experimentally established value of 4.6 MeV. Extrapolation of coupling constant κ to tensor meson values gives a significantly lower value (between 4.0 and 6.0 MeV).

2 NON-POLYNOMIAL LAGRANGIAN THEORIES

This section will give an introduction to Non-Polynomial Lagrangian methods, sufficient only to motivate the computational technique used later. Full details of the technical problems encountered will be found in references 1, 2, 3 and 8.

2-1

Examples of non-polynomial Lagrangians of physical interest are not restricted to gravitational theories. Two popular examples are: firstly, the chiral SU(2) ⊗ SU(2) Lagrangian

$$\mathcal{L} = \frac{(\partial_\mu \phi)^2}{(1+f\phi^2)^2} \tag{2.1}$$

in Weinberg's representation. The second is the intermediate-boson mediated weak Lagrangian with Stückelberg variables A, B for the W-mesons

$$W_\mu = A_\mu + \frac{1}{m}\partial_\mu B \tag{2.2}$$

This can be shown to lead to a non-polynomial parameterization. The gravitational Lagrangian is

$$\mathcal{L}_{Einstein} = \frac{g^{\mu\nu}\left(\Gamma_{\mu\rho}{}^{\lambda}\Gamma_{\nu\lambda}{}^{\rho} - \Gamma_{\mu\nu}{}^{\lambda}\Gamma_{\lambda\rho}{}^{\rho}\right)}{\kappa^2\sqrt{-\det(g_{\mu\nu})}} \tag{2.3}$$

where

$$\Gamma_{\mu\nu}{}^{\lambda} = \tfrac{1}{2}\, g^{\lambda\rho}\left(\partial_\mu g_{\nu\rho} + \partial_\nu g_{\mu\rho} - \partial_\rho g_{\mu\nu}\right) \tag{2.4}$$

If $g^{\mu\nu}$ is the fundamental field, the covariant quantity $g_{\mu\nu}$ is intrinsically non-polynomial and vice-versa.

2-2 The general form of such theories is

$$\mathcal{L}_I(x) = g : V(\phi(x)) : = g \sum_{n=0}^{\infty} \frac{u_n}{n!} : \phi^n(x) : \tag{2.5}$$

where V is some function and u_n is proportional to f^n, f being the "minor" coupling constant. As Efimov points out[1] a calculation of the peturbation series in the "major" coupling constant g,

$$S = 1 + \sum_{n=1}^{\infty} g^n S_n \tag{2.6}$$

is not so easy since the usual concept that the small peturbation changes slightly the states of a free field is not relevant. Any formalism developed to use these Lagrangians must be able to cope both with the non-renormalizable infinities arising from $f^n \phi^n$ interactions in the expansion in minor coupling constant for $n > 4$, and possible unnacceptable high-energy behaviour. The first difficulty may be tackled by completely summing the peturbation series in f^n for any fixed order g^N by a direct summation method, for example, Borel summation.

The second difficulty may be seen in second order, taking elastic scattering via a superpropagator as an example.

The S-matrix

$$S_2 = \frac{i^2}{2!}\iint d^4x_1 d^4x_2 \cdot T^*\Big(V(\phi(x_1))\ V(\phi(x_2))\Big)$$

$$= \frac{i^2}{2!}\iint d^4x_1 d^4x_2 \sum_{m_1,m_2=0}^{\infty} F^{(2)}_{m_1m_2}(x_1-x_2) : \frac{\phi^{m_1}(x_1)}{m_1!}\frac{\phi^{m_2}(x_2)}{m_2!} : \tag{2.7}$$

with

$$F^{(2)}_{m_1m_2}(x_1-x_2) = \sum_{n=0}^{\infty} \frac{u_{n+m_1}\, u_{n+m_2}}{n!}\Big[\Delta_c(x_1-x_2)\Big]^n \tag{2.8}$$

Δ_c is the causal function,

$$\Delta_c(x) = \frac{1}{(2\pi)^4 i}\int d^4p\ \frac{e^{ip\cdot x}}{m^2-p^2-i\varepsilon} \tag{2.9}$$

The Fourier transform

$$\tilde{F}^{(2)}_{m_1m_2}(p^2) = i\int d^4x\, e^{ip\cdot x} F^{(2)}_{m_1m_2}(x) \tag{2.10}$$

for elastic scattering is $\tilde{F}^{(2)}_{22}(s)$, $s = p^2$ (Fig. 1).

The high-energy behaivour of the discontinuity across the branch cut at $s = 4m^2$

$$\rho_{22}(s) = \mathrm{Im}\, \tilde{F}^{(2)}_{22}(s) \tag{2.11}$$

enables field theories to be classified as "localizable" or "non-localizable" if $\rho(p^2)$ falls faster or slower than $e^{\sqrt{|p^2|}}$ respectively. For example, $\mathcal{L}_{INT}$ of the form $g : \phi^n e^{f\phi} :$ or $g : (\bar{\psi}\psi A) e^{f\phi} :$ are localizable, whereas $g : \phi^n (1+f\phi)^{-w}$ or $g : (\bar{\psi}\psi A)(1+f\phi)^{-w}$ $(w>0)$ are not. A physical consequence of localizability is that, provided a solution exists, on-mass-shell S-matrix elements from localizable Lagrangians are expected to show Froissart high-energy boundedness (see Ref. 9).

2-3 The definition of the Fourier transform (2.10) is made difficult by the singularity at $x = 0$ in $F^{(2)}_{m_1 m_2}(x)$. The Gel'fand-Shilov procedure for evaluating the Fourier transform of a distribution like $(1/x^2)^n$ may be illustrated by considering

$$\mathcal{L}_{exp} = g\,(e^{f\phi} - 1) \tag{2.12}$$

for which the "superpropagator" $S(x)$ is

$$S_{exp}(x) = \left\langle T\left(\mathcal{L}_{exp}(\phi(x))\, \mathcal{L}_{exp}(\phi(0)) \right) \right\rangle \tag{2.13}$$

Formally

$$S_{exp}(x) = g^2 \sum_{n=1}^{\infty} \frac{(f^2)^n}{n!} \left[\Delta(x)\right]^n \tag{2.14}$$

with $$\Delta(x) = \langle T\, \phi(x)\, \phi(0) \rangle = 1/x^2 \tag{2.15}$$

for massless particles. Take the Sommerfeld-Watson transform, namely

$$S_{exp}(x) = \frac{g^2}{2\pi i} \int_C \frac{dz}{\Gamma(z+1)} \frac{1}{\tan \pi z} \left[f^2 \Delta(x)\right]^z \tag{2.16}$$

The contour C encloses the positive real axis ($z < 1$ to ∞). Rotating the contour parallel to the imaginary axis, the Fourier transform may be carried out to give

$$\tilde{S}_{exp}(p) = \int_{0<Re\,z<1} dz\, (f^2)^z \left(\frac{1}{p^2}\right)^{2-z} \frac{\Gamma(2-z)}{\Gamma(z)\Gamma(z+1)\tan \pi z} \tag{2.17}$$

Fourier transforms are generally considered in Euclidean metrics ($p^2 < 0$) and the transition to the physical region made by analytic continuation.

2-4 For a rational (non-localizable) Lagrangian,

$$\mathcal{L}_{RAT} = : \frac{g}{1+f\phi} : \tag{2.18}$$

$$S_{RAT}(x) = g^2 \sum_{n=0}^{\infty} n! \left(f^2 \Delta(x)\right)^n \tag{2.19}$$

The Borel summation method uses the relation

$$n! = \int_0^{\infty} d\zeta \, e^{-\zeta} \zeta^n \tag{2.20}$$

to formally write

$$\begin{aligned} S_{rat}(x) &= g^2 \sum_{n=0}^{\infty} \int_0^{\infty} d\zeta \, e^{-\zeta} \left(f^2 \Delta(x) \zeta\right)^n \\ &= \int_0^{\infty} \frac{1}{1 - f^2 \Delta(x) \zeta} e^{-\zeta} d\zeta \end{aligned} \tag{2.21}$$

To define a physical superpropagator, this approach takes the principal value of the integral in the ζ-plane. The Gel'fand-Shilov method for $\tilde{S}_{RAT}$ then goes through in a similar way to $\tilde{S}_{EXP}$ (equations (2.14) to 12.17).

2-5 The use of distributions like $(1/x^2)^n$ leads to ambiguities coming into the above-mentioned techniques. For a full discussion, see Refs. 3,8. The resulting "b-ambiguity" means that in (2.17) one should really replace $\left[\frac{1}{\tan \pi z}\right]$ by $\left[\frac{1}{\tan \pi z} + b(z)\right]$ where b is arbitrary. Lehmann and Pohlmeyer[10] have shown that there

exist criteria by which one can satisfactorily eliminate such ambiguities from localizable theories. In rational Lagrangians, such as the one in (2-4), the "Borel ambiguity" in the principal value further complicates matters to prevent these criteria from being applied. The difficulty in the rational case is ascribed to normal ordering, [3] but not yet solved.

In the rational co-ordinates taken for the gravitational field in the following sections the non-localizability is taken as only apparent since exponential co-ordinates could just as well have been taken and the results expected to be equivalent. The rational form is taken in most the early gravitation work (e.g. References 4,5,6) since this arises most naturally out of the requirements of general relativity, but exponential co-ordinates (e.g. equation (1.4) are becoming increasingly popular. (e.g. Ref. 3). However, no rigorous equivalence theorem exists, though the mechanism for removal of infinities to be described later is basically the same. In either exponential or rational cases, the numerical results of preliminary calculations which estimate the magnitudes of gravitational effects are pretty much the same. Specifically, b is taken as zero.

3 QUANTUM GRAVITY AND INFINITIES

3-1 The recent revival of the idea that the non-polynomial coupling of gravity to matter may provide a damping of the infinities in field theory started with a demonstration of gravity-modified quantum electrodynamics by Isham, Salam and Strathdee[4,5]. As they point out, even classically, the electron self-mass (δm) is infinite. Lorentz's calculation gives $\delta m = e^2/R$ (R is the radius of the electron). For a point electron ($R \to 0$), δm is linearly infinite. Ref. 4 traces the subsequent history of this singularity. Using quantum electrodynamics Waller[11] showed Dirac's equation to give a quadratic infinity, but this was improved on by Weisskopf[12] using positron theory, which gave (to second order)

$$\frac{\delta m}{m} = \frac{6\alpha}{4\pi} \lim_{R \to 0} \log \frac{1}{Rm} \quad + \text{finite terms} \qquad (3.1)$$

$$\left(\alpha = \frac{e^2}{4\pi}\right)$$

The logarithmic infinity in (3.1) led him to suggest a critical length R_{crit} where the theory would need alterations

$$R_{crit} \approx \frac{1}{m} \exp\left(-1/\alpha\right) \approx 10^{-56}\ m^{-1} \qquad (3.2)$$

Subsequently, the well-known Feynman-Dyson procedure confirms this result, further introducing another infinite quantity self-charge (δe) — but δe and δm are seen to be unmeasurable quantities, so however unpalateable, their presence need cause no trouble. In hadron physics, though, electromagnetic breaking of internal symmetries opens up a way in which the infinite mass shifts are observable and measurable.

3-2 The standard way of introducing gravity into any theory is by the requirement that the equations of the theory be invariant under general coordinate transformations. In Lagrangian language this means that the action integral $\int d^4x \mathcal{L}(x)$ must be invariant under this group, implying that the Lagrange function must be constructed so that it transforms as a scalar density with weight $+1$. The "weight" W of a quantity $\mathcal{T}^{\mu\ldots}_{\nu\ldots}$ transforming as a tensor density under general co-ordinate transformation $x \rightarrow x'$ is defined by

$$\mathcal{T}'^{\mu\ldots}_{\nu\ldots} = \left|\frac{dx}{dx'}\right|^W \frac{\partial x'^{\mu}}{\partial x^{\rho}} \cdots \frac{\partial x^{\sigma}}{\partial x'^{\nu}} \cdots \mathcal{T}^{\rho\ldots}_{\sigma\ldots}$$

where $|dx/dx'|$ is the Jacobean of the transformation. Tensors are tensor densities of weight zero.

A Lagrangian of weight -1 can be generated from any Lorentz invariant one by the following rules. Firstly, replace the Minkowski metric, $\eta^{\mu\nu} = diag(1, -1, -1, -1)$, wherever it appears in the Lagrangian, by the Einstein metric, $g^{\mu\nu}(x)$. Secondly, replace

the ordinary derivatives of the fields by the standard covariant derivatives of general relativity. Finally, adjust the total weight of each term in the Lagrangian to -1 by adjoining to each a factory $|\det g_{\mu\nu}|^{-\frac{w}{2}}$ which transforms as a Lorentz scalar with weight w. The crucial point about this last step is that it renders the new Lagrangian automatically non-polynomial. To the Lagrangian generated by means of these rules it is of course necessary to add a purely gravitational term. The graviton field $\phi^{\mu\nu}(x)$ is defined by

$$\kappa\,\phi^{\mu\nu}(x) = g^{\mu\nu}(x) - \eta^{\mu\nu} \tag{3.3}$$

so that $g^{\mu\nu}$ reduces to the flat space metric, $\eta^{\mu\nu}$, as $\phi^{\mu\nu} \to 0$ It has been established[5] that the scalar gravity replacement

$$\phi^{\mu\nu} \longrightarrow \eta^{\mu\nu}\,\phi \tag{3.4}$$

and so $$|\det g_{\mu\nu}| \longrightarrow \frac{1}{(1+\kappa\phi)^4} \tag{3.5}$$

gives numerical results essentially the same as tensor gravity, and use of the scalar field $\phi(x)$ is a very convenient simplification. Denoting the fields in the original Lagrangian by $A_\alpha(x)$, the overall modification now reads:

$$\mathcal{L}(A_\alpha, \partial_\mu A_\beta, \eta^{\nu\sigma}) \longrightarrow$$
$$\mathcal{L}\left(A_\alpha(1+\kappa\phi)^{-2w_\kappa},\ D_\mu A_\beta\,(1+\kappa\phi)^{-2w_\beta},\ \eta^{\nu\sigma}(1+\kappa\phi)^{-2}\right)$$
$$+\ \mathcal{L}(\text{gravity}) \tag{3.6}$$

W_α is the weight of the field A_α, D_μ is the appropriate covariant derivative.

3-3 The calculation of a finite δe and δm with a graviton-electron-photon Lagrangian was partly motivated by the results of Glimm and Jaffe[13], whose field-theory models suggested that some of the infinities could well be intrinsic to the type of Lagrangian considered, and not just ascribed to technicalities involved in an expansion about $e = 0$. If this were generally true, it would be essential to introduce a fundamental interaction effective at small distances ($\sim R_{crit}$). It is an old idea to propose gravity to remove light-cone singularities since zero-point field functuations of quantum gravity might cause a smearing of the light-cone, the definition of which is gravity-dependent in any theory of light and matter propagating in a gravitational field.

The minimal modification to the Dirac Lagrangian

$$\mathcal{L}_D = e\,\bar{\Psi}\,\gamma_\mu\,\Psi\,A_\mu \tag{3.7}$$

(Ψ and A_μ are electron and photon fields respectively) taken in reference 4 is

$$\mathcal{L}_G = e\,\frac{\bar{\Psi}\,\gamma_\rho\,A^\rho\,\Psi}{\left|\det\left(\eta^{\mu\nu}+\kappa_g\,\phi^{\mu\nu}\right)\right|} \tag{3.8}$$

The tensor gravity calculation[5] gives essentially the same results as a simplified treatment with

$$\mathcal{L}_G = e\,\frac{\bar{\Psi}\,\gamma_\mu\,A^\mu\,\Psi}{\left(1+\kappa_g\,\phi(x)\right)} \tag{3.9}$$

The corresponding Feynman graphs are shown in Fig. 2. Evaluating this with the non-polynomial techniques described in section 2 - namely the Borel summation of paragraph 2-4, with $f = \kappa_g$ - one obtains

$$\left(\frac{\delta m}{m}\right)_G \propto e^2 \int_0^\infty \frac{d(x^2)}{x^2 + \kappa_g^2 \zeta} e^{-\zeta} d\zeta \tag{3.10}$$

Without gravity one would have had the logarithmic infinity

$$\frac{\delta m}{m} \propto e^2 \lim_{R \to 0} \int_{|x| \geq R} \frac{d^4x}{(x^2)^2} \tag{3.11}$$

In fact,

$$\left(\frac{\delta m}{m}\right)_G = \frac{6\alpha}{4\pi} \log \frac{4\pi}{\kappa m} + \text{terms of order } \alpha \text{ and } \kappa\alpha$$

$$\sim \frac{2}{11} \tag{3.12}$$

with $\kappa_g = \left((2.2) \times 10^{-22}\right)\ m^{-1}$.

With an eye to possible more fundemental developments, it is often noted that the cut-off appears to come at a length related to the Schwarzschild radius of the electron, $R_{Schwartz}$ since cut-off $\sim \kappa \sim R_{Schwartz}/m\kappa$. No real discussion of any reason for this has yet been put forward.

3-4 "Strong gravity" is an extension of the concepts discussed so far, and thought to be more applicable to strong interactions. The separation of hadron from lepton electrodynamics occurs in the vector dominance model. The photon interacts directly with leptons but only indirectly with hadrons through a mixing of γ with the $\rho - \omega - \phi$ combination. It has been hypothesised[6] that analogously, the graviton couples only indirectly with hadrons, through a mixing of gravitons with massive spin-two strongly-interacting mesons. One would obtain cut-offs for ultra-violet infinities in a similar manner to that described already - with the role of Einstein's gravity played by the massive tensor mesons. The coupling constant κ_m, analogous to κ_g, would now be much larger - to within an order of magnitude, equal to the inverse of the mass of the tensor meson. In this case the cut-off comes at $\kappa_m^{-1} \approx$ a few BeV - similar to that used arbitrarily in strong interaction physics. However, the terms of order κ and κ_m, too small to be considered in the "weak" gravity case, will now not be negligible for such a large κ.

The implications of this hypothesis go further than just damping infinities. In strong interaction physics, a theory is envisaged[6,14] in which tensor mesons universally couple to the hadronic stress tensor (based on Einstein's equation for weak gravity:

$$G_{\mu\nu} \equiv R_{\mu\nu} - \tfrac{1}{2} g_{\mu\nu} R = -\frac{\kappa_g^2}{2} T_{\mu\nu} \qquad (3.13)$$

where $R = g^{\mu\nu} R_{\mu\nu}$, $R_{\mu\nu}$ is the contraction $R^{\alpha}{}_{\mu\alpha\nu}$ of the curvature tensor

$$R^{\beta}{}_{\mu\kappa\nu} = \Gamma^{\beta}{}_{\mu\kappa,\nu} - \Gamma^{\beta}{}_{\mu\nu,\alpha} + \Gamma^{\beta}{}_{\lambda\nu}\,\Gamma^{\lambda}{}_{\mu\alpha} - \Gamma^{\beta}{}_{\lambda\alpha}\,\Gamma^{\lambda}{}_{\mu\nu} \tag{3.14}$$

and $T_{\mu\nu}$ is the energy-momentum tensor.) Speculations[3] range from using strong gravity to work out general relativity geometry inside hadronic matter, to the prevention of "gravitational collapse" in objects on a cosmological scale.

The possibility of a "strong coupling" for gravity is considered in addition to ordinary gravity in the following.

4 THE π^+-π^0 MASS DIFFERENCE WITH GRAVITY

4-1 The internal SU(2) symmetry of pions is broken by the electromagnetic interaction. A physically reasonable theory of this mass shift exists, but which nevertheless gives an infinite result. The Lagrangian into which gravity will be inserted is that of Lee and Nieh[15]. Whereas for soft pions they obtain a result close to that observed experimentally, for massive pions the mass difference becomes logarithmically divergent. The same result was obtained independently by Wick and Zumino[16] and is the same as that from current algebra[17].

Lee and Nieh[15] construct a phenomenological Lagrangian appropriate to the group SU(2) X SU(2) which includes pions, ρ mesons and axial vector mesons (A_1 mesons). The $\pi^+ - \pi^0$ mass difference is then calculated to order e^2 by considering all the tree diagrams for the process $\pi^+ + \rho^0 \to \pi^+ + \rho^0$ and closing the $\rho^0 - \gamma - \rho^0$ loop as shown in Fig. 3. The relevant vertices are given by

$$
\begin{aligned}
\mathcal{L} = & -g\, f_\mu \cdot (\underline{\pi} \times \partial_\mu \underline{\pi}) \\
& + \tfrac{1}{2} g (\sqrt{2} m_\rho)^{-2} (\partial_\mu f_\nu - \partial_\nu f_\mu) \cdot \partial_\mu \underline{\pi} \times \partial_\nu \underline{\pi} \\
& + \tfrac{1}{2} g^2 (f_\mu \times \underline{\pi})^2 \\
& - \tfrac{1}{2} g (\sqrt{2} m_\rho)^{-1} (\partial_\mu \underline{a}'_\nu - \partial_\nu \underline{a}'_\mu) \cdot (\partial_\mu f_\nu - \partial_\nu f_\mu) \times \underline{\pi} \\
& - \tfrac{1}{2} g (\sqrt{2} m_\rho)^{-1} (\partial_\mu f_\nu - \partial_\nu f_\mu) \cdot (\underline{a}'_\mu \times \partial_\nu \underline{\pi} - \underline{a}'_\nu \times \partial_\mu \underline{\pi})
\end{aligned}
$$

$$-\tfrac{1}{4} g^2 (\sqrt{2}\, m_\rho)^{-2} \left[(\partial_\mu f_\nu - \partial_\nu f_\mu) \times \underline{\pi} \right]^2$$
$$+ (e/g)\, m_\rho^2\, \rho^0_\mu\, A_\mu$$

(4.1)

where A_μ, $\underline{\pi}$, f_μ and $\underline{a}'_\mu$ denote the photon, pion, ρ-meson and A_1 fields respectively; m_ρ is the mass of the ρ-meson.

For zero mass pions ($\mu^2 \to 0$), the answer is finite and in reasonable agreement with experiment

$$\mu^2(\pi^+) - \mu^2(\pi^0) \equiv \delta\mu^2 = \frac{3\alpha}{4\pi} \cdot m_\rho^2 \cdot 2\ln 2 \qquad (4.2)$$

which gives the mass difference $\delta\mu = 5.0$ MeV, the experimentally-determined value being 4.6 MeV. When the pions are massive, however, ($\mu^2 \neq 0$) the calculated mass shift is logarithmically divergent. To order $(\mu/m_\rho)^2$

$$\delta\mu^2 = \frac{3\alpha}{4\pi} m_\rho^2 \left\{ 2\ln 2 + \frac{\mu^2}{m_\rho^2} \left[\ln \frac{m_\rho^2}{\mu^2} + \frac{19}{4} \ln 2 - \frac{5}{2} + \frac{1}{8} \ln \frac{\Lambda^2}{m_\rho^2} \right] \right\}$$

(4.3)

where Λ is the ultra-violet cut-off momentum. This relation may be expressed in the form

$$\delta\mu = 6.0\ \text{MeV} + \frac{3\alpha}{4\pi} \frac{\mu}{8} \ln \frac{\Lambda}{m_\rho} \qquad (4.4)$$

It is this logarithmic infinity which it is hoped will be removed by introduction of gravity.

4-2 The inclusion of gravity is carried out by modifying the Lagrangian of Lee and Nieh using the techniques of Section 3. The most convenient co-ordinates for the calculation are those in which the weights of all the fields are equal to zero. The Lagrangian of equation (4.1) now becomes

$$
\begin{aligned}
\mathcal{L} = & -g f_\mu \cdot (\underline{\pi} \times \partial_\mu \underline{\pi})(1+\kappa\phi)^{-1} \\
& + \tfrac{1}{2} g (\sqrt{2}\, m_\rho)^{-2} (\partial_\mu f_\nu - \partial_\nu f_\mu) \cdot \partial_\mu \underline{\pi} \times \partial_\nu \underline{\pi} \\
& + \tfrac{1}{2} g^2 (f_\mu \times \underline{\pi})^2 \ (1+\kappa\phi)^{-1} . \\
& - \tfrac{1}{2} \cdot g (\sqrt{2}\, m_\rho)^{-1} (\partial_\mu \underline{a}'_\nu - \partial_\nu \underline{a}'_\mu) \cdot (\partial_\mu f_\nu - \partial_\nu f_\mu) \times \underline{\pi} \\
& - \tfrac{1}{2} g (\sqrt{2}\, m_\rho)^{-1} (\partial_\mu f_\nu - \partial_\nu f_\mu) \cdot (\underline{a}_\mu' \times \partial_\nu \underline{\pi} - \underline{a}_\nu' \times \partial_\mu \underline{\pi}) \\
& - \tfrac{1}{4} g^2 (\sqrt{2}\, m_\rho)^{-2} \left[(\partial_\mu f_\nu - \partial_\nu f_\mu) \times \underline{\pi} \right]^2 \\
& + (e/g)\, m_\rho^2 f_\mu^{\,0} A_\mu (1+\kappa\phi)^{-1}
\end{aligned}
\tag{4.5}
$$

Covariant derivatives D_μ (which would involve couplings to $\partial_\mu \phi$) do not appear in the above since [18]

$$D_\mu \underline{V}_\nu - D_\nu \underline{V}_\mu = \partial_\mu \underline{V}_\nu - \partial_\nu \underline{V}_\mu \tag{4.6}$$

for $\underline{V}$ a vector (or axial-vector) field, and

$$D_\mu \underline{\pi} = \partial_\mu \underline{\pi} \tag{4.7}$$

for $\underline{\pi}$ a scalar field. Note that only the rho-photon and some of the rho-pion vertices are changed. Those involving A_1 mesons remain the same. These modifications correspond diagrammatically to the inclusion of superpropagators between some of the vertices in the diagrams of Fig. 3 as shown in Fig. 4. However, the explicit calculation of diagrams involving more than one superpropagator is at the present time an unsolved technical problem, and we make the approximation of including only one superpropagator in each graph as shown in Fig. 5. Since only one superpropagator per diagram is sufficient to make the theory finite, this approximation still retains the main features of the gravitational regularization. The originally divergent diagrams have only one superpropagator anyway (Fig. 4 (c), (e) and (f)), and diagrams in which superpropagators are neglected gave finite contributions. The inclusion of the other superpropagators would serve only to modify slightly this already finite answer.

4-3 The calculation is performed by the standard Volkov-Salam-Strathdee momentum-space method for non-polynomial Langrangians, as outlined in section 2 and reference 8 (Volkov, Salam/Strathdee). The superpropagator in configuration space is given by

$$G(x) = \langle T\left[V[\phi(x)]\ V[\phi(0)] \right] \rangle_0 \tag{4.8}$$

where

$$V[\phi] = \frac{1}{1+\kappa\phi} = \sum_{n=0}^{\infty} (-\kappa\phi)^n \tag{4.9}$$

which gives in momentum space the (massless) superpropagator

$$\tilde{G}(p^2) = \frac{\pi}{2}(4\pi)^2 \int_{a-i\infty}^{a+i\infty} dz \left[\frac{\kappa}{4\pi}\right]^{2z} \frac{1}{\tan\pi z \sin\pi z} \times (-p^2)^{z-2} \frac{\Gamma(z+1)}{\Gamma(z)\Gamma(z-1)} \tag{4.10}$$

where $-1 < a < 0$

The pion mass difference may now be computed from the diagrams of Fig. 5,

$$\delta\mu^2 = \frac{e^2}{i}\int \frac{d^4k}{(2\pi)^4}\frac{d^4q}{(2\pi)^4} M_{\mu\nu}(k^2) D_{\mu\nu}(q^2,\lambda) \tilde{G}\left((k-q)^2\right) \tag{4.11}$$

where (with $p^2=\mu^2$ and the A_1 mass $m_a=\sqrt{2}\,m_\rho$),

$$M_{\mu\nu}(k^2) = \left[\frac{1}{k^2-m_\rho^2}\right]^2 \left[\eta_{\mu\tau} - \frac{k_\mu k_\tau}{m_\rho^2}\right]\left\{ \left(-\frac{1}{(p-k^2)-\mu^2}\right) \right.$$

$$\left. \left[(p-k)_\alpha p_\beta + p_\alpha (p-k)_\beta + (p-k_\alpha)(p-k)_\beta + p_\alpha p_\beta\right]\right.$$

$$\Big[\eta_{\tau\alpha}\eta_{\beta\delta} - (m_\rho\sqrt{2})^{-2}\eta_{\tau\alpha}(\eta_{\beta\delta}k^2 - k_\beta k_\alpha)$$
$$+\left(\tfrac{1}{2}\right)^2(m_\rho\sqrt{2})^{-4}(\eta_{\tau\alpha}k^2 - k_\tau k_\alpha)(\eta_{\beta\delta}k^2 - k_\tau k_\alpha)\Big]$$

$$+\eta_{\tau\delta} - (m_\rho\sqrt{2})^{-2}(\eta_{\tau\delta}k^2 - k_\tau k_\delta)$$

$$-\left(\frac{1}{(p-k)^2 - m_a^2}\right)(m_\rho\sqrt{2})^{-2}(\eta_{\tau\alpha}k^2 - k_\tau k_\alpha)$$

$$\left(\eta_{\alpha\beta} - \frac{(p-k)_\alpha (p-k)_\beta}{m_a^2}\right)(\eta_{\beta\delta}k^2 - k_\beta k_\delta)\Bigg\}$$

$$\left(\eta_{\delta\nu} - \frac{k_\delta k_\nu}{m_\rho^2}\right) \tag{4.12}$$

and $D_{\mu\nu}(q^2, \lambda)$ is the photon propagator. It will be instructive to work in an arbitrary covariant gauge parameterized by λ:

$$D_{\mu\nu}(k^2, \lambda) = \left(\eta_{\mu\nu} - \lambda\frac{k_\mu k_\nu}{k^2}\right)\frac{1}{k^2} \tag{4.13}$$

In equation (4.11) the internal integral around the photon-graviton loop may be carried out first and the rsult written in terms of a "modified photon propagator" $D'_{\mu\nu}(k^2)$

$$\delta\mu^2 = \frac{e^2}{i}\int\frac{d^4k}{(2\pi)^4}M_{\mu\nu}(k^2)D'_{\mu\nu}(k^2) \tag{4.14}$$

where

$$D'_{\mu\nu}(k^2) = \int \frac{d^4q}{(2\pi)^4} D_{\mu\nu}(q^2)\tilde{G}\left((k-q)^2\right) \tag{4.15}$$

Explicitly, using equations (4.10) and (4.13)

$$D'_{\mu\nu}(k^2) = \frac{\pi}{2}(4\pi)^2 \int_{a-i\infty}^{a+i\infty} dz \left(\frac{k}{4\pi}\right)^{2z} \frac{1}{\tan\pi z \sin\pi z}$$

$$\times \frac{\Gamma(z)}{\Gamma(z)\Gamma(z-1)} \int \frac{d^4q}{(2\pi)^4}\left(\eta_{\mu\nu} - \frac{\lambda q_\mu q_\nu}{q^2}\right)\frac{1}{q^2}$$

$$\times \left[-(k-q)^2\right]^{z-2} \tag{4.16}$$

Here we have changed the order of integration, the contour integral will always be performed last in accordance with usual non-polynomial techniques. Evaluating the q integral,

$$D'_{\mu\nu}(k^2) = \frac{\pi}{2i} \int_{a-i\infty}^{a+i\infty} dz \frac{(k^2/16\pi^2)^z}{\sin\pi z \tan\pi z\ \Gamma(z)} (-k^2)^{z-1}$$

$$\cdot \left\{\eta_{\mu\nu}\left(1 - \frac{\lambda z}{2(z+1)}\right) - \lambda \frac{k_\mu k_\nu}{k^2}\left(1 - \frac{2z}{z+1}\right)\right\} \tag{4.17}$$

Substituting this expression into equation (4.14) and performing the momentum integration, to order (μ^2/m_φ^2) one obtains:

$$\delta\mu^2 = \frac{3\alpha}{4\pi}\cdot\frac{i}{2\pi^2}\int_{a-i\infty}^{a+i\infty} dz\ \frac{(m_\varphi^2 K^2/16\pi^2)^z}{\sin^2\pi z\cdot\tan\pi z\cdot\Gamma(z)}$$

$$\left\{2m^2(2^z-1)+\mu^2\left[\left(\tfrac{1}{2}z^2-2\tfrac{1}{2}z+4\tfrac{3}{4}\right)2^z\right.\right.$$

$$\left.\left.-\left(\tfrac{3}{2}z+3\tfrac{7}{8}\right)-\frac{2}{\sqrt{\pi}}\frac{\Gamma(z+1/2)}{\Gamma(z+3)}\left(\frac{4\mu^2}{m_\varphi^2}\right)^z\right]\right\}$$

$$\left\{1-\frac{\lambda z}{2(z+1)}\right\} \qquad (4.18)$$

which is linear in λ. The contour along which the integral in equation (4.18) is taken stands to the left of z = 0, where the integrand has a double pole. Collapsing the contour around the positive real axis also picks up the singularities at z = 1,2,3 ... which are tripoles. The full expression for $\delta\mu^2$ will be given at the end of this section (Equation (4.25) for reference purposes. With λ =0,

$$\delta\mu^2 = (\delta\mu^2)_{z=0} + \frac{1}{2}\frac{3\alpha}{4\pi}m_\varphi^2\sum_{n=1}^{\infty}C_n(k)\left(\frac{K^2m_\varphi^2}{16\pi^2}\right)^n \qquad (4.19)$$

where

$$(\delta\mu^2)_{z=0} = \frac{3\kappa}{4\pi} m_\varsigma^2 \left[2\ln 2 + \frac{\mu^2}{m_\varsigma^2} \left\{ \ln \frac{m_\varsigma^2}{\mu^2} + \frac{19}{2}\ln 2 - \frac{5}{2} + \frac{1}{8}\left(\ln \frac{16\pi^2}{\kappa^2 m_\varsigma^2} + \psi(1) \right) \right\} \right] \tag{4.20}$$

and the power series coefficients are:

$$\begin{aligned} c_n(\kappa) = \frac{1}{(n-1)!} \Bigg[& \Big\{ 2.(2^n - 1) + 4\psi(n).\ln a \\ & - 2\phi(n)\ln^2 a - 2^{n+2}.\psi(n)\ln 2a + 2^{n+1}\phi(n)\ln^2(2a) \Big\} \\ & + \frac{\mu^2}{m_\varsigma^2} \Big\{ \left(\frac{n^2}{2} - \frac{5n}{2} + \frac{19}{4}\right) 2^n - \left(\frac{3n}{2} + 3\,7/8\right) \\ & - 2\left(2^n (n - 5/2) - 3/2\right)\psi(n) + 2^n \phi(n) \\ & + \left(2\left(\frac{3n}{2} + 3\,7/8\right)\psi(n) - 3\phi(n) \right) \ln a \\ & - \left(\frac{3}{2}n + 3\,7/8\right)\phi(n)\ln^2 a + \Big((2n-5)\phi(n) \\ & - 2\left(1/2\, n^2 - 5n/2 - 4\,3/4\right)\psi(n) \Big) 2^n \ln 2a \\ & + \left(\frac{1}{2}n^2 - \frac{5n}{2} + 4\,3/4\right) 2^n \phi(n)\ln^2(2a) \Big\} \Bigg] \end{aligned} \tag{4.21}$$

where $a = m_g^2 \kappa^2 / 16\pi^2$

$$\phi(n) = \psi^2(n) - \psi'(n)$$

$$\psi(n) = \frac{\partial}{\partial z} \ln \Gamma(z)\Big|_{z=n}$$

$$\psi'(n) = \frac{\partial}{\partial z} \psi(x)\Big|_{z=n}$$

Note that $\delta\mu^2 = 2\mu\,\delta\mu$

4-4 It has been pointed out in Reference 5 that computation with only one superpropagator is not a gauge-invariant procedure. In this calculation, the gauge-dependence of $\delta\mu$ is made manifest by the explicit appearance of the gauge parameter λ in equation (4.17). As a multiplier of $k_\mu k_\nu / k^2$ it is harmless: after integrating over k this part will vanish by symmetric integration. As a multiplier of $\frac{z\,\eta_{\mu\nu}}{2(z+1)}$, however, it exhibits the non gauge invariance of the result, since, as can be seen by equation (4.18), λ still remains in the expression for $\delta\mu^2$ even after the momentum integrations have been carried out. However, on evaluating equation (4.18), the coefficient of λ is only 0.005 MeV when $\kappa = \kappa_g$ of graviton theory ($\sim 2 \times 10^{-22} m_e^{-1}$) and still only 0.01 MeV when $\kappa = \kappa_m$ of tensor meson theory (~ 1 BeV^{-1}).

The smallness of such gauge dependent effects increases optimism that the problem of gauge invariance is not as serious as one might first expect. All numerical results in §5 are quoted with $\lambda = 0$.

4-5 In the calculation described in paragraph 4-3 the weights of the fields were all taken to be zero. A more general approach should be able to take arbitrary weights and still obtain a unique result. This would involve a concept called "κ-renormalization" which may be illustrated in the context of the pion mass difference. It should be stressed that no rigorous proof of equivalance under field re-definitions is being attempted.

If the fields in the Lagrangian (4.1) are taken with non-zero weight, then the powers of $(1+\kappa\phi)$ at the various vertices will be quite different to those of (4.5). The approximations involved in taking one superpropagator per diagram (Fig. 3) would then not be the same. However, for the purposes of this illustration, we will take one superpropagator per diagram as before - but field re-definitions will be generally represented by taking for the form of the superpropagator,

$$G_\ell(x) = \left\langle \frac{1}{(1+\kappa\phi(x))^\ell} \; \frac{1}{(1+\kappa\phi(0))^\ell} \right\rangle \qquad (4.22)$$

ℓ is an arbitrary integer. $G_\ell(x)$ replaces $G(x)$ of the previous calculation. The massless superpropagator in momentum

space is

$$\tilde{G}_\ell(p^2) = (4\pi)^2 \frac{\pi}{2} \int_{a-i\infty}^{a+i\infty} dz \left(\frac{K^2}{(4\pi)^2}\right)^z \frac{(-p^2)^{z-2}}{\tan\pi z \sin\pi z} \times \frac{\Gamma(z+1)}{\Gamma(z)\,\Gamma(z-1)} \times \left[\frac{\Gamma(\ell+z)}{\Gamma(z+1)\,\Gamma(\ell)}\right]^2 \tag{4.23}$$

which reduces to (4.10) for $\ell = 1$. The net result of using $\tilde{G}_\ell(p^2)$ to evaluate

$$\delta\mu_\ell^2 = \frac{e^2}{i} \int \frac{d^4k}{(2\pi)^4} \frac{d^4q}{(2\pi)^4} M_{\mu\nu}(k^2) D_{\mu\nu}(q^2,\lambda) \tilde{G}_\ell\left((k-q)^2\right) \tag{4.24}$$

is that the integrand of equation (4.18) acquires an extra factor of $\left[\frac{\Gamma(\ell+z)}{\Gamma(z+1)\,\Gamma(\ell)}\right]^2$.

This factor will introduce an ℓ-dependence into the residues of the singularies at $z = 0,1,2\ldots$ in this integrand.

Both $(\delta\mu^2)_{z=0}$ and $C_n(K)$ of equation (4.19) become ℓ dependent.

The full expression for $\delta\mu$ as a function of ℓ and the gauge parameter λ is given below in equation (4.25) et seq. Equation (4.19) may be obtained by setting $\ell=1$ and $\lambda=0$.

$$\delta\mu^2(\kappa,\lambda,\ell) = \delta\mu^2_{z=0}(\kappa,\lambda,\ell) + \frac{1}{2}\cdot\frac{3\alpha}{4\pi}\cdot m_s^2 \sum_{n=1}^{\infty} \frac{1}{(n-1)!}\left[\frac{(\ell+n-1)!}{(\ell-1)!\,n!}\right]^2 \left(\frac{\kappa^2 m_s^2}{16\pi^2}\right)^n S_n(\kappa,\lambda,\ell) \tag{4.25}$$

The term at the origin is

$$\delta\mu^2_{z=0}(\kappa,\lambda,\ell) = \frac{3\alpha}{4\pi} m_s^2 \left[2\ln 2 + \frac{\mu^2}{m_s^2}\left\{ \ln\frac{m_s^2}{\mu^2} + \frac{19}{4}\ln 2 - \frac{5}{2} + \frac{\lambda}{16} - \frac{1}{8}\ln\left(\frac{\kappa^2 m_s^2}{16\pi^2}\right) - \frac{1}{8}\left(2\psi(\ell) - 3\psi(1)\right)\right\}\right] \tag{4.26}$$

and the power series coefficients are

$$S_n(\kappa,\lambda,\ell) = A_n^{(1)}(\kappa,\ell) - \lambda\left[\frac{1}{2}\frac{n}{n+1}A_n^{(1)}(\kappa,\ell) + \frac{1}{(n+1)^2}A_n^{(2)}(\kappa,\ell) - \frac{1}{(n+1)^3}B_n\right] \tag{4.27}$$

The quantities $A^{(1)}$, $A^{(2)}$ and B are

$$B_n = 2(2^n-1) + \frac{\mu^2}{m_s^2}\left[\left(\frac{n^2}{2} - \frac{5n}{2} + \frac{19}{4}\right)2^n - \left(\frac{31}{8} + \frac{3n}{2}\right)\right]$$

$$A_n^{(1)}(k,\ell) = 2\,C_n(k,\ell)\,D_n + B_n\left[\left(C_n(k,\ell)\right)^2 + 2\psi'(\ell+n) - 2\psi'(n+1) - \psi'(n)\right] + E_n$$

$$A_n^{(2)}(k,\ell) = C_n(k,\ell)\,B_n + D_n \qquad (4.28)$$

where $$D_n = 2^{n+1}\ln 2 + \frac{\mu^2}{m_s^2}\left[2^n \ln 2\left(\frac{n^2}{2} - \frac{5n}{2} + \frac{19}{4}\right) - \frac{3}{2} + 2^n(n-2)\right]$$

$$C_n(k,\ell) = \ln\left(\frac{k m_s}{4\pi}\right)^2 + 2\psi(\ell+n) - 2\psi(n+1) - \psi(n)$$

$$E_n = 2^n\left[2\ln^2 2 + \frac{\mu^2}{m_s^2}\left\{2\ln 2.(n-2) + 1 + \ln^2 2\left(\frac{n^2}{2} - \frac{5n}{2} + \frac{19}{4}\right)\right\}\right] \qquad (4.29)$$

5 NUMERICAL RESULTS AND CONCLUSIONS

5-1 When κ is put equal to κ_g of graviton theory ($\kappa_g = 4.3 \times 10^{-22}$ (MeV)$^{-1}$) the power series contribution of the tripoles (equation 4.21) is negligible — 2×10^{-35} MeV. The contribution of the leading dipole (equation (4.20) clearly reproduces the ordinary zero gravity result (equation (4.3) except that there remains a dependence on κ in the form of an effective cut-off:

$$\Lambda \sim \frac{4\pi}{\kappa} \tag{5.1}$$

The important point is that the ultra-violet infinity in the old theory has disappeared via the mechanism of the induced cut-off. The ultra-violet infinity still leaves its mark as a singularity in the κ-plane and re-appears if the limit $\kappa \longrightarrow 0$ is taken. Equation (4.20) gives

$$\delta_\mu = 6.9 \text{ MeV} \tag{5.2}$$

for massive pions. Thus gravity-modified hadron electrodynamics produces a finite pion mass difference not much greater than that observed.

5-2 A rigorous calculation of the effects of tensor meson dominance of gravity is not possible at the present time since the analytic form of the massive superpropagator is unknown. Also the effects of the approximations in neglecting superpropagators become more serious. However, if one assumes that the behaviour of the zero mass propagator provides a good approximation to the massive case, the effects of strong gravity may be estimated by extrapolating to large values of κ. For values of κ of the order of one $(BeV)^{-1}$ the contribution of the tripoles is no longer negligible and the whole of equation (4.19) must be taken. Taking as a typical tensor meson mass that of the $f(1260)$, Figure 6 ($\ell = 1$) shows $\delta\mu$ as a function of κ. The variable on the axis is the quantity G defined by

$$\kappa_m = \frac{G}{m_f} \tag{5.3}$$

The range of G typical of tensor meson theory is

$$10^{-1} < G < 10 \tag{5.4}$$

It can be seen from Fig. 5 that the value of $\delta\mu$ decreases from about 5.7 MeV to about 4.1 MeV in this range, thus enclosing the physical value 4.6 MeV. The curve does not

start to rise appreciably towards the weak gravity result until $G \sim 10^{-2}$ and so this cannot be drawn in. (As $G \to 0$, $\delta_\mu \to \infty$ logarithmically.)

5-3 If one wished to estimate the value of κ in a tensor meson theory, then the decay channel of the appropriate meson would enable a direct physical evaluation to be made. In the representation of field re-definitions taken in section 4-5, a naive physical argument implies that since the relevant meson $\longrightarrow 2\pi$ term in the total Lagrangian originates from the expansion

$$\frac{\partial_\mu \pi \, \partial_\mu \pi}{(1+\kappa\phi)^{\ell}} = (\partial_\mu \pi \partial_\mu \pi)\left[1 - (\kappa\ell)\phi + \cdots\right] \tag{5.5}$$

then the coupling at the vertex is proportional to $\kappa\ell$. Thus, approximately, one would expect that the physical coupling constant κ_m was "renormalized" by field re-definitions. In a full tensor theory, the dependence of κ_m on ℓ will be very complicated. In this scalar example, roughly one expects

$$\kappa_m(\ell) \sim \kappa \cdot \ell \tag{5.6}$$

Since a detailed spin-two meson calculation was not performed for the pion mass difference, an accurate text of a "κ-renormalization" effect or comparison with an experiment like $f \to 2\pi$ is not possible. However, it is very interesting

to note that with the inclusion of $\widehat{G}_\ell(p^2)$ as described in section 4-5, in the region (5.4) $\delta_\mu(\kappa,\ell)$ shows approximate dependence on the single variable $\kappa\ell$. Figure 6 shows δ_μ as a function of ("bare") κ for various values of ℓ and Figure 7 shows δ_μ as a function of the variable $\kappa_\ell = \kappa.\ell$ for the same ℓ values. All the curves in the latter lie close together in the strong gravity region, though there is no explicit $\kappa\ell$ dependence in the expression evaluated. This indicates that, within the model taken, a renormalization of coupling could be occuring.

The effect also happens for weak gravity, where the power series in κ is negligible and only the log terms survive. Then, since $\psi(\ell)$ behaves like $\log\ell$ (especially for large ℓ) the typical combination $\left[\log\frac{1}{\kappa} - \psi(\ell)\right]$ will behave as $\log(\kappa\ell)$.

5-4 To summarize briefly, the pion mass difference provides a quantifiable test of gravity-modified hadron electrodynamics. "Weak" gravity gives numerical results - though finite - a little too high (6.9 MeV). That weak gravity is not completely unsuitable to regularizing strong interactions stems from the hadron model whose logarithmic ultra-violet divergence is proportional to μ^2. However, extrapolation of κ to values

representative of "strong" gravity for which

$$10^{-1} < k \cdot m_f < 10$$

gives $$5.7\,\text{MeV} > \delta_\mu > 4.1\,\text{MeV} \qquad (5.7)$$

indicates that a complete tensor meson theory would give a more physically reasonable prediction.

REFERENCES (PART 2)

1. See, for example, "Review on Methods in Non-Linear Quantum Field Theory" G. V. Efimov: Cern preprint TH 1087 (1969)

2. See, for example, the review talk "Non-Polynomial Lagrangian Theories" A. Salam: Proc. Miami Conference, Coral Gables (1970)

3. See, for example, the review talk "Computation of Renormalization Constants" A. Salam: Proc. Miami Conference, Coral Gables (1971) Trieste Preprint IC/71/3 (1971)

4. A. Salam, J. Strathdee: Nuovo Cimento Letters 4, 101 (1970)

5. C. J. Isham, A. Salam, J. Strathdee: ICTP Trieste preprint IC/70/131 (1970); to be published in The Physical Review

6. C. J. Isham, A. Salam, J. Strathdee: ICTP Trieste preprint IC/70/108 (1970); to be published in The Physical Review

7. Sections 4 and 5 contain material also appearing in M. J. Duff, J. Huskins, A. Rothery: I.C. preprint ICTP/70/17 (1971)

8. A. Salam, J. Strathdee: Phys. Rev. D1, 3296 (1970);
and
M. K. Volkov: Annals of Physics (NY) 49, 202 (1968)

9. H. Epstein, V. Glaser and A. Martin: Comm. Math. Phys. 13, 257 (1969)

10. H. Lehmann, K. Pohlmeyer: DESY preprint 70/26 (1970)

11. I. Waller: Zeits. Phys. 62 673 (1930)

12. V. Weisskopf: Zeits. Phys. 89, 27 (1934); Phys. Rev. 56 72 (1939)

13. A. Jaffe, J. Glimm: Commun. Math. Phys. 11, 9 (1968)

14. A. Salam: (Kiev Conference) ICTP Trieste preprint IC/70/106 (1970)

15. B. W. Lee and H. T. Nieh: Phys. Rev. 166, 1507 (1968)

16. G. C. Wick and B. Zumino: Phys. Letters 25 B, 479 (1967)

17. I. S. Gerstein, B. W. Lee, H. T. Nieh, H. J. Schnitzer: Phys. Rev. Letters 19, 1064 (1967)

18. See, for example, J. L. Anderson: "Principles of Relativity Physics" (Academic Press, London, 1967).

FIGURES FOR PART TWO

FIGURE CAPTIONS

Figure 1. Schematic representation of $\tilde{F}_{22}^{(2)}(s)$.

Figure 2. (a) Electron self-mass graph.

(b) Modification to (a) with graviton exchanges.

Figure 3. Feynman graphs from the chiral Lagrangian. The wavy line, double line, and thick line represent the photon, pion, rho and A_1, respectively. (a), (b) and (c) differ by the powers of momenta at the vertices; similarly for (d) and (e).

Figure 4. Full gravity-modified graphs. The dotted line represents the multi-graviton propagator.

Figure 5. Single-superpropagator graphs evaluated.

Figure 6. $\delta\mu_l$ as a function of "bare" coupling constant κ . $G = \kappa \cdot m_f$, with values between 0.0 and 10.0 for strong gravity. The curve rises below $G = 0.01$ and eventually becomes infinite for $G = 0.0$. The weak gravity result is indicated.

Figure 7. $\delta\mu_l$ as a function of "renormalized" κ_1 i.e. $G.l$ ($= \kappa_1 \cdot m_f$).

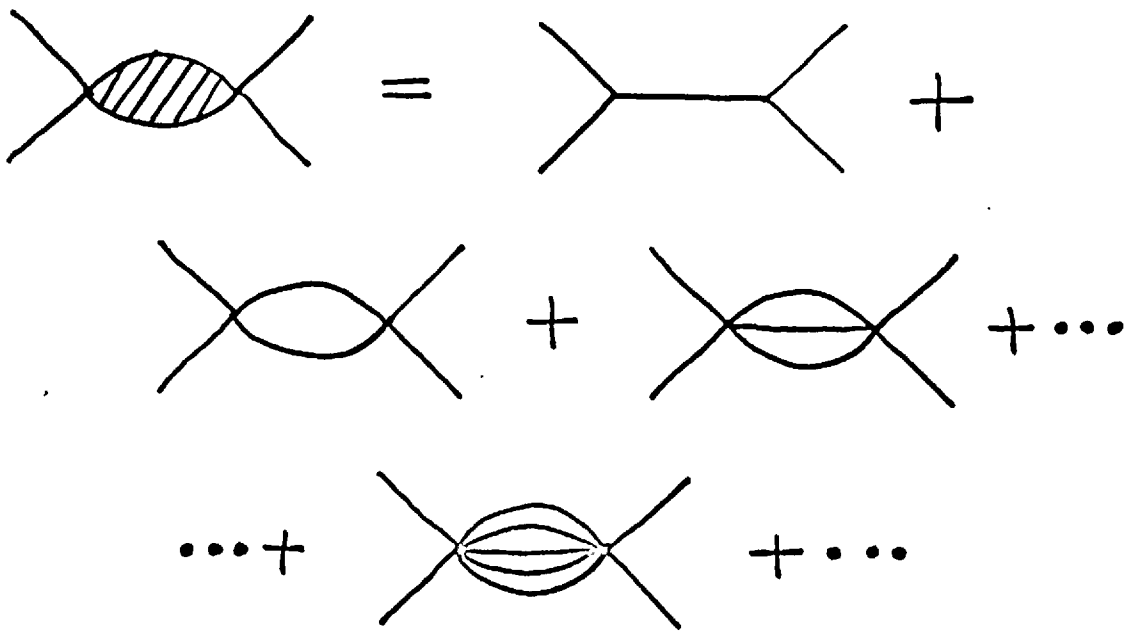

FIG. 1

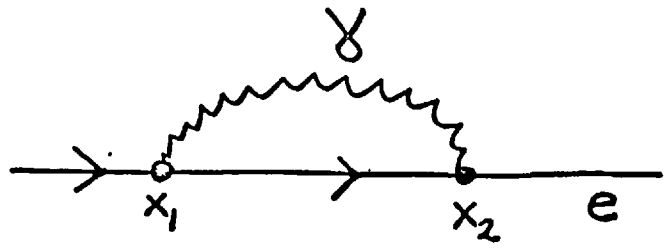

(a)

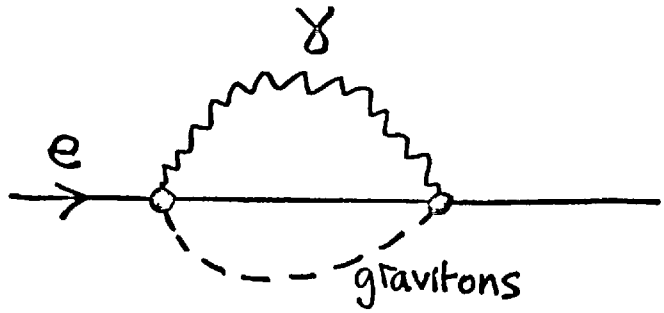

(b)

FIG. 2

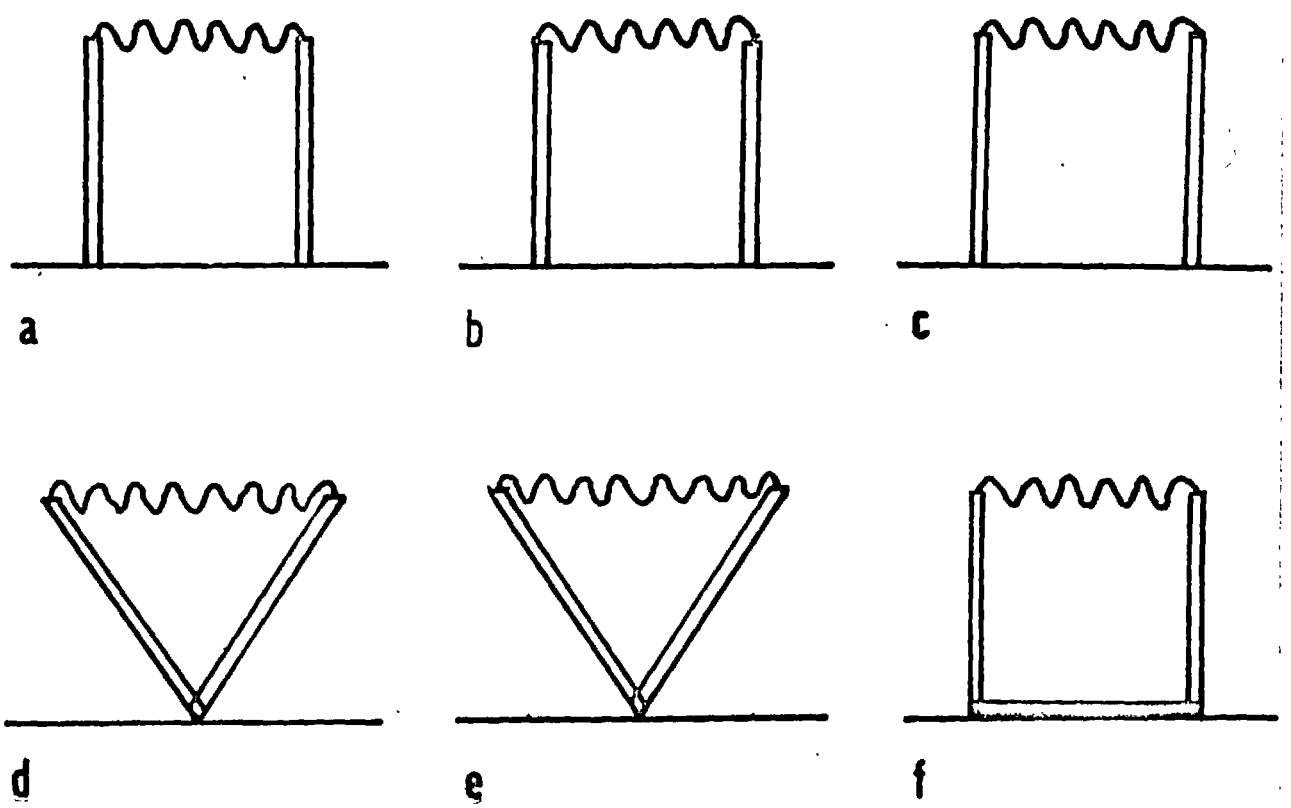

Fig. 3

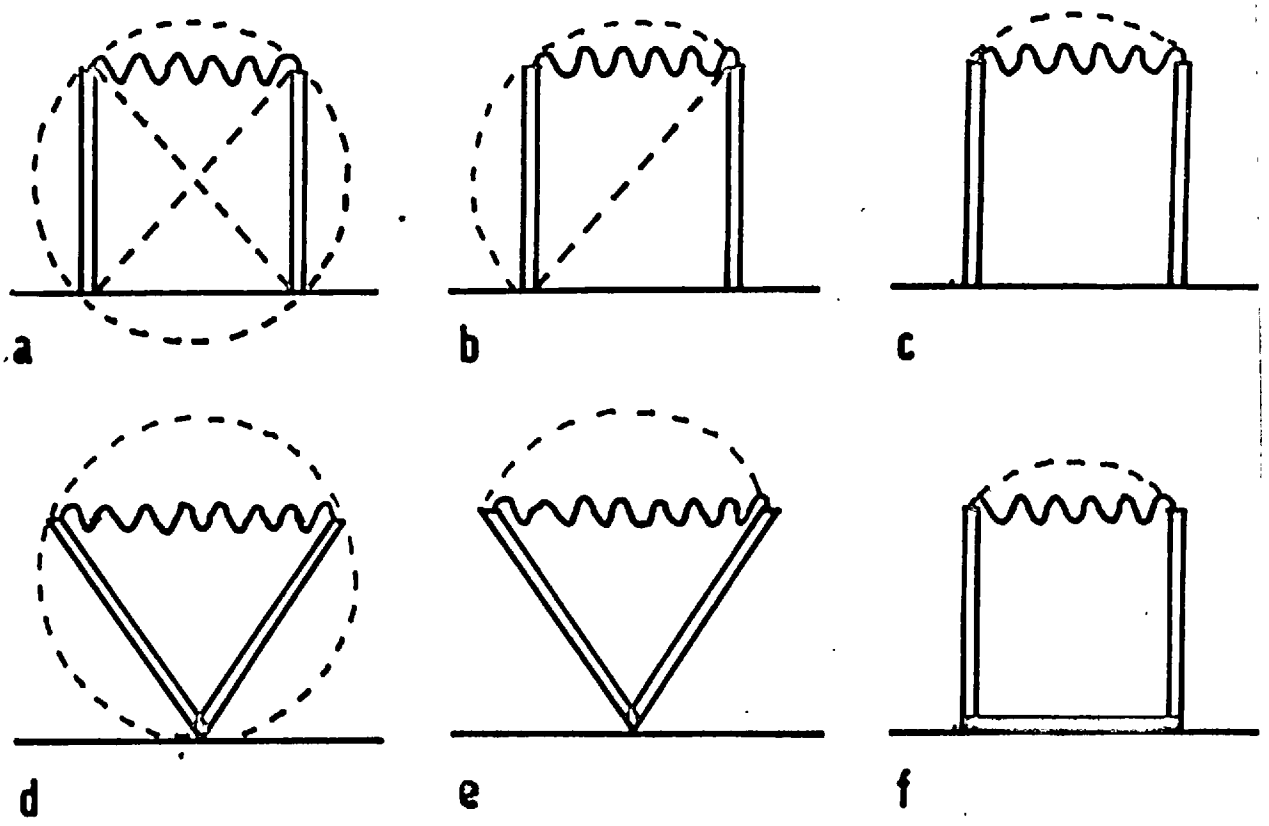

Fig. 4

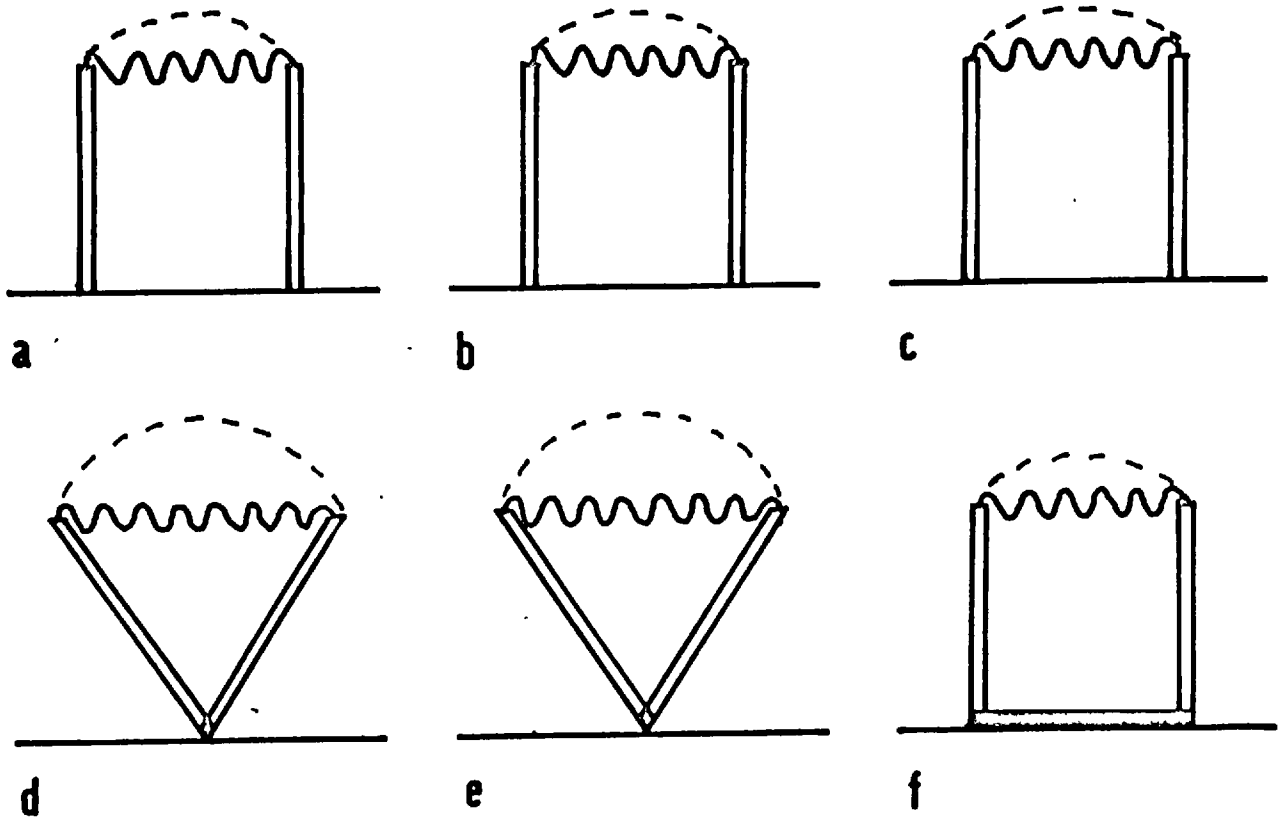

Fig. 5

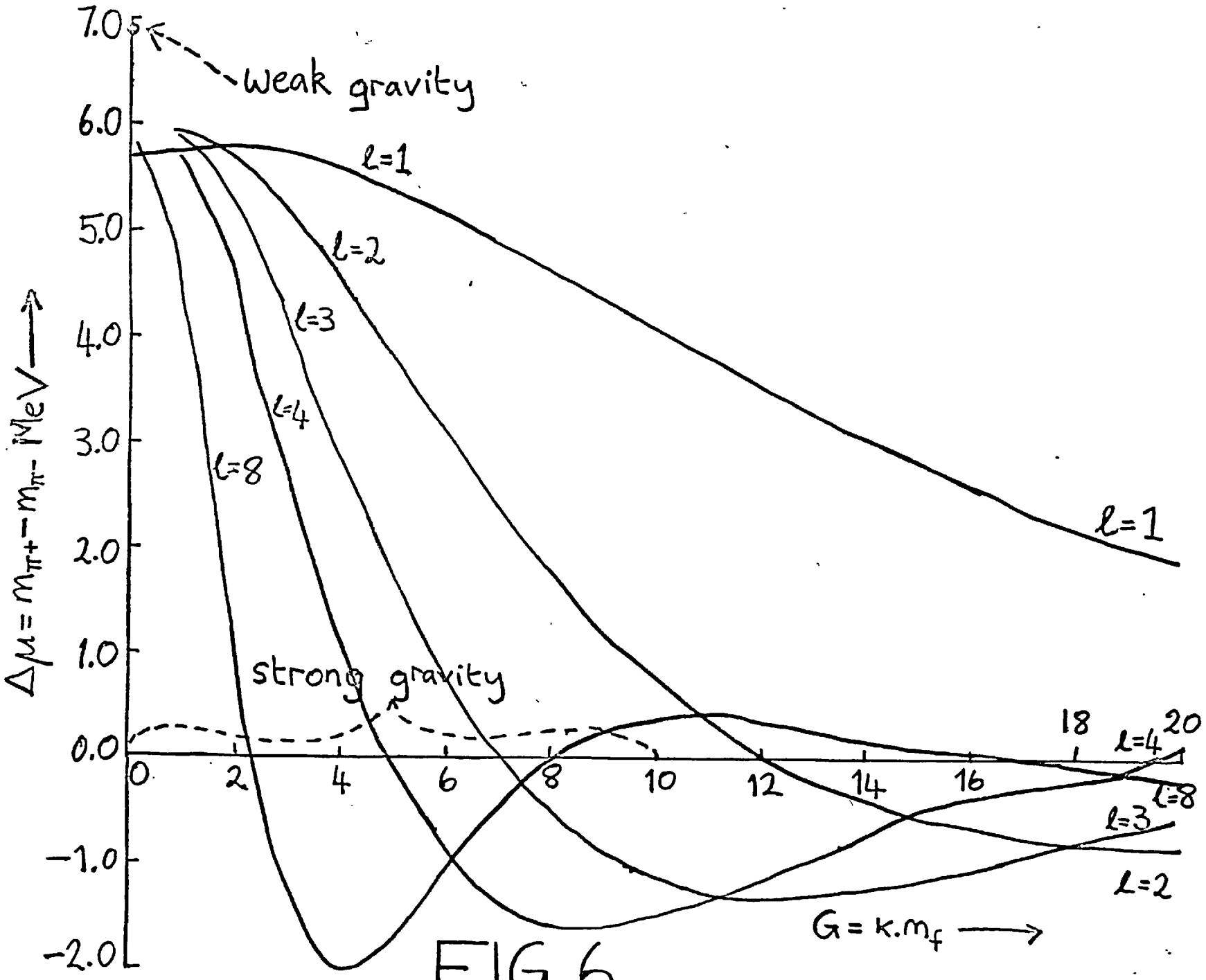
7.0
6.0
5.0
4.0
3.0
2.0
1.0
0.0
−1.0
−2.0
0
2
4
6
8
10
12
14
16
18
20
Weak gravity
strong gravity
ℓ=1
ℓ=2
ℓ=3
ℓ=4
ℓ=8
ℓ=1
ℓ=4
ℓ=8
ℓ=3
ℓ=2
Δμ = m_π+ − m_π− MeV
G = k.m_f

FIG.6

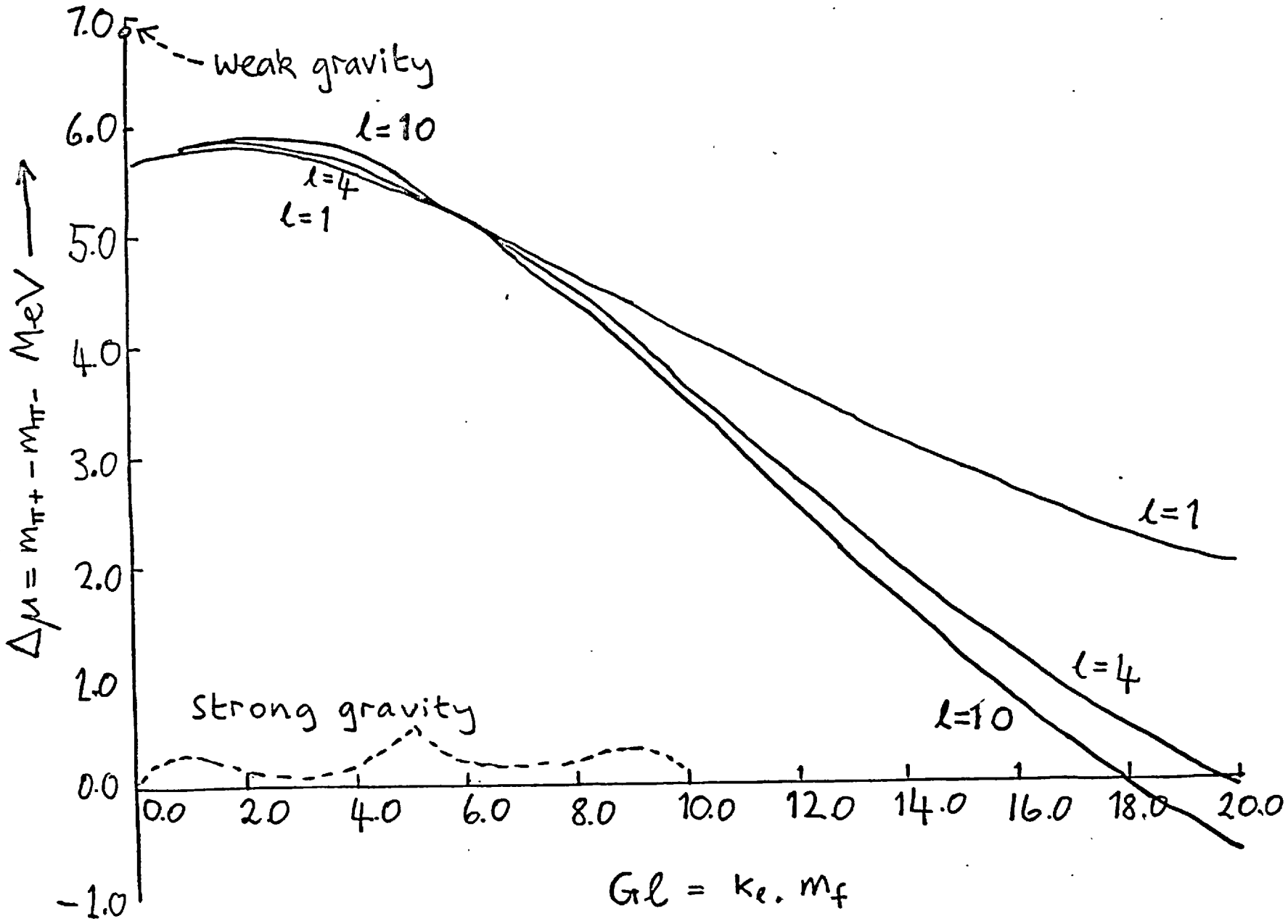
7.0
6.0
5.0
4.0
3.0
2.0
1.0
0.0
-1.0
weak gravity
l=10
l=4
l=1
l=1
l=4
l=10
strong gravity
0.0
2.0
4.0
6.0
8.0
10.0
12.0
14.0
16.0
18.0
20.0
Δμ = mπ+ - mπ- MeV
Gl = ke . mf

FIG. 7